The improvement and application of topically applied double stranded RNAs to control *Sclerotinia sclerotiorum* and *Hyaloperonospora arabidopsidis*

by

Christopher L. Manchur

A thesis submitted to the Faculty of Graduate Studies of

The University of Manitoba

in partial fulfillment of the requirements of the degree of

MASTER OF SCIENCE

Department of Biological Sciences

University of Manitoba

Winnipeg, Manitoba, Canada

ABSTRACT

Hyaloperonospora arabidopsidis and *Sclerotinia sclerotiorum* are plant pathogens of significance to both agricultural research and production. While chemical pesticides are effective at controlling these pathogens, increasing environmental concerns and pathogen resistance pose serious problems for their continued use. The need to develop environmentally-friendly alternatives is now a major focus for crop protection. RNA interference (RNAi) is a process that utilizes double-stranded RNA to reduce mRNA transcript accumulation and has potential to provide species-specific, sequence-dependent crop protection applications. Using a combination of novel *in vitro* assays, I identified a set of candidate *H. arabidopsidis*- and *S. sclerotiorum*-targeting dsRNAs that reduced germination rates and growth of both pathogens. Using plate-based assays adaptable to high-throughput screening, I screened multiple dsRNAs and demonstrated dsRNA dose-responses within the pathogens. Foliar application of dsRNAs on *Arabidopsis thaliana* caused transcript knockdown within *H. arabidopsidis*, confirming that the impaired growth was RNAi-mediated. Comparisons of Dicer gene sequences in *H. arabidopsidis* and *S. sclerotiorum* with homologous sequences in other fungi and oomycetes confirmed that while both pathogens shared this conserved RNAi pathway gene, the evolution of Dicer fits with the phylogenetic divergences of these rather different phytopathogens. This research provides valuable insights into novel assays that can be used for evaluating dsRNA treatments in both pathogens, and the optimization of dsRNA treatments can lead towards the development of RNAi-based crop protection products against both downy mildew and Sclerotinia stem rot.

ACKNOWLEDGEMENTS

I would like to thank the people who have made my graduate experience a positive one and have encouraged me to put my best foot forward as a researcher and as a person. I'd like to extend my gratitude to Dr. Steve Whyard and Dr. Mark Belmonte for the opportunity to work in their labs; it has been an absolute pleasure and I am grateful for their support in both my research and personal development. I'm grateful for the financial support received during my graduate studies from the Natural Sciences and Engineering Research Council of Canada, the Canadian Agricultural Partnership fund in concert with the Canola Council of Canada and provincial canola growers associations, the University of Manitoba, the Faculty of Science, the Faculty of Graduate Studies, and the Department of Biological Sciences.

While the COVID-19 pandemic introduced many challenges, I am thankful for all the help and advice received from the both the Belmonte and Whyard research groups, offered either in-person or online (Nick Wytinck, Phil Walker, Dylan Ziegler, Aditi Singh, Daniel Heschuk, Michael Wood, Sharon Felix, and Elizabeth Jonson). I am especially thankful for the help and guidance from Alison Tayler, who has instilled in me a strong work ethic and skills in molecular biology. It's been a pleasure working with all of you, and I have thoroughly enjoyed the company and accompanying puns.

I am thankful for my family and friends for their continuous support; the shared enthusiasm of my work has been an excellent motivator to keep pushing forward. I'd also like to thank the farmers of both Canada and Ukraine - your dedication to agriculture has been a continuous inspiration for me. Lastly, I'd like to extend a heartfelt thank you to my fiancé Laura Brinkman. Your love, encouragement, and support over these past two years have been a blessing and have made it a pleasant journey to no end.

TABLE OF CONTENTS

LIST OF TABLES

LIST OF FIGURES

LIST OF SUPPLEMENTARY TABLES AND FIGURES

NON-COMMON ABBREVIATIONS

AGO	ARGONAUTE
BLAST	basic local alignment search tool
bp	base pairs
DCL	DICER-LIKE
DCR	DICER
DMI	demethylation inhibitor
dsRBD	dsRNA-binding domain
dsRNA	double-stranded RNA
EC_{50}	half maximal effective concentration
GMO	genetically modified organism
GO	gene ontology
GUS	β-glucuronidase
HIGS	host-induced gene silencing
hpi	hours post inoculation
miRNA	micro RNA
mRNA	messenger RNA
MUSCLE	multiple sequence comparison by log- expectation
OD_{600}	optical density at 600 nanometer wavelength
PDB	potato dextrose broth
piRNA	piwi-interacting RNA
PTGS	post-transcriptional gene silencing
QOI	quinone outside inhibitor
qRT-PCR	reverse transcription quantitative real-time PCR
RdRp	RNA-dependent RNA polymerase
RISC	RNA-induced silencing complex
RNAi	RNA interference
RNA-seq	RNA sequencing
SDHI	succinate dehydrogenase inhibitor
shRNA	short hairpin RNA
SID	systemic RNA interference defective proteins
SIGS	spray-induced gene silencing
SIL	SID-like proteins
siRNA	short interfering RNA
SSR	Sclerotinia stem rot

CHAPTER 1: INTRODUCTION TO RNA INTERFERENCE AS A CROP PROTECTION TOOL FOR CONTROLLING PLANT PATHOGENS

1.1 Current Management of Plant Diseases in Agriculture

Providing a sustainable source of food for our growing population is a common goal amongst agricultural producers. With a population projection of approximately 9.7 billion by 2050, food production will need to increase by almost 50% to satisfy the growing caloric needs (FAO 2018; Gouel and Guimbard 2018). Expanding cropland to meet these needs is only possible if forests are cultivated into arable land, but this exacerbates the already significant losses in habitat, biodiversity, and carbon sequestration (Molotoks et al., 2018; Eitelberg, et al., 2014). In current agricultural regions, abiotic stressors such as drought, heat, cold, and salinity can negatively impact crop growth, and often facilitate further damage from biotic stressors such as diseases caused by plant pathogens (Pandey et al., 2017). These plant diseases can account for significant crop losses, and producers worldwide are challenged by pathogens that hamper the production of high quality food products.

In staple food crops such as wheat, rice, and maize, plant pathogens can be responsible for approximately 20% of estimated yield losses worldwide (Savary et al., 2019), with pathogens such as Fusarium head blight (*Fusarium graminearum*) in wheat, rice sheath blight (*Rhizoctonia solani*), and Gibberella stalk rot (*Gibberella zea*) in maize representing some of most economically important destructive species. Besides yield losses, plant diseases impact postharvest food products and can produce toxins that make them unsafe for consumption. Pathogens such as *Botrytis cinerea, Alternaria,* and *Penicillium* are causal agents of rots and molds that are major contributors of the 25-50% postharvest losses in fruits and vegetables (Barkai-Golan, 2001; Nunes, 2012), and mycotoxins produced by *Fusarium* found in wheat

kernels can cause gastric complications in both humans and animals (Snijders, 1990). To combat these diseases, producers employ plant disease management plans with the goals of reducing the frequency and severity of infection.

An integrated plant disease management plan involves a combination of cultural, genetic, and chemical methods to efficiently prevent pathogens from becoming an issue in producers' fields or greenhouses. The objective is to limit the levels of starting inoculum, reduce the rate of infection, and reduce the interaction time between pathogen and host populations (Ciancio and Mukerji, 2007). Some cultural practices producers use include rotating to crops that are not hosts to pathogens present, altering planting dates to shift the plant's susceptible growth stage away from the critical period of infection, and removal of alternative hosts in the area, such as some weed species. Producers can also choose to use cultivars that are genetically resistant to pathogens. Using conventional breeding or by genetic engineering using transgenic/genome-editing tools, producers now have access to varieties that can overcome a pathogen's infection either completely or enough to be economically viable. As of 2020, there have been 29 transgenic events conferring genetic resistance to diseases (Kumar et al., 2020), and there are many other instances where genetic resistance was provided through conventional breeding. While genetic resistance and cultural controls are commonly used, producers also choose to apply chemical fungicides to prevent infection in their crops.

In Canada, 38% of field crop farms use fungicides (Statistics Canada, 2017), and in the Canadian Prairie Pothole Region, approximately 1,600 metric tonnes of fungicide were applied in 2015 (Malaj et al., 2020). While there is a vast selection of commercial fungicide brands available, these chemicals can be broken down into groups based on their mode of action. Some of the most common modes of action are demethylation inhibitors (DMI's), quinone outside

inhibitors (QOI's), and carboxamides (Kuck et al., 2012). These chemicals target critical pathways in pathogens such as sterol biosynthesis or cellular respiration and are commonly applied as a broad-spectrum solution to control a variety of pathogens. While many of the fungicides used today are effective and cost-efficient, there are many downsides that could result in severe challenges for producers in the future if left unchecked.

Pathogen resistance to fungicides is one of the major concerns for producers and researchers. For a pathogen to develop resistance, there are a few key factors involved: the genetic diversity of the pathogen; potential for rapid production/dispersal of propagules; and need for repeated application of fungicide to provide disease management annually (Brent and Holloman, 2007). Once a pathogen develops genetic resistance to a fungicide, that resistance can become heritable and could potentially confer cross-resistance to other fungicides that target the same mechanism. This can result in a complete breakdown of a particular mode of action for a particular fungal species, and if producers are applying these chemicals as a broad spectrum solution, this option may no longer be viable. One case of pathogen resistance in Canada in recent years is in *Leptosphaeria maculans*, the causal agent of blackleg in canola. The effective concentration to inhibit fungal growth by 50% (EC_{50}) of the fungicide pyraclostrobin against isolates collected from stubble in 2016 increased 4-fold compared to baseline isolates collected in 2011 (Wang et al., 2020). As one of the three registered active ingredients available in Canada to control blackleg, reduced efficacy severely limits producers' options for chemical control of this serious pathogen.

Along with pathogen resistance, there are environmental concerns regarding the foliar and seed treatment-based applications of fungicides. Through runoff into local water systems, fungicides could alter aquatic ecosystems by inhibiting the growth of benign fungal species and

thus favoring growth of toxic cyanobacteria (Lu et al., 2019). As foliar fungicides are often applied when the crop is in bloom, fungicides may contaminate the pollen on which bees feed, and a recent study has shown that the combination of boscalid and pyraclostrobin fungicides could impair colony health of honeybees (Fisher et al., 2021).

Consumers today are also becoming more concerned about from where their food comes and how safe it is for themselves and the environment, spurring governments to introduce strict regulations and bans on products. Chlorothalonil, a fungicide used to control Septoria leaf blotch in wheat, has been banned in the European Union (EU) following its classification as a Category 1 Carcinogen by the European Chemicals Agency (Case, 2019). Another chemical, mancozeb, has also been banned by the EU, pushing farmers to seek out alternative solutions to controlling potato late blight (Clarke, 2021). While either of these two chemicals are not currently banned in Canada, there are strict regulations on the use of them, such as preventing their use as a seed treatment or increased restrictions on entry into sites where they have been applied (PMRA, 2018, 2020). It is yet to be seen if greater restrictions of these fungicides will be implemented in Canada, but producers and manufacturers of these chemicals should be prepared to find alternative control methods.

Fungicides are effective tools for farmers to control and mitigate infection in their fields, but the overall reliability of many of these chemicals is in question. If fungicides are no longer usable due to pathogen resistance, adverse environmental impacts, or legislation, producers will have one of their greatest instruments removed from their integrated disease management strategy. Because of this, there is a real need for an alternative control method that is environmentally harmless, effective, and can be readily adopted by producers. One technology

being developed that could offer species-limited control of certain fungal pathogens is RNA interference.

1.2 Overview of the RNA Interference Mechanism

In 1998, Andrew Fire and colleagues discovered a mechanism in the nematode *Caenohabditis elegans* (Fire et al., 1998). By microinjecting an annealed mixture of sense- and antisense RNA covering a 742-nucleotide segment of the *unc-22* gene into *C. elegans*, Fire observed significantly greater frequencies of *unc-22* loss-of-function mutant phenotypes when compared to microinjecting sense- or antisense RNA on their own. This annealed mixture, known henceforth as double-stranded RNA (dsRNA), was determined to be the causal agent of a mechanism known as RNA interference (RNAi).

Before the term "RNAi" was coined, there were previous discoveries that lead to the 1998 landmark paper by Fire. In the early 1990s, quelling and post-transcriptional gene silencing (PTGS) was described. Quelling is the term coined by Romano and Macino (1992) to describe the inactivation of an endogenous gene in the fungus *Neurospora crassa* following the introduction of antisense RNA of the gene introduced via transformation. This was later determined to be a form of RNAi, with the transformed plasmid DNA expressing a dsRNA that could induce the silencing effect (Zhang et al., 2013). A similar phenomenon, originally called transgene silencing in plants, was also observed by multiple research groups in 1994; each group transformed plants to produce antisense RNAs that targeted either an endogenous gene or a viral RNA that would infect that plant (Dehio and Shell, 1994; Smith et al., 1994; Blokland et al., 1994). In all cases, a post-transcriptional silencing event was the product, where the targeted gene was suppressed. Later, it was determined that PTGS and quelling were carried out by the same overall mechanism as RNAi.

The RNAi mechanism is separated into two distinct steps: biogenesis of small RNAs; and degradation of mRNAs through the RNA-Induced Silencing Complex, or RISC. There are three classes of small RNAs that can play a role in RNAi, and they differ by their origin and function. PIWI-interacting RNAs (piRNAs) are 24-31 nucleotides long and are produced by the host as a mechanism for regulating transposon activity and other mobile genetic elements (Iwasaki et al., 2015). Micro-RNAs (miRNAs) originate from the host or other organisms as single-stranded RNA precursors that contain a hairpin structure, allowing a short-hairpin RNA (shRNA) to be produced and regulate host gene expression (Betti et al., 2021). Lastly, small interfering RNAs (siRNAs) can originate from both the host or other organisms and are generated from double-stranded RNA precursors that can vary in length (Li et al., 2010).

In all three classes of sRNAs, the RNA precursors need to be processed by Dicer. Dicers (DCRs) or dicer-like proteins (DCLs) are ribonucleases that convert the precursors into 21-24 nucleotide duplexes that are ready for loading into RISC. In most species, there are six domains within Dicer: DEAD box, helicase C, DUF283, PAZ, RNase III (usually two domains), and the dsRBD. The most critical domains are the PAZ, RNase III, and dsRBD, where the PAZ domain binds single- or double-stranded RNA, and the dsRBD (dsRNA-binding domain) also binds dsRNA and aids in RISC's specificity for double-stranded vs single stranded RNAs. The RNase III domains are responsible for the catalytic action of the protein and cleavage of the RNAs (Liu et al., 2009). In most organisms there are two Dicer genes, although some species can have more. In *Arabidopsis*, for example, there are four Dicer genes, each with a different function; DCL1 processes miRNAs as well as sRNAs from endogenous inverted repeats, DCL2 and DCL3 produce siRNAs for viral resistance and chromatin modification, and DCL4 has been associated with post-transcriptional silencing (Henderson et al., 2006). Another distinguishing feature of

these Dicer proteins are the size of the dsRNA molecule they generate, which can range from 21-24 nucleotides (Kaur et al., 2016). Conversely, there appears to be a loss of this RNAi silencing machinery in some fungal organisms. *Ustilago maydis*, *Cryptococcus deuterogatti*, *Candida albicans*, *Naumovozyma castelli*, and *Saccharaomyces cerevisiae* all lack Dicer proteins, which has resulted in the loss of regulatory and defense roles the RNAi machinery can provide (Lax et al., 2020). In some of these species like *U. maydis* and *S. cerevisiae*, this disadvantage is overcome by retaining the ability to have a symbiotic relationship with dsRNA killer viruses. These viruses give the host a competitive edge in communities with high microbial densities but couldn't persist in a host that has active RNAi machinery (Laurie et al., 2012; Pieczynska et al., 2013).

The subsequent step in RNAi involves the RISC and the eventual degradation of mRNAs. Small RNAs generated by DICER unwind to become single-stranded and are loaded into the center of the RISC, Argonaute (AGO) protein. The AGO protein family has different clades, with each clade of the AGOs matching to a particular sRNA (Kaur et al., 2016). Once the sRNA is loaded, the single-stranded sRNA acts as a guide and base pairs with the corresponding RNA (often mRNA). RNase activity within the PIWI domain of the Argonaute protein induces cleavage of the target RNA, and the cut RNA is then degraded by cellular nucleases. The reduction in the amount of the targeted mRNA then leads to less protein, thus generating the so-called gene silencing effect of RNAi.

1.3 Applications and Interactions of RNA Interference in Agriculture and Plant Pathogens

While RNAi is a mechanism found in many organisms, where it serves as either an antiviral defense or a gene regulation mechanism, RNAi can be utilized in agricultural settings to selectively target species deemed antagonists to agriculture production. This can be achieved by

introducing to target species foreign dsRNA or sRNAs that are specifically designed to target mRNAs that are critical for growth, feeding, or infection. Because these RNAs can be designed to be host-specific by having no complementarity to other species in the final 21-24 bp sequence, RNAi has a great advantage over traditional pesticides that are often non-discriminatory (Christiaens et al., 2018). This species-specific, sequence-dependent mechanism offers researchers and agricultural producers another way to protect plants without any considerable drawbacks to the environment.

Two methods by which RNAi can be used in agricultural settings is Host-Induced Gene Silencing (HIGS) and Spray-Induced Gene Silencing (SIGS). Many plant species use RNAi as an antiviral defense mechanism, and researchers can provide specific dsRNAs for protection by genetically transforming the plants with dsRNA-expressing transgenes. A variation of HIGS is Viral-Induced Gene Silencing (VIGS), where plants can be infected with a virus that produces the dsRNAs or siRNAs needed to initiate RNAi within the plant's cells (Lee et al., 2015). While VIGS uses non-replicating viruses, there are concerns that this technology could be difficult to contain, when recombinant viruses are used. HIGS, is considered a safer approach, as it relies on well-tested transformation techniques. Using the transformation vector *Agrobacterium tumefaciens*, a genetic construct containing sequences used to generate dsRNAs can be inserted into the host plant's genome to provide protection against pathogens like fungi or viruses (Koch et al., 2013; Tomar et al., 2018). Stable and consistent expression of dsRNA within the transgenic plant is a great advantage for heritable protection, and thanks to the activity of RNA-dependent RNA polymerases (RdRp's) within plants, the dsRNAs can be amplified by the plant to provide longer-lasting protection (Nunes and Dean, 2012). While no commercial RNAi products are available to control pathogens yet, Bayer CropScience and Corteva have announced

corn seed products that contain HIGS technology to help control corn rootworm (Business Wire, 2022; Gullickson, 2022). However, HIGS has some challenges that could prevent its widespread adoption into agricultural systems. Not all species are amenable to *Agrobacterium*-based transformation, and there are many regulatory restrictions in place that are influenced by public perception of GMOs which discourage new genetic events from reaching the market (Anjanappa and Gruissem, 2021).

In contrast to HIGS, SIGS, or topical application of dsRNA, could offer equal or better protection, without the limitations associated with transgenic technology. SIGS is an alternative of RNAi-based pest and pathogen management that involves spraying dsRNA molecules on their own or conjugated with nanoparticles onto leaves, flowers, or fruits. When applied to plants, the dsRNA has two possible routes to enter the pathogen: direct internalization from the surface of the plant or the abiotic environment into the pathogen; or indirectly through penetration into the plant's tissues. Most pathogens acquire dsRNA from the plant surface, where there is the greatest amount of biologically active dsRNAs available. DsRNA acquired from within plant tissues presents more challenges, as the dsRNA needs to overcome the hydrophobic cuticle and be protected from nucleases (Bennett et al., 2020). DsRNA delivery into the plant can offer more robust protection by being processed by the host plant's RNAi machinery, amplification of the dsRNA by RdRp's, and translocation throughout the vascular system of the plant to areas that did not have direct contact with the spray (Koch et al., 2016). Topical application of dsRNA has proven successful in a variety of agriculturally important pathogens such as *Botrytis* grey mold on tomatoes, strawberries, grapes, lettuce, and onion (Wang et al., 2016), *Phytophthora* late blight on potatoes (Kalyandurg et al., 2021), *Fusarium* blight on barley and wheat (Koch et al., 2016; Yang et al., 2021), and *Sclerotinia* on canola (McLoughlin et al., 2018). Foliar application

of dsRNA against fungal pathogens has also been improved by encapsulating dsRNA using layered double-hydroxide nanosheets (aka BioClay) (Mitter et al., 2017; Mosa and Youssef, 2021) or using *E. coli*-based minicells (Islam et al., 2021). Mitter's (2017) BioClay has been used to facilitate better delivery in plant cells, however the exact mechanism responsible for the transport of dsRNA is currently unknown. Using these nanocarriers, the researchers observed extended protection of the plants from the pathogens under greenhouse conditions, which they attributed to reduced degradation by RNases, improved internalization of dsRNAs into plant tissues, and/or prolonged release of the dsRNA over time.

1.4 Challenges in the Application of SIGS as a Crop Protection Product

While there has been a steady increase in the number of reports of effective RNAi directed against fungal pathogens, the use of SIGS as a crop protection product in fields will require further enhancements to maximize its efficiency. Prior to uptake into the target pathogen, dsRNAs need to be readily available in the pathogen's immediate environment. Rainwater, UV light, and RNases can negatively impact dsRNA stability (Rank and Koch, 2021). In one study, soybean plants treated with 100 bp-length dsRNA applied with a backpack sprayer in a field showed almost 99% reduction in concentration on the leaves after 7 days (Bachman et al., 2020). While naked dsRNA appears to degrade quickly, dsRNA loaded onto BioClay has shown to be still detectable even after 30 days by Northern blot analysis (Mitter et al., 2017). In soils, dsRNA appears to degrade rapidly due largely to microbial nuclease activity, with very little detected after 48 hours (Dubelman et al., 2014; Parker et al., 2019). This rapid degradation in soil will ensure that off-target effects, even on related beneficial fungi, will be limited. But a short half-life also means it will be challenging to control pathogens within the soil, such as *Rhizoctonia* spp. and *Plasmodiophora brassicae,* which attack the root systems of species such as canola.

This limitation may, however, be overcome with future developments of nanoparticle carriers that protect the dsRNA from soil microbes, with one research group developing a cationic polymer that binds to dsRNA which can extend its stability by 3 weeks (Whitfield et al., 2018).

The rate of cellular uptake of dsRNA can be another barrier for efficient RNAi, and it is still not fully understood how dsRNA can access the cell's cytoplasm to reach the RNAi machinery. In *Caenorhabditis elegans,* systemic RNA interference defective (SID) proteins facilitate dsRNA uptake (Hinas et al., 2012), and orthologous SID-like (SIL) proteins appear to have a role in uptake in some insects, such as the Western corn rootworm and the Colorado potato beetle (Miyata et al., 2014; Cappelle et al., 2016). Conversely, insects such as the flour beetle *Tribolium castaneum,* desert locust *Schistocerca gragaria*, and diamondback moth *Plutella xylostella* do not appear to utilize SIL proteins in the dsRNA uptake process (Tomoyasu et al., 2008; Wynant et al., 2014; Wang et al., 2014). Instead, these species, and other insects examined to date, can use clathrin-mediated endocytosis for dsRNA uptake (Saleh et al., 2006; Abbasi et al., 2020). Similarly, in the fungus *Sclerotinia sclerotiorum,* Wytinck (2020) demonstrated that clathrin-mediated endocytosis was a primary dsRNA uptake mechanism. Because fungi lack orthologs of the SID proteins, endocytic pathways like clathrin-mediated endocytosis may be the primary modes of uptake for dsRNA for many of these organisms, but to date, there are only a small number of studies that have examined dsRNA uptake in fungi and related phytopathogens (Wytinck et al., 2020). Recently, Qiao et al. (2021) observed that uptake efficiency varies in different phytopathogen species, resulting in the failure of RNAi to suppress pathogen infections of some host plants. In that study, the oomycete *Phytophthora infestans* exhibited limited uptake of dsRNA across cell types and developmental stages, but in fungal pathogens like *Botrytis cinerea, Sclerotinia sclerotiorum,* and *Verticillium dahliae,* there was

highly efficient uptake, resulting in effective plant protection. While *Phytophthora* was found to be recalcitrant to topical dsRNA applications, it was effectively controlled by HIGS in transgenic potato lines (Sanju et al., 2015). While different targets were utilized between these studies, it raises questions on how SIGS can be better optimized for the target pathogen, and if there are other factors that influence SIGS or HIGS success.

In studies involving the protection of plants from viruses, insects, and fungal pathogens using topical applications of dsRNA, the application devices, areas sprayed, and dosages vary amongst them, making it challenging to provide direct comparisons (Rank and Koch, 2021). It is currently estimated that 2-10 grams of dsRNA is required for every hectare of land, but can vary depending on type of application, target pathogen sensitivity, and if they are conjugated with nanoparticle carriers (Das and Sherif, 2020). The cost of production via *in vitro* dsRNA transcription is currently around $100 USD per gram (Dalakouras et al., 2019), making commercial application of SIGS using this method of dsRNA synthesis uneconomical. To solve this, microbial platforms to manufacture dsRNA at costs as low as $0.50 USD per gram are currently under development (Guan et al., 2021; Nino-Sanchez et al., 2021). If SIGS is to be adopted to field-scale applications where dsRNA may be sprayed on many hectares of land, the minimum effective concentration is a crucial factor in maximizing the cost effectiveness of SIGS and making it an economically viable alternative.

Developing new fungicides products with unique modes of action or formulations can take years and involves a substantial investment, upwards of $300 million USD per fungicide (Arnason, 2017; Leadbeater, 2015). Developing fungicidal dsRNA molecules has its own set of challenges. To determine which genes should be selected as RNAi targets, research groups utilize their own “target identification pipeline” to narrow down candidate genes to a manageable

number. Researchers can take advantage of RNA-seq data, GO-term enrichment, and essential gene data of their selected pathogen, but these resources have not been fully developed for all fungal pathogens or are not well annotated. Consequently, the list of candidate targets may still be extensive, creating a burden on researchers to screen them. Current analytical techniques *in planta* are often impractical for research groups, as they require plant material to be grown in growth chambers or greenhouses, taking valuable space, and in the case of spray applications, special barriers/ventilation equipment to prevent drift would be required. For *in vitro* analyses, molecular biological techniques such as quantitative PCR are effective in determining transcript knockdown, but when evaluating many different RNAi molecules, with multiple technical and biological replicates, the cost of reagents can quickly skyrocket. For these reasons, high-throughput and cost-effective methods to screen for RNAi targets are needed to enable research groups to identify the best molecules to develop as plant protection agents.

1.5 *Sclerotinia sclerotiorum* and its Role in Canadian Crop Production and RNAi Development

Among the plant pathogens of the Canadian Prairies, one of the most devastating on crop yields is *Sclerotinia sclerotiorum* (Lib.) de Bary. This pathogen has a broad host range, infecting over 400 species including agronomically important ones such as soybeans and peas (Boland and Hall, 1994). In Canada, *S. sclerotiorum* is of particular concern to *Brassica* crops, namely the edible oilseed crop canola (*Brassica napus*).

Canola's importance to the Canadian agriculture cannot be understated, having an overall national economic impact of almost $30 billion CAD annually with approximately 20 million tonnes of canola seed produced domestically every year (Canola Council of Canada, 2022). This seed is destined to become either canola oil, a healthy cooking oil with high levels of oleic acid

and a high smoke point, or as canola meal, a protein-rich product that is excellent for livestock production (Lin et al., 2013; Canola Council of Canada, 2022). While high-performance canola cultivars, agronomic practices, and integrated pest management strategies have increased canola yields across the Prairies, *Sclerotinia* is still a problem pathogen in these fields.

Sclerotinia stem rot (SSR) is present across Canada, with symptoms commonly observed in canola fields in Alberta, Saskatchewan, and Manitoba (Canadian Journal of Plant Pathology, 2020). The severity of symptoms depends on field and plant conditions, with the pathogen thriving in high humidity and high soil moisture conditions with a dense canola leaf canopy (Sharma et al., 2015). The average yield of canola decreases by approximately 0.5% for every 1% increase in *S. sclerotiorum* disease incidence in the field, as the fungus ultimately decreases the quality of the seed and its overall oil content (del Rio et al., 2007; Sharma et al., 2015). *Sclerotinia* spends most of its lifecycle overwintering in soil as hard and melanized resting structures known as sclerotia (Fig. 1.1). Germination of sclerotia is initiated by changes in soil temperature and moisture, producing apothecia fruiting bodies that rise from the soil. Ascospores are then ejected from the apothecium, landing on healthy host tissues. In the case of canola infection, ascospores adhere to senescing petals, which land onto the plant's leaves where watery lesions then develop. As a necrotroph, *Sclerotinia* produces oxalic acid to aid in plant cell death, by forming lesions that become necrotic. These lesions enable mycelial growth to spread quickly throughout the plant, invading the vascular system to fully infect the plant. Eventually, infection becomes systemic, with mycelial tissue completely overtaking the stem of plant; new sclerotia are produced inside the stem, which are returned to the soil via stubble degradation (Sharma et al., 2015; Bardin and Huang, 2000; Purdy, 1979).

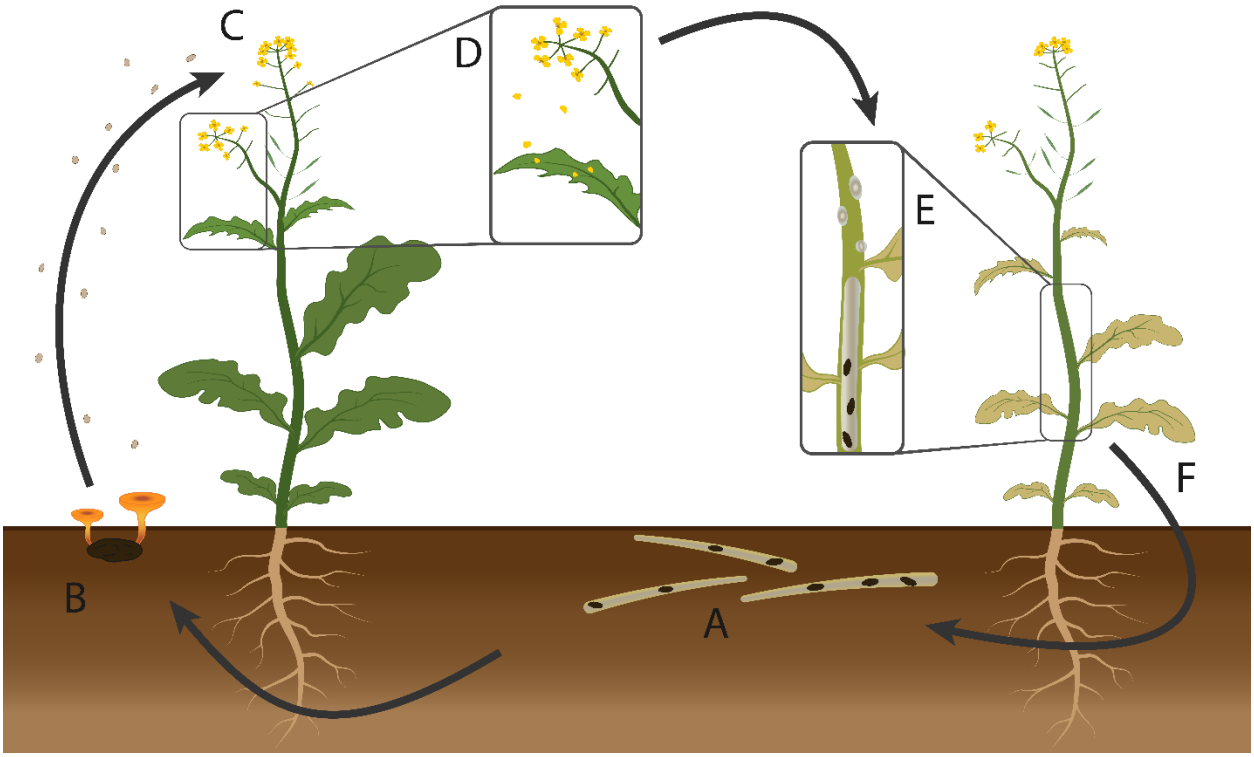

Figure 1.1. Disease cycle of *Sclerotinia sclerotiorum* on the host *Brassica napus*. (a) Sclerotia resting structures reside in soil overwinter within plant stubble. (b) Sclerotia germinate ascospore-producing apothecia. (c) Ascospores infect *B. napus* petals. (d) Infected petals land on leaves and stems, distributing infection throughout the plant. (e) Fungal lesions and mycelia progress through the stem, forming new sclerotia. (f) Diseased stubble containing sclerotia return to the soil.

Management of *S. sclerotiorum* in canola fields is challenging, owing to its highly aggressive rate of infection, broad host range, and its ability for long-term survival in soil as sclerotia (Bolton et al., 2006). Complete genetic resistance to *Sclerotinia* has yet to be seen in commercial cultivars, but quantitative gene resistance has the potential of lessening the impact of the disease, with other *Brassica* species (such *B. juncea*, *B. carinata*, and *B. nigra*) showing promise as sources of resistant germplasm (Taylor et al., 2015). Because of this, current control methods are based on integrated disease management practices including agronomic principles, cultural practices, and chemical applications. To limit the impact *Sclerotinia's* impact, producers can implement optimal row spacing to improve lodging resistance and canopy density, crop

rotation away from host species, and use of sclerotia-free seed (Kamal et al., 2016; Derbyshire and Denton-Giles, 2016). Soil inoculum can also be managed by using tillage to burrow sclerotia deep under the soil, alter the soil moisture content, and using soil amendments (Derbyshire and Denton-Giles, 2016). While this integrated approach to control is useful, chemical fungicides are by and large the most effective means of control. Chemicals with modes of action such as succinate dehydrogenase inhibitors, demethylation inhibitors, and quinone outside inhibitors are effective, but maximum effectiveness depends on the application window (early bloom for canola), weather conditions, and foliar coverage (Zamani-Noor and Molinero-Ruiz, 2021; Bradley et al., 2007; Kamal et al., 2016). As mentioned previously, fungicides have some significant drawbacks if used improperly or excessively, leaving the potential for *Sclerotinia* to become a major concern. Because of this, there is active research that looks to use RNAi as a potential alternative or to complement current controls regarding *Sclerotinia*.

Considerable progress has been made to develop RNAi as a viable control option in Canada, and as one of the primary pathogens of focus here and worldwide, *Sclerotinia* has been an ideal candidate for RNAi studies. Its ability to be grown quickly *in vitro* from both ascospores and sclerotia is an advantage over slower growing pathogens, and there are many protocols available depending on inoculum type and inoculation method that can produce reliable and replicable results (Yin et al., 2010; Pethybridge et al., 2015). Recently, both HIGS and SIGS studies have shown success in controlling *Sclerotinia*. Transgenic *Arabidopsis thaliana* lines producing dsRNAs targeting pathogen effector genes, appressorium formation, and oxalic acid production genes have resulted in decreased pathogenesis (Maximiano et al., 2022; Ding et al., 2021; Rana et al., 2022). Topical applications of dsRNA on canola, *Arabidopsis*, lettuce and collard greens targeting a variety of genes have also shown increased levels of protection

(McLoughlin et al., 2018; Qiao et al., 2021). While many gene targets have been successfully identified in both HIGS and SIGS systems, there is still uncertainty about which targets would be most effective as a treatment for field crop protection, what doses should be applied as a foliar application, and if other phytopathogens can be similarly controlled by targeting the ortholog genes in other fungal species. Research in RNAi within *Sclerotinia* pathosystems is showing great promise and has the capability to be utilized as a model organism to further develop these RNAi technologies and to answer key biological questions.

1.6 Downy Mildews and the Model Pathogen *Hyaloperonospora arabidopsidis'* Role in RNAi Development

Oomycete pathogens present many challenges to producers, and downy mildew diseases are major culprits of yield loss in field and greenhouse crops. Evolutionarily distinct from true fungi, oomycetes are more closely related to algae and other protists and differ from fungi by having a cellulose cell wall with a high glucan content instead of chitin, and they demonstrate non-septate growth (Thines, 2014; Bartnicki-Garcia, 1968). Plant pathogenic oomycetes and fungi evolved similar lifestyles and morphology through convergent evolution, filling the same ecological niches, filamentous growth, and similar modes of nutrition (Richards et al., 2006). The downy mildew clade is a major group within the oomycetes, with over 700 described species belonging to the Peronosporaceae downy mildew family. Each pathogen species is host species-specific, with many targeting agronomically important crops such as sunflower (*Plasmopara halstedii*), canola (*Peronospora parasitica*), and field peas (*Peronospora viciae*). Downy mildew can be the causal agent of significant crop loss, with severe situations resulting in up to 75% loss of yield in field peas (Chang et al., 2013) and near destruction of the French grape harvest in 1915 (Gessler et al., 2011). Downy mildew infection is suppressed using fungicides that target

functions such as mitochondrial respiration, RNA polymerase, sterol binding, and cellulose synthesis (Cohen et al., 2015). Chemicals with unique modes of action such as metalaxyl and dimethomorph perform well against oomycetes, but pathogen resistance risk is high, with many species developing resistant isolates worldwide (Gisi and Sierotzki, 2008). While cultural practices used to limit disease severity in fungi can also be applied to oomycetes, the inability to use fungicides to control downy mildew leaves crops susceptible if other control methods are not found.

Because of the number of unique downy mildew species, it is practical for researchers to focus on one species to act as a model pathogen for others. Due to its relation to the model plant *Arabidopsis thaliana*, *Hyaloperonospora arabidopsidis* is often used as the model for downy mildew pathosystems (Coates and Beynon, 2010). *Hyaloperonospora* has two infection cycles: primary infection from overwintering oospores, and secondary infection from conidia (Fig. 1.2). High humidity and cool temperatures between 16-18°C are ideal for infection and germination in a laboratory setting, but temperatures between 8-24°C can initiate disease in the field (Slusarenko and Schlaich, 2003). Thousands of conidiospores are dispersed from heavily colonized plants within 7-10 days in ideal conditions, quickly propagating across an entire plant population (McDowell, 2014). Infection progresses rapidly, with appressorium and germ tube formation within 6 hours of first contact. Hyaloperonospora has a latent phase of at least 4 days, where hyphae grow within intercellular spaces, until haustoria form for nutrient uptake (Slusarenko and Schlaich, 2003; McDowell, 2014). After one week of infection, thick-walled oospores are produced sexually in the leaves, eventually returning to the soil until favorable conditions initiate germination again (Coates and Beynon, 2010). A range of pathosystem interactions have been identified, characterized by infectivity on Arabidopsis leaves. In

compatible oomycete-plant reactions, the pathogen shows extensive growth and induces chlorosis in the host plant. To define the considerate number of *Hyaloperonospora* isolates, a nomenclature system has been developed, whereby the last two letters of the *Hyaloperonospora* isolate matches that of the *Arabidopsis* isolate, such as the *Hyaloperonospora* isolate Noco2 and its Arabidopsis isolate Col-0, or Emoy2 and Oy-0 (Holub et al., 1994). In incompatible reactions, the plant produces a hypersensitive response resulting in only small necrotic lesions, thereby resisting the oomycete.

Research with *Hyaloperonospora* is often limited to *in planta* studies due to its obligate biotrophic nature; the oomycete has proven highly difficult to culture *in vitro* or to produce viable transformants (McDowell, 2014). Isolated spores also cannot be stored, requiring fresh or frozen infected plant tissue as starting inoculum. Because of these restrictions, RNAi and ultimately SIGS studies have been limited to *in planta* studies, with one study by Bilir (2019) demonstrating that sRNAs targeting cellulose synthase genes could limit the infection on Arabidopsis leaves. This same study did, however, also describe an *in vitro* method of studying spore germination on cellophane, although growth of the oomycete could not persist on this artificial medium. Beyond *Hyaloperonospora*, RNAi was used successfully to reduce growth of the grape downy mildew *Plasmopara viticola* (Marciano et al., 2021; Haile et al., 2021), but future research on this pathogen may be limited by the slow generation time for grapevine plants. A testing system using fast growing *Arabidopsis* plants would help accelerate the development of RNA-based mildew control technologies.

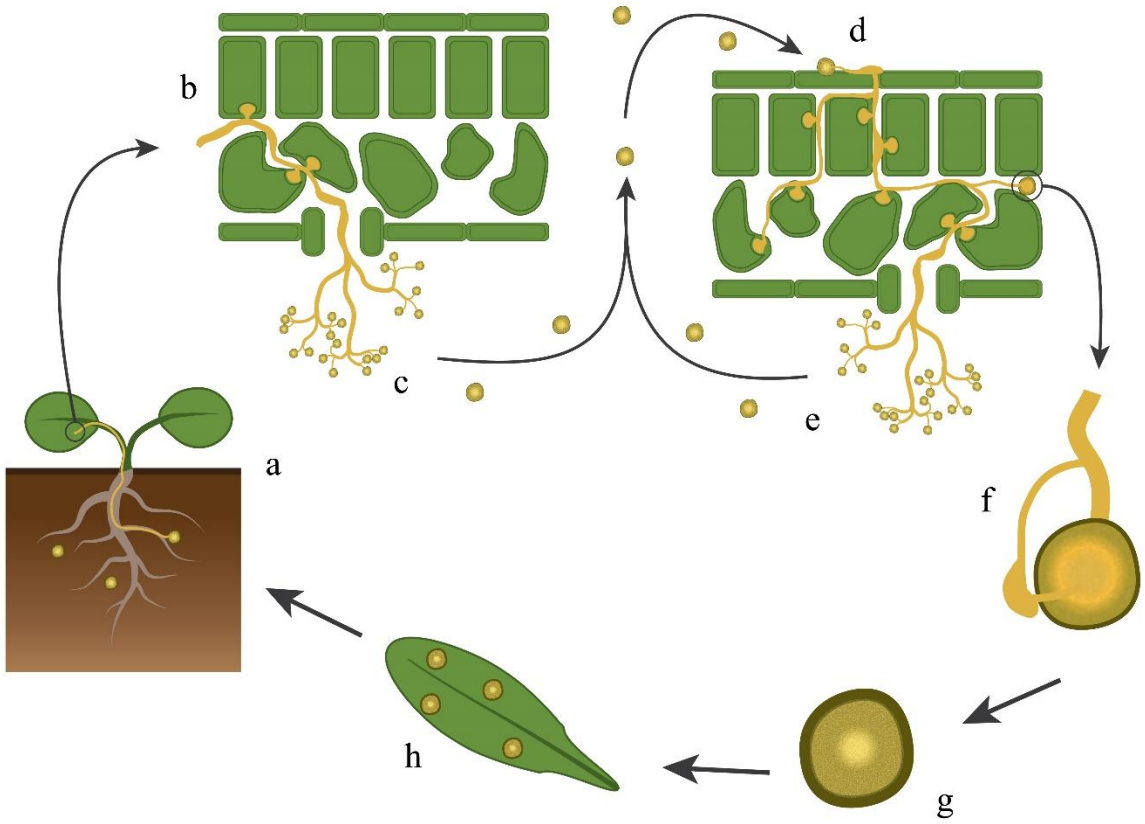

Figure 1.2. Disease cycle of *Hyaloperonospora arabidopsidis*. (a) Oospores germinate and infect from decomposed leaf tissue. (b) Leaves are colonized by hyphae within intercellular spaces, with haustoria feeding on nearby cells. (c) Conidiophores arise from stomata, producing conidiospores that release into the air. (d) Conidiospores land on nearby leaves, reintroducing infection. (e) Additional rounds of infection are produced from germinating conidia. (f) Oospheres contained within the female sexual organs (oogonia) are fertilized by male antheridia growing through its outer wall. (g) Fertilized oospheres form into mature oospores with a thick outer wall. (h) Leaves heavily infected with oospores reside in soil litter for future germination.

1.7 Research Objectives

Crop production worldwide is constantly being challenged by pathogens that lower yield, impact food quality, and limit a producer's ability to provide food for our growing population. While fungicides are one of our first choices to control these pathogens, our ability to use them to their fullest potential is being eroded by fungal resistance, government legislation, and a push

for more environmentally friendly alternatives. These challenges present an opportunity for RNAi to be developed into a tool for crop protection, using topically-applied dsRNA. As the field of RNAi-based protection technologies expands, there is a growing need for the understanding of how to apply our knowledge of RNAi across pathosystems, and to optimize assays for quick and efficient screening of RNAi products for their future use in field or greenhouse studies. The overall objective of my research is to compare the application of RNAi between the fungus *Sclerotinia sclerotiorum* and the oomycete *Hyaloperonospora*. By developing novel assays to evaluate both new and previously identified dsRNAs, I will demonstrate the similarities and differences between these pathogens and how these unique approaches can contribute towards the advancement of SIGS and crop protection.

1.7.1 Development of a Multiwell Plate Assay to Assess dsRNA Efficacy Against *Sclerotinia sclerotiorum in vitro*

Question: Can a high-throughput assay be developed to compare dsRNAs in vitro within S. sclerotiorum?

I hypothesize that I can identify significant differences between dsRNA treatments by developing an *in vitro* assay that can be scaled for selection of dsRNA targets in a cost effective and efficient manner. Using a programmable multi-well plate reader, I will demonstrate the difference in *S. sclerotiorum* growth inhibition across dsRNA treatments. Using this assay, I will evaluate different doses dsRNA and different dsRNA targets, to assess the utility of this novel assay as a method of identifying promising dsRNAs for future analysis.

1.7.2 Target Identification and Development of RNAi Technologies to Control *Hyaloperonospora arabidopsidis*

Question: How can RNAi targets be evaluated within H. arabidopsidis? Can an in vitro assay be used to identify successful RNAi targets? Are genes that encode fungicide targets good RNAi targets? Can a foliar application of dsRNA targeting H. arabidopsidis genes reduce gene expression?

I hypothesize that dsRNA targets that successfully inhibit growth of *H. arabidopsidis* can be identified via a target identification pipeline that combines publicly available genomic data, literature, and RNA-seq data. Using a novel cellophane-droplet assay, I will analyze germination rate and germination tube length of *H. arabidopsidis* when treated with synthesized dsRNAs within a high-resolution fluorescence microscope. Using successful dsRNA treatments, I will measure the ability of these dsRNAs to reduce transcript levels *in planta* by a foliar treatment on *Arabidopsis* seedlings. Finally, I will measure the approximate amount of dsRNA applied in this SIGS assay per unit area to accurately determine the required concentration when applying dsRNAs as a topical application.

1.7.3 Comparison of Oomycete and Fungal RNAi Responses

Question: Is RNAi equally effective in both S. sclerotiorum and H. arabidopsidis? Do differences in a key RNAi component, Dicer, agree with the evolutionary divergences between H. arabidopsidis and S. sclerotiorum?

I hypothesize that dsRNAs that specifically target either *S. sclerotiorum* or *H. arabidopsidis* impact growth differently, even at comparable doses. By comparing *in vitro* growth using similar droplet germination assays, I will investigate how both pathogens respond to varying dsRNAs doses to confirm RNAi efficacy varies between pathogens. To investigate if

Dicer protein structure is conserved across plant pathogens, a phylogenetic analysis of the two agronomically important pathogens will be performed.

CHAPTER 2: MATERIALS AND METHODS

2.1 Selection of RNAi Gene Targets and Criteria for dsRNA Construct Creation

Selection criteria of *Hyaloperonospora arabidopsidis* followed a unique target identification pipeline based on previous literature (Bilir et al., 2019) on *Hyaloperonospora arabidopsidis*, fungicidal modes of action (FRAC, 2021), and research using SIGS to control other plant pathogens (McLoughlin et al., 2018); See Fig. 2.1.). Putative functions were identified using GO-term data of *H. arabidopsidis* Emoy2 strain from UniProt (https://www.uniprot.org/) and supported with ortholog data from FungiDB (https://fungidb.org/fungidb/app). Genes were further selected based on size to create sufficiently long (300-350 bp) dsRNAs and without any 21-mer overlaps with species that would be considered important to ecosystems where *Hyaloperonospora* can be found (similar plant pathogen species were not considered).

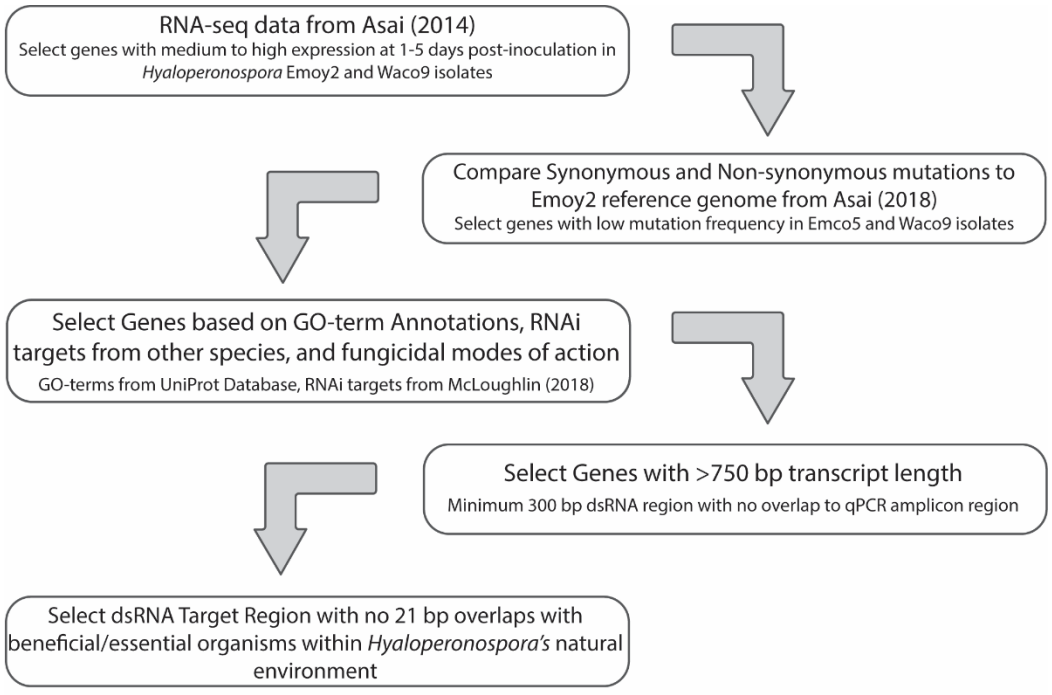

Fig. 2.1. Target Identification Pipeline for *H. arabidopsidis* dsRNA selection. RNA-seq data retrieved from Asai (2014) and mutation data from Asai (2018). GO-terms exported from UniProt database.

2.2 *In vitro* Production of dsRNAs

Hyaloperonospora arabidopsidis gene sequences were retrieved from FungiDB and primers were designed to amplify the gene fragments using NCBI Primer-BLAST (https://www.ncbi.nlm.nih.gov/tools/primer-blast/) and confirmed with Primer3 (https://bioinfo.ut.ee/primer3-0.4.0/). The primer sets were designed to amplify an approximately 300 bp exon region of the transcript with a primer melting temperature between 58 and 62° C. A BLAST query was performed on the primer sets to confirm no 21-bp overlap with genomes of non-related species and to confirm that there are no overlaps within the genome of *Hyaloperonospora*. Primers then had restriction sites *KpnI, XhoI, or XbaI* appended to the 5' end of each primer with a "GTATA" overhang. The complete primer list for cloning *Hyaloperonospora* gene fragments can be found in Table 2.1.

Table 2.1. Complete list of primers used to clone *H. arabidopsidis* gene fragments to synthesize dsRNAs.

Target	Primer Sequence (5' -> 3')	Product Size
HpaG803990 - F	GTATAGGTACCGGCGACGATCACCTACAAAC	302
HpaG803990 - R	GTATACTCGAGAACGGCGCCACTGATGTAG	
HpaG809065 - F	GTATAGGTACCAGGAAGCGAACGATGTGGTT	319
HpaG809065 - R	GTATACTCGAGCAAAGATCATGGGCGCCTTG	
HpaG813906 - F	GTATAGGTACCCCTGCAGCTCCTACTTCGTC	304
HpaG813906 - R	GTATACTCGAGACTCTCCGCCTTCTTCTCCT	
HpaG810051 - F	GTATAGGTACCGGCCTCAATCAGCTCTCGAT	322
HpaG810051 - R	GTATACTCGAGCGCTTGGCTCTTACTGTTCA	
HpaG806090–1 - F	GTATAGGTACCCATCGGTCTTCTGCAGGTGT	303
HpaG806090–1 - R	GTATACTCGAGTAATCACCACACCGCCGTAC	
HpaG806090–2 - F	GTATAGGTACCATCGGAAACTGCACGCTTTG	318
HpaG806090–2 - R	GTATACTCGAGGTACACGGGCGTCACTACTG	

HpaG812588 - F	GTATAGGTACCACTCGTCCTTCCGGCTCTAT	309
HpaG812588 - R	GTATACTCGAGAATGCTGTGCGTCTTTCCTG	
HpaG808599 - F	GTATATCTAGATGCGGACAATACGACCTGAA	307
HpaG808599 - R	GTATACTCGAGGTTGGTGATGAGGGTGTCGT	
HpaG800629 - F	GTATAGGTACCACTTTGAGACGGACCGCATC	323
HpaG800629 - R	GTATACTCGAGTCCCTCAAATGGCTCACGTC	
HpaG807348 - F	GTATAGGTACCGGGCATGGGTGGTATGTTCA	308
HpaG807348 - R	GTATACTCGAGCACCTTCCACTCCTGCGATT	

Using *Arabidopsis thaliana* tissues infected with *Hyaloperonospora arabidopsidis*, RNA was extracted using a RNeasy Plant Mini RNA Extraction Kit (Qiagen Sciences, Germantown MD, USA) following the manufacturer's protocol with the optional DNase I on-column treatment. RNA was eluted in 50 µL of nuclease-free water and checked for purity via spectrophotometric analysis (Synergy H1 Multimode Plate Reader, Biotek Instruments, Winooski, VT, USA). RNA was treated a second time to remove contaminating DNA using TURBO DNase (ThermoFisher Scientific, Waltham, MA, USA) following manufacturer's protocol and inactivated using EDTA. From the DNase treated RNA, cDNA was synthesized using qScript cDNA Supermix (QuantaBio, Beverly, MA, USA) following the manufacturer's protocol. Target gene sequences were amplified using a SimpliAmp PCR Thermal Cycler (Applied Biosystems, Waltham, MA, USA) and Econotaq PLUS Green 2X Master Mix (Lucigen, WI, USA) under the following conditions: 95 °C for 3 min; followed by 40 cycles of: 95 °C for 10 s, 60 °C for 15 s, and 72 °C for 15 s; and a final extension of 72 °C for 5 min. PCR products were visualized on a 1.5% agarose gel with ethidium bromide and excised from the gel. The PCR product was purified using the E.Z.N.A. Gel Extraction Kit (Omega Biotek, Norcross, GA, USA) and subsequently digested using FastDigest Green *KpnI, XhoI, or XbaI* enzymes (ThermoFisher Scientific, Waltham, MA, USA) following the manufacturer's protocol. At the same time an empty pL4440 plasmid vector was similarly digested using the above enzymes,

whereafter both the digested PCR products and digested plasmid was run on a 1.5% agarose gel stained with ethidium bromide. The corresponding DNA fragments were excised, purified using the E.Z.N.A Gel Extraction Kit, and ligated together using T4 DNA Ligase (ThermoFisher Scientific, Waltham, MA, USA). The constructed plasmids were transformed into Subcloning Efficiency DH5α Chemically Competent *Escherichia coli* cells (Invitrogen, Carlsbad, CA, US) following the manufacturer's protocols of the heat shock method. Cells were suspended in SOC broth (2% tryptone, 0.5% yeast extract, 10 mM NaCl, 2.5 mM KCl, 10 mM $MgCl_2$, 10 mM $MgSO_4$, and 20 mM glucose) and an aliquot was pipetted onto ampicillin-amended Lysogeny Broth (LB) agar plates (1% tryptone, 0.5% yeast extract, 0.5% NaCl, 1.8% agar, and 50 μg/mL ampicillin). Plates were incubated at 37° C upright for 30 minutes, then incubated upside-down overnight. For each RNAi target, up to 10 *E. coli* colonies were selected for a PCR colony screen, using target-specific primers and the same reaction conditions as above, but with an extended initial denaturation step of 95° C for 10 minutes. Successful transformations were confirmed on a 1.5% agarose gel stained with ethidium bromide. For each target gene fragment successfully cloned into *E. coli*, 1 colony was streaked onto a master LB-ampicillin plate, grown overnight, then used to inoculate 4 mL of LB broth amended with 50 μg/mL ampicillin which was placed on an orbital shaker at 225 rpm at 37° C overnight. Plasmids with the inserts were purified using the E.Z.N.A Plasmid DNA Mini Kit (Omega Biotek, Norcross, GA, USA) and eluted in molecular-grade water. Glycerol stocks of each target were also prepared using 500 μL of the broth culture and 500 μL of glycerol and stored at -80° C. The sequences of the gene fragment inserts were confirmed using Sanger sequencing (The Centre for Applied Genomics Sick Kids, Toronto, ON, Canada). Using pL4440 primers that amplify the plasmid region containing both the insert and the T7 promoter regions, a 100 uL Econotaq PCR reaction of each

target was prepared using the same thermocycling conditions as previously described. The PCR product was once again purified and eluted into molecular-grade water to be used as the template for dsRNA synthesis. DsRNA was synthesized using the MEGAScript RNAi kit (Invitrogen, Carlsbad, CA, US) according to the manufacturer's protocol with each reactant volume doubled until the wash steps to obtain a final yield of approximately 1,000 ng/μL. Size, concentration, and purity of dsRNA molecules were confirmed by agarose gel electrophoresis, spectrophotometry, and by using the Agilent 2100 BioAnalyzer with the DNA 1000 chip (and its corresponding manufacturer's protocol).

DsRNAs used for the *Sclerotinia*-based assays were taken from *E. coli* glycerol stocks previously prepared by Austein McLoughlin (Department of Biological Sciences, University of Manitoba). DsRNAs were synthesized exactly as described above beginning with the LB-broth culture step.

2.3 Arabidopsis thaliana Growth Conditions

For *Hyaloperonospora* spore propagation, *Arabidopsis* Col-0 seeds were lightly sprinkled on moistened Sunshine Mix #1 (SunGro Horticulture, Agawam, MA, USA) soil inside plastic trays (8 cm x 12 cm x 6 cm) and kept in a growth chamber with a 16-hour light and 8-hour dark photoperiod at 22° C. *Arabidopsis* lawns were periodically watered until inoculated with *Hyaloperonospora* spores.

For Spray-Induced Gene Silencing Assays, *Arabidopsis* seeds were sterilized through successive ethanol washes and plated onto Murashige and Skoog (MS) media (Caisson Labs, Smithfield, UT, USA) with 0.6% Phytagel (Sigma-Aldrich, St. Louis, MO, USA). *Arabidopsis* seeds were placed in a 4° C fridge in the dark for 4 days, before being transferred to a controlled

growth chamber where they were kept at a 16-hour light and 8-hour dark photoperiod at 24° C for 5 days. Empty Fisher-brand micropipette tip boxes were filled with moist Sunshine mix soil about 2/3rds full and autoclaved on a 20-minute liquid cycle with the tip box lids on. After the soil and boxes have sufficiently cooled off, *Arabidopsis* seedlings (still at the cotyledon stage) were aseptically transferred into the boxes with 5 seedlings across, and 3 down for a total of 15 seedlings per box. The tip boxes were sealed with 3M micropore tape (The 3M Company, St. Paul, MN, USA) then placed in a growth chamber with a 16-hour light and 8-hour dark photoperiod at 24° C for 11 days. After inoculation with *Hyaloperonospora*, the *Arabidopsis* plants were kept at 17° C for 7 days until collection.

2.4 *Sclerotinia sclerotiorum* and *Hyaloperonospora arabidopsidis* Growth Conditions

Sclerotinia sclerotiorum ascospores were generously donated by Agriculture and Agri-Food Canada (Morden Research and Development Centre, Morden, MB, Canada) and kept on aluminum foil discs inside a container in the dark with desiccant at 4° C.

Hyaloperonospora arabidopsidis Noco2 spores were generously provided by Dr. Keiko Yoshioka from the Department of Cell & Systems Biology, University of Toronto. Spores were received by infected *Arabidopsis* tissues. Infected leaves/seedlings displaying conidiophores/conidiospores were collected into a 15 mL Falcon tube containing 10 mL of tap water. Spores were dislodged by vortexing for 30 seconds, and aliquoted into a fine misting spray bottle. *Arabidopsis* lawns 12-15 days old occupying half a flat were sprayed with the spore solution until all leaves are noticeably wet. The flat was also watered to provide additional moisture. A clear plastic lid was misted with tap water and placed over the lawns in a plastic tray and sealed with packaging tape to retain moisture. After 7-8 days, infected tissues were collected in 1.5 mL microfuge tubes on ice and placed in a -20° C freezer overnight before storing at -80°

C for long-term storage. *Hyaloperonospora* infection was also maintained by inoculating from lawn-to-lawn, using the same procedure as described above.

2.5 *Sclerotinia sclerotiorum* In Vitro Multiwell Plate Assays

While working aseptically on the day of the assay, a small piece of foil containing *Sclerotinia* ascospores was cut and placed in 10 mL of ¼-strength potato dextrose broth (PDB) (BD Difco, ThermoFisher Scientific, Waltham, MA, USA). Using a fine horsehair brush, ascospores were brushed off the foil, and using a magnetic stir bead the spores were stirred at high speed for 30 minutes. Using a hemocytometer, an aliquot of the spore solution was adjusted to a concentration of 2.5×10^4 spores/mL.

A 10 mg/mL solution of Boscalid fungicide (Sigma-Aldrich, St. Louis, MO, USA) was prepared by dissolving powder in 100% methanol. DsRNAs were adjusted to a 100 ng/µL working stock concentration for all assays. In a 24-well Greiner CELLSTAR multiwell culture plate (Sigma-Aldrich, St. Louis, MO, USA), the following was added to each well: 1.5 mL of 1/8-strength PDB, 1.5 µL 50 mg/mL ampicillin, and 10 µL of the ascospore solution (approximately 250 spores/well). Either dsRNA or Boscalid was added to the corresponding wells with 4 biological replicates per treatment, and the plate was then placed into the Synergy H1 multimode plate reader.

At room temperature (22° C), the plate was scanned for absorbance at the 600 nm wavelength in a 9x9 grid centered in the middle of the well. Optical density at 600 nm (OD600) was measured every 6 hours, for 96 hours. Prior to each scan, the plate was shaken using the orbital shaker option for 5 minutes.

Mean OD600 values across all 81 scan points were calculated, and 0-hour scan point values were subtracted to account for any background absorbance in each well. The mean OD600 value and standard error across all 4 biological replicates was calculated in Microsoft Excel, then plotted using GraphPad Prism 9.0 software (GraphPad Software, San Diego, CA, USA). Statistical analysis of endpoint values was calculated using one-way ANOVA with Tukey's Multiple Comparisons Test ($p < 0.05$).

2.6 *Sclerotinia sclerotiorum* In Vitro Droplet Assays

Cellophane squares 1 cm x 1 cm were autoclaved in distilled water and placed onto Petri plates with Murashige and Skoog media with 1.5% agar as a gelling agent and a pH of 5.7 (+/- 0.05). As previously described, *Sclerotinia sclerotiorum* ascospores was prepared in ¼-strength PDB at a concentration of 2.5×10^4 spores/mL and supplemented with 100 µg/mL of ampicillin. In a Level 2 Biosafety Cabinet, 2 µL of the spore suspension was pipetted onto each cellophane square, and 2 µL of the corresponding dsRNA was added and then mixed by pipetting up and down. Each droplet represents 1 biological replicate with up to 4 biological replicates per cellophane square. For the fungicide positive control, 2 µL of a 20 ppm Boscalid fungicide (diluted from the 10 mg/mL stock using molecular-grade water) was added in the same manner. Plates were sealed with Parafilm and incubated within a 17° C growth chamber and wrapped in aluminum foil.

After a 48-hour incubation, cellophane squares containing the spore/dsRNA treatments were placed into 6-well Greiner multiwell plates, with one square per well. To each droplet, 1 µL of 0.2 µm filtered, 0.1% Calcofluor White stain (Sigma-Aldrich, St. Louis, MO, USA) was added and 1 µL of molecular-grade water. An 18 mm x 18 mm coverslip was gently placed over

the cellophane square and droplets, then imaged using the DAPI fluorescent filter set on the ImageXpress Micro 4 cellular imager (Molecular Devices, San Jose, CA, USA). High-resolution images were obtained by stitching together a grid of images taken using the 40X objective with autofocus at each individual image. Images were exported as .tiff images for further analysis.

High-resolution .tiff images of *Sclerotinia* growth were imported into ImageJ Fiji image analysis software (https://imagej.net/software/fiji/). Images were cropped to contain a single droplet and converted to an 8-bit file type. Colour threshold was then adjusted to only highlight fungal material with minimal background highlight that could be caused by detritus on the cellophane, and any highlighted background that is positively identified to not be fungal material is coloured to the same as the black background. Total pixels highlighted per droplet were measured and imported into GraphPad Prism for calculation of mean, and standard error. Statistical significances between treatments were calculated using one-way ANOVA test with Tukey's Multiple Comparisons Test ($p < 0.05$). Each treatment was compared with a minimum of 3 biological replicates and a maximum of 7 biological replicates.

2.7 *Hyaloperonospora arabidopsidis* In Vitro Droplet Assays

MS media with cellophane squares was prepared as previously described. Infected *Arabidopsis* tissues containing *Hyaloperonospora* Noco2 spores previously frozen at -80° C were thawed for 2 hours on ice, and approximately 1 mL of sterile distilled water was added to each tube. Tubes were vortexed for 30 seconds on high and filtered through a coarse insect mesh netting to remove plant and soil debris. Aliquots of the spore solution were centrifuged at 10,000 x g for 30 seconds, and the supernatant was drawn off. Another 1 mL of sterile distilled was added and vortexed again, then spun with the same conditions to rinse the spores. The supernatant was drawn off once more, then suspended in sterile distilled water and adjusted to a

final concentration of 5 x 10^4 spores/mL. In a sterile Biosafety cabinet, 2 µL of a vortexed spore solution was pipetted onto the cellophane squares, with 2 µL of the corresponding dsRNA treatment added and mixed by pipetting up and down. For the fungicide positive control, 2 µL of a 0.2 mg/mL Metalaxyl was added. Plates were sealed with Parafilm and incubated for 48 hours at 17° C in a growth chamber with a 16-hour light and 8-hour dark photoperiod.

After a 48-hour incubation, cellophane squares containing the spore/dsRNA treatments were placed into 6-well Greiner multiwell plates, with one square per well. To each droplet, 1 µL of 0.2 µm filtered, 0.1% Calcofluor White stain (Sigma-Aldrich, St. Louis, MO, USA) was added. Droplets were then imaged using the DAPI fluorescent filter set on the ImageXpress Micro 4 cellular imager (Molecular Devices, San Jose, CA, USA). High-resolution images were obtained by stitching together a grid of images taken using the 40X objective with autofocus at each individual image. Images were exported as .tiff images for further analysis.

High-resolution images of germinating *Hyaloperonospora* spores were imported into ImageJ Fiji image analysis software (https://imagej.net/software/fiji/). Using the line drawing tool, germinating and non-germinating spores were traced from the center of the spore to the tip of the germination tube. In the case of a non-germinating spore, the line is kept as a very short line segment with 10 pixels in length as the cut-off between germinated/non-germinated. Germinated percentages for each biological replicate were calculated, and mean germination percentages per treatment was plotted using GraphPad Prism. Statistical analysis was carried out by One-way ANOVA and Tukey's Multiple Comparisons Test ($p < 0.05$). Frequency distribution of germination tube lengths were plotted using GraphPad Prism with 20-pixel bin ranges and values below 10 pixels omitted. Statistical analysis of mean germination tube length

of 100 ng/µL treatments compared to the GUS negative control was carried out by Student's t-test with Welch's correction ($p < 0.05$).

2.8 Foliar Application of dsRNAs to *Arabidopsis* Seedlings Infected with *Hyaloperonospora*

As previously described, 16-day old *Arabidopsis* seedlings were grown in micropipette tip boxes in a 5x3 seedling arrangement. In a biosafety cabinet, 2.75 mL of a 10 ng/µL solution was prepared in a small fine-misting spray bottle. Each tip box will receive 6 pumps of the corresponding treatment equating to approximately 1.25 mL of the dsRNA treatment, with two tip boxes per treatment. Tip boxes were left opened to dry for 30 minutes to dry the treatment. *Hyaloperonospora* spores on *Arabidopsis* tissues frozen at -80° C were thawed on ice for 2 hours and then placed into a 15 mL Falcon tube. Sterile tap water was added and vortexed to dislodge spores, and to let the dirt/detritus settle to the bottom of the tube with the spores still in suspension. The spore suspension was drawn off and pipetted into a small fine-misting spray bottle and the concentration adjusted to 5×10^4 spores/mL. Each tip box received 8 pumps of the spore solution to sufficiently wet the seedlings, and 5-6 pumps of sterile tap water was sprayed on the inside of the tip box lid to maintain humidity. Tip boxes were sealed with micropore tape and incubated in a 17° C growth chamber with a 16-hour light and 8-hour dark photoperiod.

2.9 Tissue Collection, RNA Extraction, cDNA synthesis, and Relative Transcript Abundance Following Foliar dsRNA Application

After 7 days of incubation with the *Hyaloperonospora* spores and the treatments, seedlings were septically transferred into Eppendorf 1.5 mL Safe-Lock tubes (ThermoFisher Scientific, Waltham, MA, USA) and frozen immediately by dipping in liquid nitrogen. Seedlings were collected without root tissue to minimize soil transfer, and each biological replicate consisted of 5 seedlings in each tip box, for a total of 6 biological replicates.

Tissues were ground using 1.4 mm metal beads in a Bullet Blender at max settings (Next Advanced, Troy, NY, USA) with 450 µL of Buffer RLT containing 1% β-mercaptoethanol from the Qiagen RNeasy Plant Mini RNA Extraction kit. RNA extraction continued following the manufacturer's protocol including the DNaseI on-column treatment and eluted in 50 µL of RNase-free water. Quality and quantity of RNA was assessed by spectrophotometry and was subsequently synthesized into complementary DNA using the qScript cDNA Supermix as previously described.

Quantitative reverse-transcriptase PCR (qRT-PCR) was used to quantify relative transcript abundance using the SsoFast EvaGreen Supermix (Bio-Rad Laboratories, Hercules, CA, USA) and Bio-Rad CFX96 Connect Real Time System (Bio-Rad Laboratories, Hercules, CA, USA). Reaction volumes were 15 µL and were prepared according to the manufacturer's protocol. Primers and their primer efficiencies were previously calculated and are listed in Table _. Thermocycler conditions are as followed: 95° C for 3 min, and 40 cycles of 95° C for 5 seconds, 60° C for 5 seconds, and 72° C for 5 seconds. Melt curve analysis started at 60° C and reached a final temperature of 95° C in 0.5° C increments to confirm absence of primer dimers or contamination. Relative transcript abundance was calculated using the $2^{-\Delta\Delta CT}$ method with transcript abundance compared to the GUS non-target dsRNA negative control and normalized using the *Hyaloperonospora* Actin housekeeping gene. All reactions were repeated in duplicate (technical replicates) and 6 biological replicates were analyzed for each gene target. A one-way Student's t-test was performed determine significant changes in expression between the negative control and the dsRNA treatment ($p < 0.05$).

Table 2.2. *H. arabidopsidis* primer sequences and primer efficiencies for qRT-PCR.

Target	Primer Sequence (5' -> 3')	Primer efficiency (%)
HpaG807716 (Actin) – F	GTTTACTACCACGGCCGAGC	99.34
HpaG807716 (Actin) - R	CGTACGGAAACGTTCATTGC	
HpaG809065 - F	GGTTCCCCACGCTCAAGTTT	106.98
HpaG809065 - R	TCAATCTCGGCAGCTGTACG	
HpaG807348 - F	CAGAATGACGCATTGGAGCG	91.25
HpaG807348 - R	ATGGCTTCAGCTGTCCAACA	

2.10 Quantification of dsRNA Spray Application

Using UltraPure Salmon Sperm DNA (ThermoFisher Scientific, Waltham, MA, USA) as an proxy to dsRNA with a fragment size less than or equal to 2000 bp, a standard curve measuring fluorescence using Quant-iT PicoGreen (ThermoFisher Scientific, Waltham, MA, USA) was prepared. Six dilutions of DNA, from 100 ng/µL to 0.01 ng/µL, was prepared with TE buffer, salmon sperm DNA, and PicoGreen reagent (mixed according to the manufacturer's protocols) with a total reaction volume of 200 µL. Solutions were aliquoted into a 96-well round-bottom multiwell plate with 3 replicates per dilution. Fluorescence was measured in each well using the Synergy BioTek Multimode Plate Reader at 480 nm excitation wavelength and 520 nm emission wavelength. Using the averages between replicates, a formula was calculated from the standard curve to correlate fluorescence with concentration of DNA.

In a fine-misting spray bottle of the same type used for the SIGS foliar applications, approximately 3.5 mL of a 10 ng/µL solution of salmon sperm DNA was prepared in molecular-grade water. On a new 96-well round-bottom plate, the spray was applied in the same manner as applied over the *Arabidopsis* seedlings in the tip boxes, with 6 pumps of the spray bottle

equating to approximately 1.25 mL across the plate. Using a Kimwipe, the surface of the plate was gently dabbed to absorb any liquid that did not reach the inside of the wells. The plate was then spun down in a plate spinner to collect the liquid in the bottom of the well. Across the plate, 32 wells will be selected (See Fig. _). In each of the wells selected, 100 µL of TE buffer and 100 µL of diluted PicoGreen reagent was added and mixed. In a separate clean 96-well plate, 3 wells had only TE buffer and PicoGreen added to serve as blanks. In the same manner described previously, the plates were scanned for fluorescence and concentration of DNA was calculated using the standard curve. Using digital calipers, the surface area of each well was calculated, and the total DNA applied per unit area was determined.

Using the formula generated from the standard curve, the concentration of each well was calculated. Based on a total volume of 200 µL and the area of the wells, the amount of DNA per cm^2 was determined. Additionally, a violin plot was created to analyze the distribution of DNA across all 32 wells and to compare against each plate.

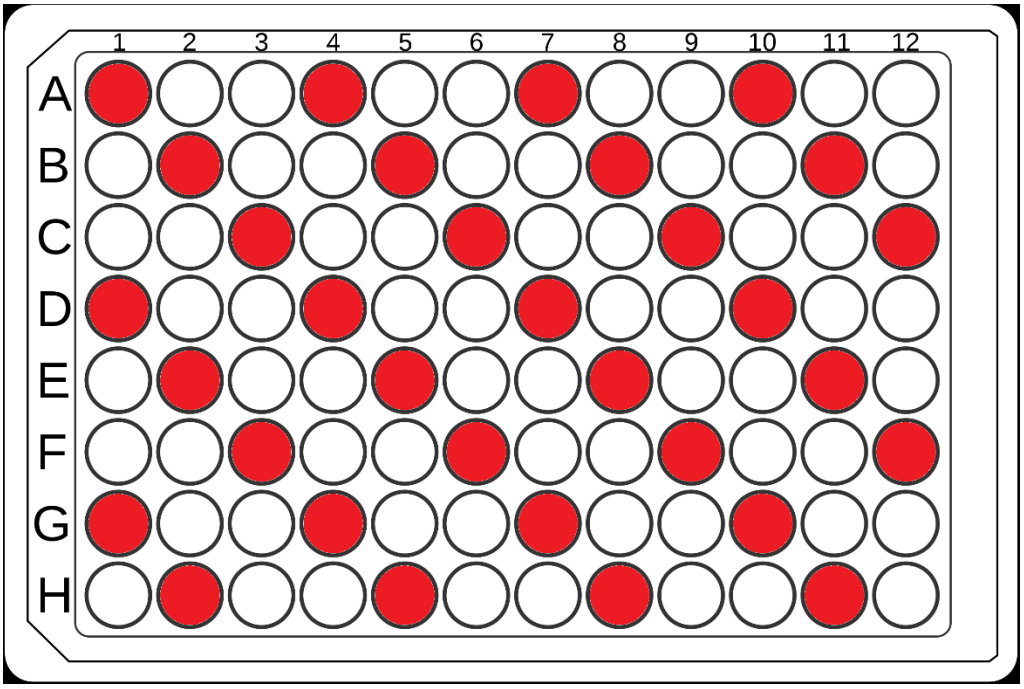

Fig 2.2. Well selection for DNA quantification. Highlighted wells indicate wells scanned with PicoGreen reagent and buffer.

2.11 Phylogenetic Analysis of DICER Genes Across Plant Pathogens

Phylogenetic analysis of DICER genes across agronomically important plant pathogens was carried out by creating a selection of pathogens across both oomycete and fungal clades. For reference, species were selected outside of these groups which are considered model species for similar analyses.

Amino acid sequences for all DICER genes within each species was acquired from published literature, FungiDB-annotated orthologs, and BLASTp of closely related species with annotated DICER genes. Using the Batch Web Conserved Domain-Search Tool (https://www.ncbi.nlm.nih.gov/Structure/bwrpsb/bwrpsb.cgi), domains of each amino acid sequence were identified across the CDD database, a superset of domains from NCBI-curated domains, Pfam, SMART, COG, PRK, and TIGFRAM databases. From the domain hit data, the longest RNase domains from all databases were selected for phylogenetic analysis.

Full-length amino acid sequences were imported into Geneious Prime (https://www.geneious.com/download/) and modified to contain only the RNase III domain sequences. Full-length and RNase III sequences were imported into the MEGA Phylogenetic Analysis Program (https://www.megasoftware.net/) and aligned separately using the MUSCLE algorithm with default parameters. Phylogenetic trees were constructed using the Maximum Likelihood method using default parameters. The phylogeny test was performed using the bootstrap method with 500 bootstraps. Constructed trees were displayed with bootstrap values above 70. Aligned RNase III domain amino acid residues imported into Jalview (https://www.jalview.org/) to visualize consensus regions. Aligned residues with BLOSUM62

scores of 100 or greater kept in visualization, with residues coloured according to Clustalx colour scheme.

CHAPTER 3: RESULTS

3.1 Selection of *Hyaloperonospora arabidopsidis* and *Sclerotinia sclerotiorum* Gene Targets

Nine *Hyaloperonospora* genes were selected to design ten dsRNAs to examine inhibition of growth *in vitro*. Following the target identification pipeline developed to narrow potential gene candidates, genes were selected to cover a diverse range of biological processes, including ones that are also targeted by oomycete-directed pesticides (Table 3.1 and Table 3.2). HpaG810051 (cellulose synthase), HpaG800629 (ubiquinol cytochrome c reductase), and HpaG807348 (oxysterol binding protein) were selected based on oomycete fungicides targeting similar modes of action in related species (Blum et al, 2012; Mitani et al, 2001; Pasteris et al, 2016). HpaG803990 (pectinesterase), HpaG809065 (protein disulfide isomerase), HpaG813906 (histone exchange protein), HpaG806090 (glucan synthase), HpaG812588 (RNA polymerase III Transcription Factor), and HpaG808599 (polysaccharide cellulase) were selected given that they had previously been proven effective in suppressing Sclerotinia growth by McLoughlin *et al.* (2018). Ten dsRNAs were synthesized from the 9 gene targets, with two unique dsRNAs designed to target different regions of the HpaG806090 transcript. For comparison, three dsRNAs were also designed to target *S. sclerotiorum* that were previously identified by McLoughlin (2018) to show significant effects on transcript accumulation *in vitro* and *in planta* and lesion size *in planta* (Table 3.3).

While some of the genes selected possessed both synonymous and non-synonymous mutations between the Waco9 and Emco5 isolates when compared to the reference isolate Emoy2, none of these mutations occurred within the dsRNA target region. Sanger sequencing

also confirmed a similar number of mutations within the Noco2 isolate (Supplementary Table 3.1), with 0-2 mutations within the dsRNA target regions compared to Emoy2, which suggests these dsRNAs could similarly be tested on this *H. arabidopsidis* isolate too. Expression levels of the nine target genes varied between Emoy2 and Waco9 isolates, but were typically within a 2-fold change of one another (Table 3.1)

Table 3.1. Summary table of genes selected for RNAi. [a] Putative function inferred by orthologs of related species. [b] Gene accessions retrieved by FungiDB. [c] Synonymous and non-synonymous polymorphisms to Emoy2 reference isolate. [d] Expression levels represented as TPM (Tags per million) of total reads aligned to *Hpa* Emoy2 genome. [e]Conidiospores.

			Emco5 Polymorphisms[c]		Waco9 Polymorphisms[c]		Expression Levels of Emoy2 Isolate[d]		Expression Levels of Waco9 Isolate[d]			
Putative Function[a]	**Gene Accession[b]**	**Transcript Length (bp)**	**Syn**	**Non-syn**	**Syn**	**Non-syn**	**Cs[e]**	**1 dpi**	**Cs[e]**	**1 dpi**	**3 dpi**	**5 dpi**
Pectinesterase	HpaG803990	918	0	0	0	0	1.6	0	4.1	139.7	287.5	24.8
Protein Disulfide Isomerase	HpaG809065	1575	0	0	0	0	757.6	753.1	660.6	938	1254.6	850.9
Histone Exchange Protein	HpaG813906	969	1	0	1	0	9.6	58.3	21.9	93.1	290	162.1
Cellulose Synthase	HpaG810051	3435	1	1	0	1	3830.9	1266.3	1659.5	804.6	559.1	589.1
Glucan Synthase	HpaG806090	7932	1	1	6	3	11.3	110.5	14.8	299.2	170	122.9
RNA Polymerase III Transcription Factor	HpaG812588	1845	1	1	0	2	61.2	102.5	108.5	92.9	65.4	43.2
Polysaccharide Cellulase	HpaG808599	756	3	3	0	2	6.7	235.3	1.4	505.1	982.6	1350.9
Ubiquinol to Cytochrome C Reductase	HpaG800629	825	3	0	1	0	413.8	226.9	375.4	0	586.2	331.1
Oxysterol Binding Protein	HpaG807348	2922	0	0	1	1	106.2	58.8	123.3	0	85.1	42.1

Table 3.2. Summary of GO terms for selected *H. arabidopsidis* genes.

		Gene Ontology (GO) Terms		
Putative Function	**Gene Accession**	**Biological Process**	**Cellular Component**	**Molecular Function**
Pectinesterase	HpaG803990	cell wall modification [GO:0042545]; pectin catabolic process [GO:0045490]		aspartyl esterase activity [GO:0045330]; pectinesterase activity [GO:0030599]
Protein Disulfide Isomerase	HpaG809065	cell redox homeostasis [GO:0045454]	cell [GO:0005623]	protein disulfide isomerase activity [GO:0003756]
Histone Exchange Protein	HpaG813906	histone exchange [GO:0043486]; regulation of transcription, DNA-templated [GO:0006355]	nucleus [GO:0005634]	
Cellulose Synthase	HpaG810051	cellulose biosynthetic process [GO:0030244]	integral component of membrane [GO:0016021]	cellulose synthase (UDP-forming) activity [GO:0016760]
Glucan Synthase	HpaG806090	(1->3)-beta-D-glucan biosynthetic process [GO:0006075]; (1->6)-beta-D-glucan biosynthetic process [GO:0006078]	1,3-beta-D-glucan synthase complex [GO:0000148]; integral component of membrane [GO:0016021]	1,3-beta-D-glucan synthase activity [GO:0003843]; hydrolase activity, hydrolyzing O-glycosyl compounds [GO:0004553]
RNA Polymerase III Transcription Factor	HpaG812588	regulation of transcription, DNA-templated [GO:0006355]; transcription preinitiation complex assembly [GO:0070897]	transcription factor TFIIIB complex [GO:0000126]	metal ion binding [GO:0046872]; RNA polymerase III general transcription initiation factor activity [GO:0000995]; TBP-class protein binding [GO:0017025]
Polysaccharide Cellulase	HpaG808599	polysaccharide catabolic process [GO:0000272]		cellulase activity [GO:0008810]
Ubiquinol to Cytochrome C Reductase	HpaG800629		mitochondrial inner membrane [GO:0005743]; respirasome [GO:0070469]	2 iron, 2 sulfur cluster binding [GO:0051537]; ubiquinol-cytochrome-c reductase activity [GO:0008121]
Oxysterol Binding Protein	HpaG807348			lipid binding [GO:0008289]

Table 3.3. Summary of *S. sclerotiorum* target genes. Fragments per kilobase million (FPKM) values are from fungal growth collected 24 hours post-inoculation *in planta* and 3 days post-inoculation *in vitro*.

				Gene Ontology (GO) Terms		
Putative Function	**Gene Accession**	**FPKM *in vitro***	**FPKM Westar**	**Biological Process**	**Cellular Component**	**Molecular Function**
Mitochondrial Import Inner Membrane Translocase (TIM44)	SS1G_06487	87.3	82	protein import into mitochondrial matrix [GO:0030150]; protein transport [GO:0015031]; intracellular protein transport [GO:0006886]	membrane [GO:0016020]; mitochondrion [GO:0005739]; mitochondrial inner membrane [GO:0005743]	chaperone binding [GO:0051087]
Aflatoxin Biosynthesis	SS1G_01703	45.1	307			hydrolase activity [GO:0016787]
Thioredoxin Reductase	SS1G_05899	268.7	259.1	removal of superoxide radicals [GO:0019430]	cytoplasm [GO:0005737]	oxidoreductase activity [GO:0016491]; thioredoxin-disulfide reductase activity [GO:0004791]

3.2 DsRNA Reduces Growth of *H. arabidopsidis in vitro*

To investigate which dsRNA targets are effective at inhibiting growth of *H. arabidopsidis*, a spore germination test in droplets on MS media overlaid with cellophane squares was carried out. Each 4 µL droplet on the cellophane contained 400 ng or 80 ng of dsRNA and 200 *H. arabidopsidis* spores. For the positive control, 400 ng of Metalaxyl fungicide, which targets RNA polymerase I enzyme (FRAC, 2021), was used, and 400 ng of dsRNA targeting the GUS gene, not present in *H. arabidopsidis*, was used as a negative control. Previous germination tests and research by Bilir (2019) showed germination on cellophane pieces overlaid on MS media is possible, but germination rates vary across initial inoculum stocks. It was also found that obtaining a consistent concentration across such small volumes is challenging, requiring continuous suspension of spores in solution.

Using the tracing and line segment measuring tools in the ImageJ Fiji Software package, germination percentages were calculated across the ten treatments at two doses, and the controls (Fig 3.1). In the 100 ng/µL dsRNA treatments, seven of the ten targets showed significant reductions in germination percentages compared to the GUS negative control, with three showing greater rates of inhibition than the Metalaxyl fungicide positive control (one-way ANOVA). While the maximum germination rate observed in the negative control did not exceed 50% and can be likely attributed to non-viable spores, there is a clear difference between the control and treatments, and that different dsRNA targets result in varying degrees of inhibition. Of the top three dsRNAs at 100 ng/µL, two targeted known fungicidal molecular targets (Oxysterol binding protein and Ubiquinol cytochrome C reductase) and the other dsRNA targeted protein disulfide isomerase, which impacts a similar pathway to a successful dsRNA target targeting thioredoxin reductase identified by McLoughlin (2018) in *S. sclerotiorum*. In Figure 3.1a, the GUS negative control showed germinated tubes that contained multiple appressorium-like features, whereas the more potent dsRNA treatments, with low germination rates, had no obvious appressorium features. The 20 ng/µL treatments did not show any significant differences in germination across treatments, yet the Metalaxyl positive control still provided effective germination inhibition. In this separate assay, the germination rate of the dsRNA treatments was consistently higher than that of the higher dsRNA concentration assay. Even the most effective dsRNAs, seen in the 100 ng/µL treatments, failed to show any degree of inhibition at the 20 ng/µL dose.

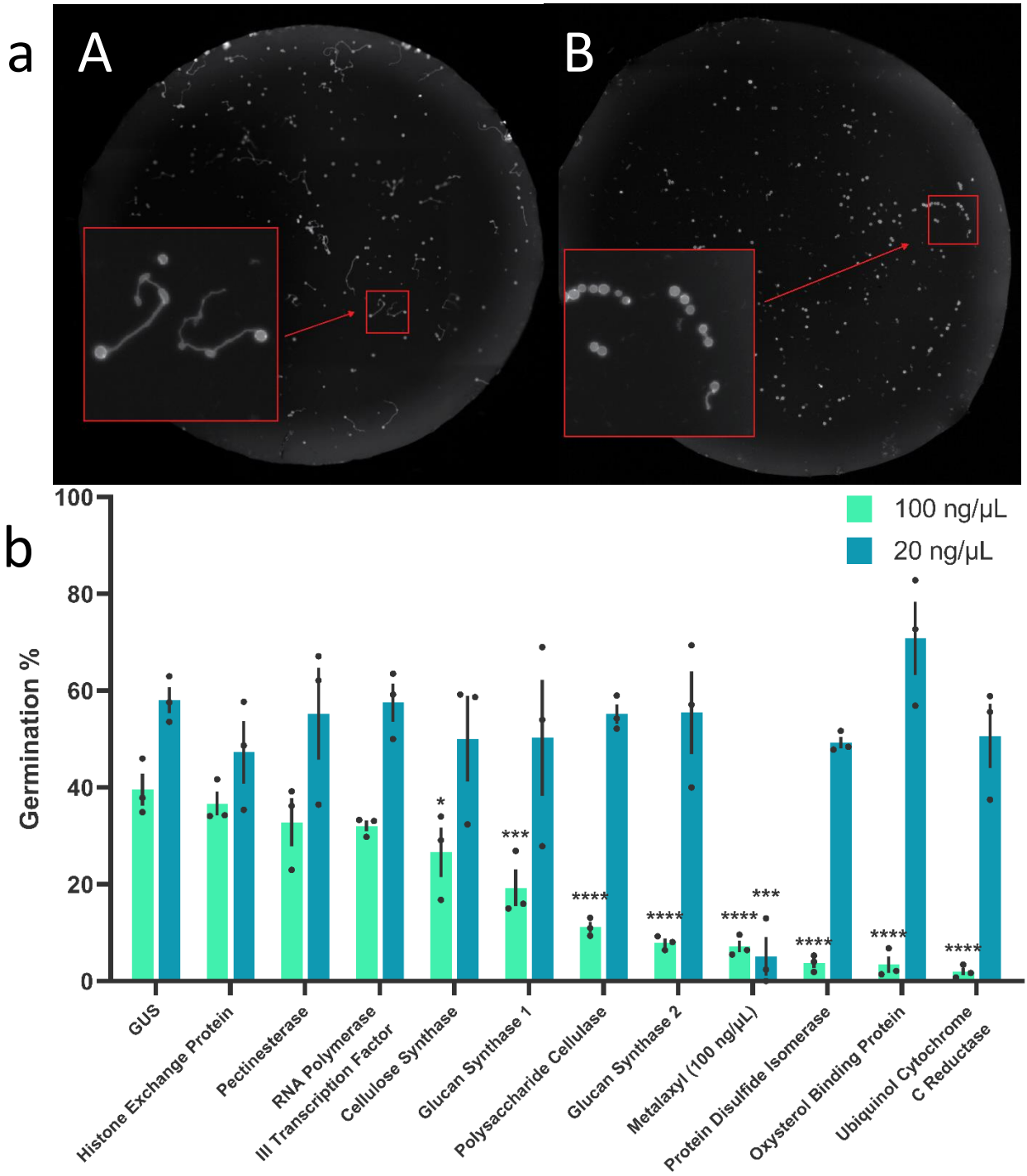

Figure 3.1. Germination of *H. arabidopsidis* spores are inhibited at high dsRNA doses. (**a**) 100 ng/µL doses of GUS dsRNA (A) and Protein Disulfide Isomerase-targeting dsRNA (B). Droplets imaged with 0.1% Calcofluor White stain and DAPI filter set. (b) Average germination percentage (n = 3 droplets) with standard error bars. Significant difference (One-way ANOVA; $p < 0.05$) from the respective GUS negative control treatment is denoted by asterisks (* = $P < 0.05$, ** = $P < 0.01$, *** = $P < 0.001$, **** = $P < 0.0001$).

To further investigate how the dsRNA treatments at both doses impacts the growth of *H. arabidopsidis'* germination tubes, a frequency distribution of germination tube lengths across all biological replicates was assessed (Fig. 3.2 and Supplementary Figure 3.1). At the 100 ng/µL dose, all dsRNA treatments showed a significant reduction in the mean length of the germination tubes compared to the GUS negative control (Student's t-test with Welch's correction). A shortening of germination tubes was also observed in treatments that did not show a significant difference in germination percentage compared to the control, including treatments targeting histone exchange protein (HpaG813906), pectinesterase (HpaG803990), and RNA polymerase III transcription factor (HpaG812588). Treatments that showed lower germination percentages compared to Metalaxyl showed similar distributions to that of the positive control, with no germination tubes exceeding 100 pixels in length. For the lower 20 ng/µL dose, the differences in distribution between the GUS negative control and dsRNA treatments were minimal, with most treatments showing a distribution of germination tube lengths similar to that of the negative control. Between doses, the germination tube lengths were longer for the 20 ng/µL concentration across all dsRNA treatments.

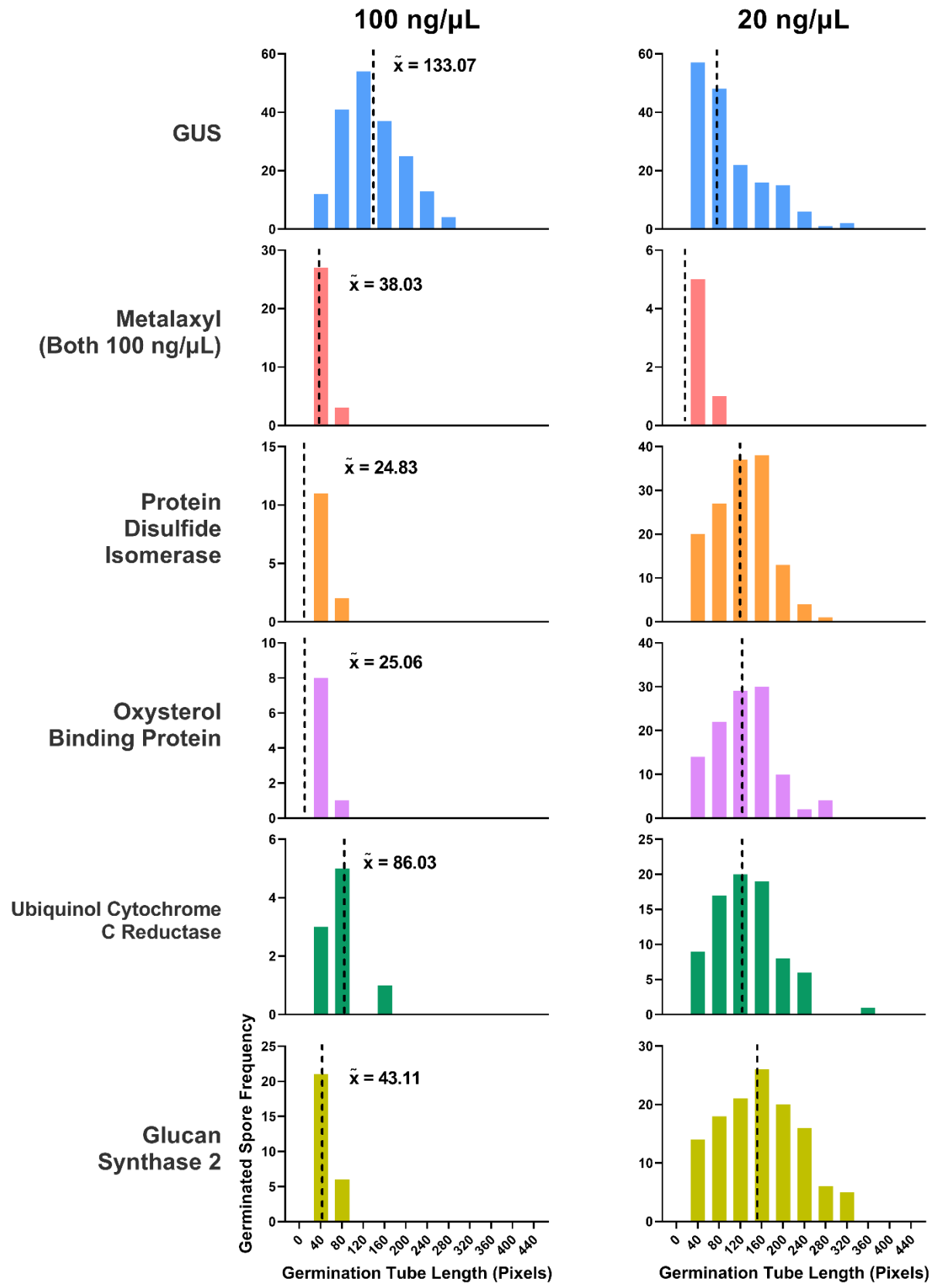
100 ng/µL
20 ng/µL
GUS
Metalaxyl
(Both 100 ng/µL)
Protein
Disulfide
Isomerase
Oxysterol
Binding Protein
Ubiquinol Cytochrome
C Reductase
Glucan
Synthase 2
x̃ = 133.07
x̃ = 38.03
x̃ = 24.83
x̃ = 25.06
x̃ = 86.03
x̃ = 43.11
Germinated Spore Frequency
Germination Tube Length (Pixels)
Germination Tube Length (Pixels)

Figure 3.2. Frequency distribution of *H. arabidopsidis* germination tubes. Total number of germinated tubes across 3 biological replicates for each treatment distributed across 40-pixel length bin ranges. Dotted line indicates median value. Metalaxyl positive control concentration of 100 ng/µL for both dsRNA dose tests. All mean germination lengths of 100 ng/µL treatments compared to the respective GUS negative control were significant (Student's t-test with Welch's correction, $p < 0.05$).

3.3 Foliar Application of dsRNAs Reduces Transcript Abundance

While dsRNAs at a high dose can prevent and slow the germination of *H. arabidopsidis in vitro*, it is important to investigate if and to what degree the impact a foliar dsRNA application has on *Arabidopsis thaliana* seedlings when they are at susceptible growth stages. Using two of the top performing dsRNA targets from the *in vitro* assay, a 10 ng/µL foliar spray of dsRNA was applied to a 5 by 3 grid of 16-day old *Arabidopsis* seedlings contained within a micropipette tip box. After 7 days of incubation following dsRNA treatment and inoculation with *Hyaloperonospora* spores, symptoms were assessed, and plant tissues collected. At 7 days post-inoculation, it was noted that the degree of infection was consistent across treatments, with no differences in the level of infection between the GUS negative control and the dsRNA treatments targeting either the oxysterol binding protein (HpaG807348) or protein disulfide isomerase (HpaG809065). Symptoms included slight chlorosis of leaves, and presence of conidiophore reproductive structures already producing conidiospores.

In contrast, differences were observed in the relative transcript abundance of both dsRNA treatments. There was a significant reduction in transcript accumulation in both dsRNA treatments when compared to the GUS negative control, with a 30.7% reduction in the Protein Disulfide Isomerase-targeting treatment (HpaG809065) and a 25.4% reduction in the Oxysterol Binding Protein-targeting treatment (HpaG807348) (Fig. 3.3). Transcript accumulation nevertheless varied across biological replicates, as it proved difficult to ensure identical growth

conditions (light exposure and soil moisture), and spore infection rates and dsRNA exposures to all leaves of the plants.

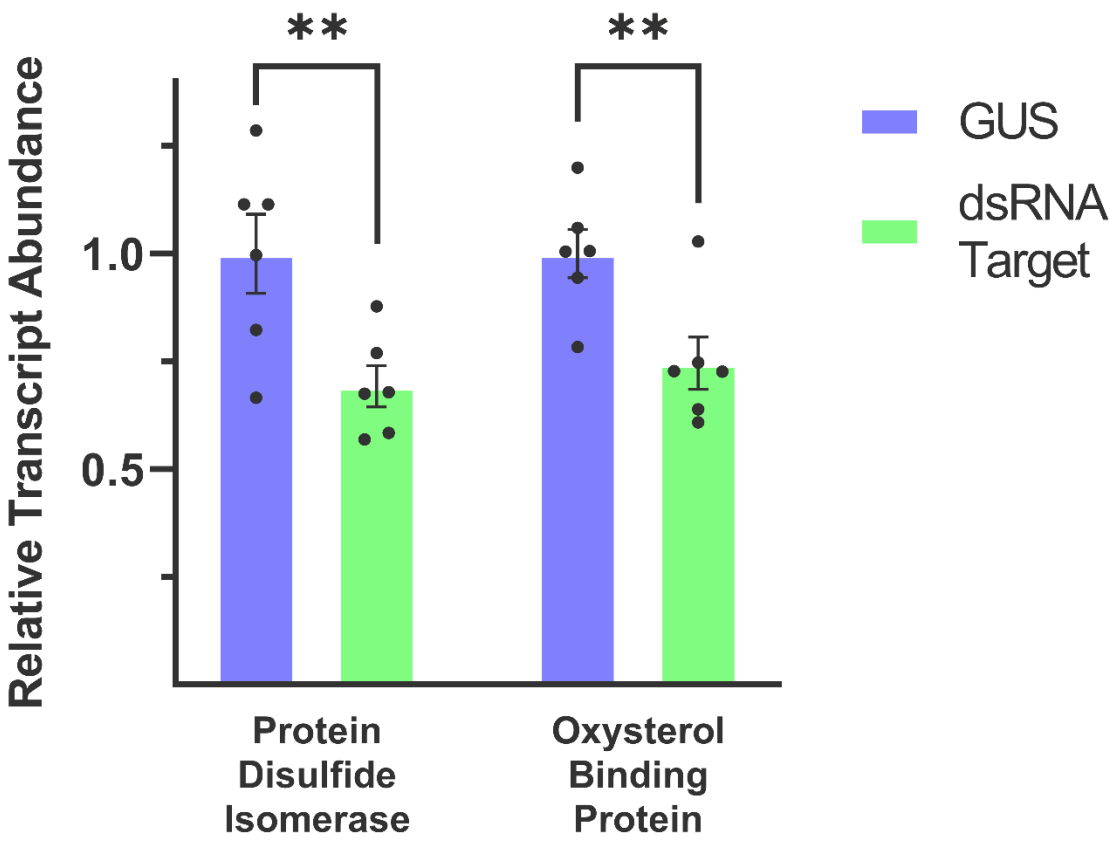

Figure 3.3. Relative transcript abundance of Protein Disulfide Isomerase (HpaG809065) and Oxysterol Binding Protein (HpaG807348) dsRNA treatments. Transcript levels measured 7 days post treatment with 10 ng/µL foliar spray of dsRNA. Data relative to GUS dsRNA non-target control and Actin (HpaG807716) reference gene. Data represents 6 biological replicates with error bars representing standard error. Significant difference (One-way Student's t-test; $p < 0.05$) from respective GUS negative control denoted by asterisks (** = $P < 0.01$)

3.4 Application of dsRNA Spray is Inconsistent Across Treatment Area

Due to the differences in relative transcript accumulation across biological replicates in the treatments, an assay was carried out to measure the approximate amount of dsRNA that could reach the leaf surface of *Arabidopsis* seedlings in the SIGS assay. Using known quantities of salmon sperm DNA determined by spectrophotometry aliquoted into a 96-well plate, a standard curve was generated to associate total fluorescence in each well with a defined concentration (Fig. 3.4). Using salmon-sperm DNA as an proxy to dsRNA, a 10 ng/µL spray was applied over two 96-well plates that simulates the same volume and spray pattern as was done in the SIGS assay (Fig. 3.5). The distribution of DNA across the plate was found to be highly inconsistent, with values ranging from as low as 9.40 ng/cm^2 to as high as 68.50 ng/cm^2. By applying the DNA in two rows of three pumps from the spray bottle, there appears to be no consistent pattern found between plate replicates. This 7-fold difference in DNA applied across both plates may explain the difference in transcript knockdown in the *Hyaloperonospora* SIGS assay replicates

3.5 Measuring Optical Density of *in vitro S. sclerotiorum* Growth Can Identify Dose-Response of dsRNAs

To quickly measure *S. sclerotiorum* growth *in vitro* in the presence of dsRNA treatments, an assay was designed to be highly automated, take measurements that is not subject to human error, and can screen multiple treatments at a time. The method ultimately developed involves measuring the optical density at 600 nm of *S. sclerotiorum* growth in a liquid culture within multi-well plates. Previous attempts to measure growth using multi-well plates included growing *S. sclerotiorum* on a thin layer of potato dextrose agar within a multi-well plate and staining the wells with a fluorescent stain (Calcofluor White) that binds to chitin before scanning. There were a few limitations with this method. First, the agar absorbed the stain, resulting in a high level of

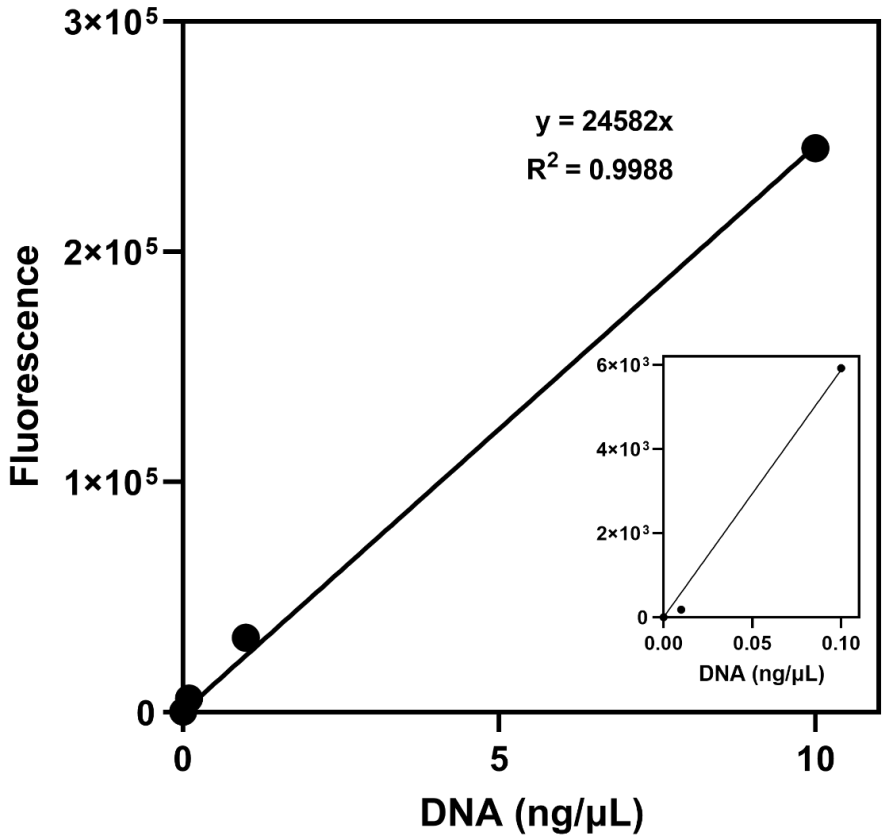

Figure 3.4. Standard curve of salmon sperm DNA and fluorescence. Six DNA concentrations (100 ng/µL to 0.01 ng/µL) with 3 replicates plotted against fluorescence values (480 nm excitation, 520 nm emission) captured in 96-wells using the Quant-iT PicoGreen Assay and Synergy BioTek Multimode Plate Reader. Standard curve equation calculated using a linear regression model.

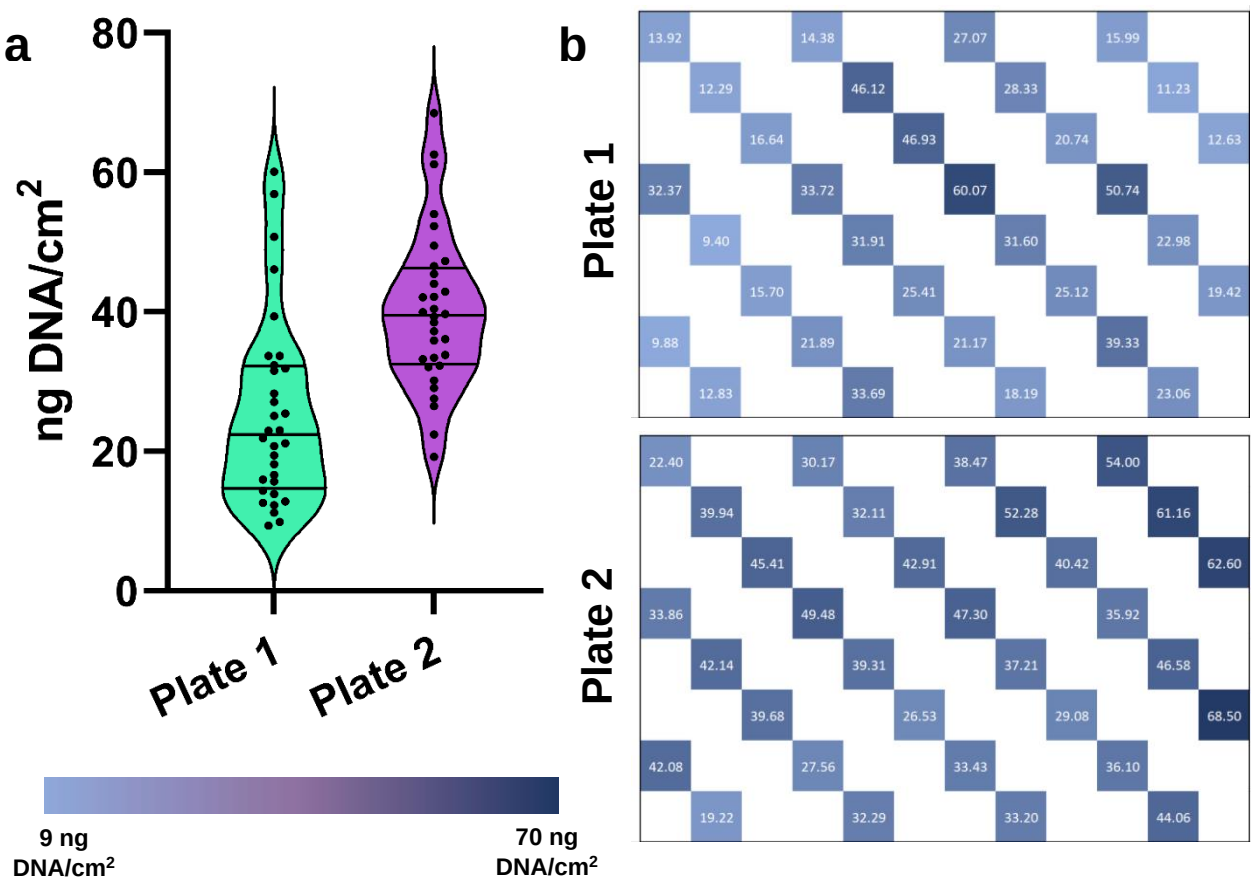

Figure 3.5. Spray application results in inconsistent amounts of DNA per unit area. (**a**) Violin plot of DNA mass per unit area (cm^2) across two independent spray applications. Median and interquartile ranges displayed, with 32 samples taken across a 96-well plate. (**b**) Heat map displaying DNA mass per unit area (cm^2) across 96-well plates.

background fluorescence. Secondly, the staining process stopped growth of the fungus, making measurements over an extended period of exposure to dsRNA impractical. And thirdly, the thinness of the agar (needed to minimize background fluorescence) resulted in a meniscus forming, causing greater nutrient accumulation and fungal growth around the around the well's periphery, which was difficult to quantify using the plate reader. Growing *S. sclerotiorum* in a much larger volume of liquid culture resolved the uneven nutrient density within the well and scanning at 600 nm is a non-invasive and non-toxic method to measure light scattering caused by growth of the fungus. This can be done multiple times during the assay, allowing for a time-series analysis.

To confirm that significant differences between dsRNA treatments and controls can be identified, an initial test of three unique dsRNA targets at the same concentration were compared against two negative controls (water and GUS dsRNA) and a positive control (Boscalid fungicide) (Fig. 3.6). Due to a programming error, this assay ended after 90 hours of growth, with all other assays extending to 96 hours of growth. All treatments, including the Boscalid control, exhibited a gradual increase in OD_{600} values up to 60 h, and thereafter, the Boscalid treated fungus stopped growing, whereas all other treatments continued to show increased growth. However, significant differences between dsRNA treatments and negative controls were observed after 90 hours of growth (one-way ANOVA, $p < 0.0001$), with 1703-dsRNA (SS1G_01703) having a 50.4% reduction, 5899-dsRNA (SS1G_05899) a 56.7% reduction, and 6487-dsRNA (SS1G_06487) a 66.2% reduction of growth relative to the GUS-dsRNA negative control. At 90 hours, the 6487-dsRNA treatment showed no statistical difference from the Boscalid fungicide treatment (one-way ANOVA) while the 1703-dsRNA and 5899-dsRNA treatments showed slightly higher growths than the positive control (one-way ANOVA, $p <$

0.05). Because OD_{600} measurements do not discriminate between living and dead cells, the plateau of the Boscalid positive control may indicate complete termination of growth after the 60–66-hour time point, with scans only measuring dead cells following this time point. The small difference between the GUS-dsRNA and water negative control treatment was not statistically significant (one-way ANOVA). It is notable that this assay provided highly consistent growth rates of the four GUS biological replicates, more so than the water control.

Given that this plate-based assay could readily measure differential growth of the fungus exposed to different dsRNAs, its ability to evaluate impacts of different dsRNA concentrations was then investigated. Using the most effective and least effective of the three dsRNA treatments selected previously (SS1G_01703 and SS1G_06487), *S. sclerotiorum* growth was compared at 1 µg/mL and 5 µg/mL dsRNA concentrations, with a GUS negative control and Boscalid positive control (Fig. 3.7). At 96 hours of growth, both 1 µg/mL dsRNA treatments showed no difference in growth relative to the GUS negative control (one-way ANOVA) but with the 5 µg/mL treatments, both dsRNAs showed a significant reduction in fungus growth (41.4% reduction for 1703 and 67.9% reduction for 6487; one-way ANOVA, $p < 0.0001$). The 5 µg/mL 1703 treatment appears to have a similar impact on fungus growth as the 2.5 µg/mL treatment from the previous assay, but by the 96-hour mark, fungus growth begins to increase rapidly, which suggests that the treatment is potentially losing efficacy. For the 5 µg/mL 6487-dsRNA treatment, the fungal growth is similar to the 2.5 µg/mL treatment, but with this dsRNA, the accumulation of fungus was not significantly greater than that of the Boscalid control at the 96-hour mark. To confirm the similarities in growth between 2.5 µg/mL and 5 µg/mL doses, another assay with both treatments and doses were conducted simultaneously (Supplementary Figure 3.2). For both dsRNA treatments, the differences in growth were not significantly significant

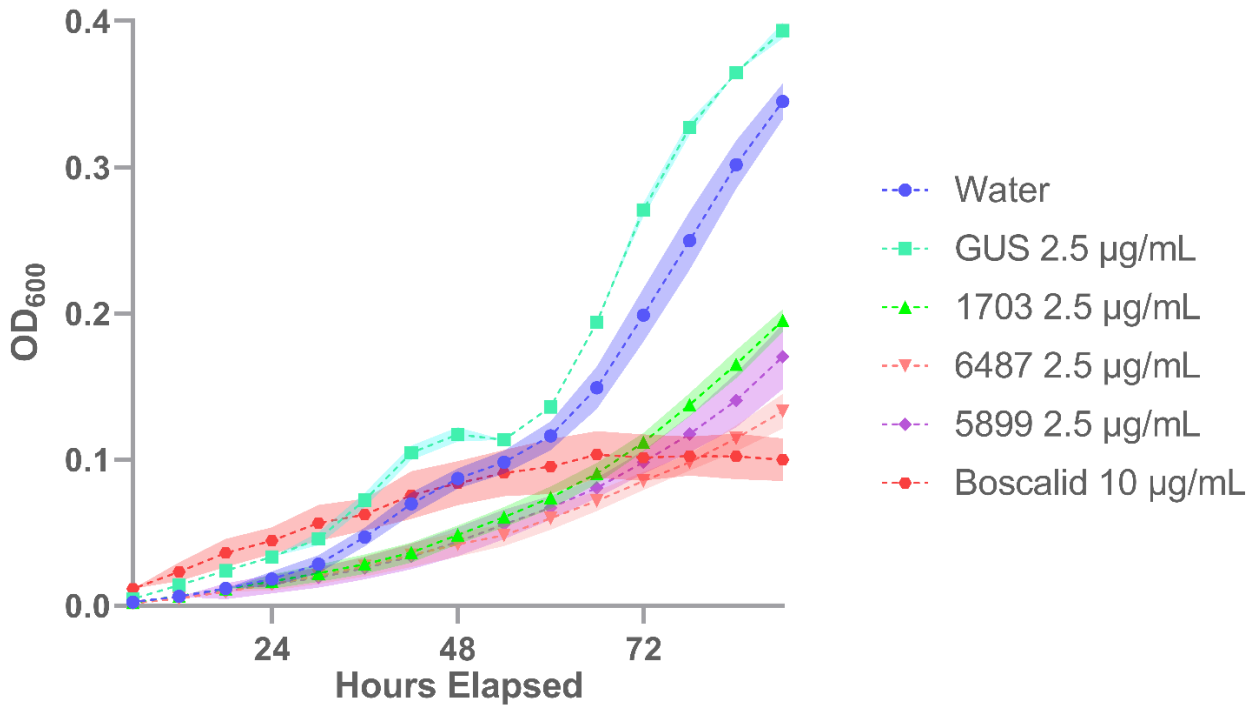

Figure 3.6. DsRNA treatments slow down growth of *S. sclerotiorum*. OD_{600} measurements scanned every 6 hours in a 9x9 scan grid in each well. Time point 0 hrs measurement subtracted from each subsequent time point. Plotted points represent mean value across 4 biological replicates with standard error plotted as shaded area.

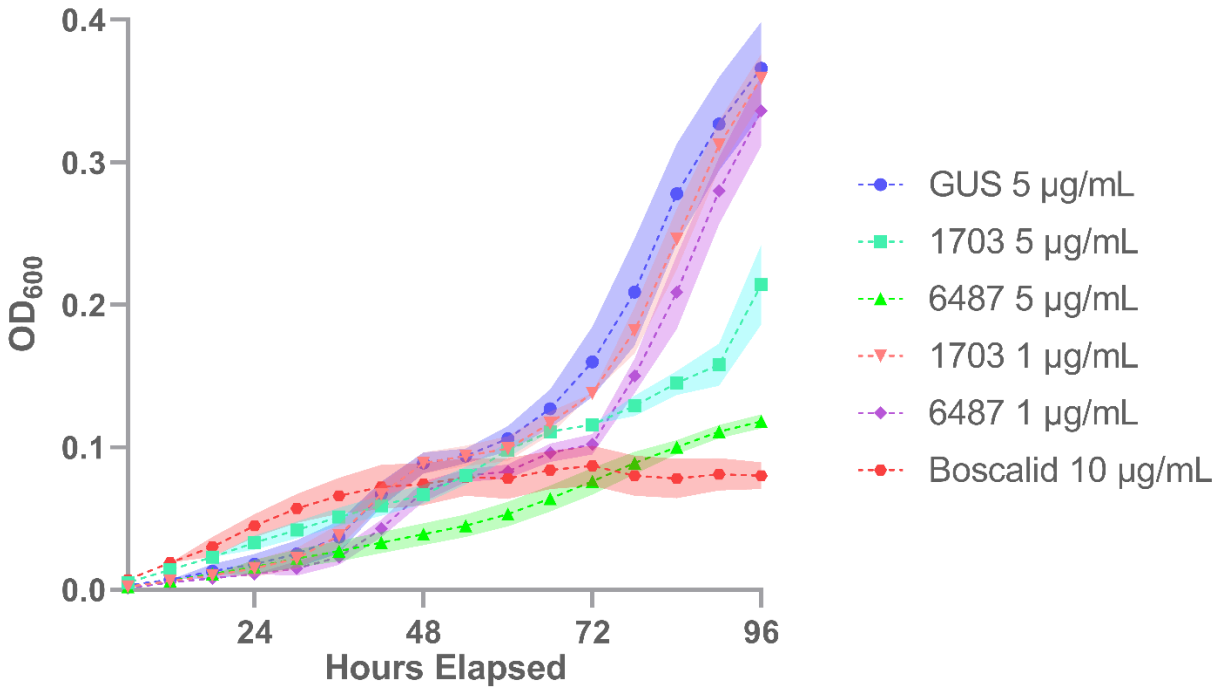

Figure 3.7. DsRNA concentration impacts growth inhibition of *S. sclerotiorum*. OD_{600} measurements scanned every 6 hours in a 9x9 scan grid in each well. Time point 0 hrs measurement subtracted from each subsequent time point. Plotted points represent mean value across 4 biological replicates with standard error plotted as shaded area.

(one-way ANOVA) and the combination of 1703 and 6487 treatments at 2.5 µg/mL did not improve growth inhibition significantly.

With growth inhibition observed across all dsRNA treatments, a final test was carried out to examine if applying half of the dsRNA midway through the assay would result in improved inhibition. Using the 1703-dsRNA, fungal cultures were treated with either a single 5 µg/mL dose at the time 0, or with a 2.5 µg/mL dose at time 0 and a second 2.5 µg/mL dose at the 48-hour mark (Supplementary Figure 3.3). There was no statistical significance between the single vs double treatments after 96 hours, with both showing approximately a 53.8% and 56.1% reduction in growth between the initial full treatment and the supplemented treatment, respectively (one-way ANOVA).

Across all assays, the growth of the GUS negative control experienced a plateau or even an apparent reduction of fungus growth at the 48-hour mark, which was then followed with a rebound in growth thereafter. This growth pattern was also observed in the water control in Figure 3.6 and the 1 µg/mL dsRNA doses in Figure 3.7 and may reflect a natural fungal growth pattern in this liquid culturing system. Regardless of this lull in growth, the plate-based assay demonstrated clear responses to the fungus-specific dsRNAs.

3.6 Hyphal Growth of *S. sclerotiorum in vitro* is Reduced at Higher dsRNA Doses

While the previous tests revealed that dsRNAs targeting the SS1G_06487, SS1G_05899, and SS1G_01703 genes can reduce growth of *S. sclerotiorum* over 4 days, it does not explain the impact these treatments have at earlier growth stages and what effect a high dose of dsRNA can have on the morphology of the pathogen. To investigate this, a similar assay to one used with *H. arabidopsidis* was developed, which utilizes high-resolution imaging of hyphal growth stained with a fluorescent stain that binds to chitin and cellulose, Calcofluor White. Because of *S.*

*sclerotiorum'*s highly aggressive growth and high germination rate, this assay was modified to analyze total growth within a droplet rather than measuring each individual germinating spore, as their hyphae would clump and overlap each other, which would hinder efforts to visualize individual hyphal strands. To reduce the rate of growth, the nutrient concentration was reduced to the same concentration used in the multiwell assays, and spores were incubated at 17° C. Germinated spores were imaged and then analyzed for total white pixel count in each droplet using ImageJ, indicating the total amount of fungal growth within each droplet.

DsRNA treatments 1703 and 6487 were tested at two doses, 5 ng/µL (5 µg/mL) and 50 ng/µL (50 µg/mL), with the same concentration in the GUS-dsRNA negative control, and with a 5 ng/µL Boscalid fungicide positive control (Fig. 3.8). *S. sclerotiorum* growth was significantly reduced in the 50 ng/µL 6487-dsRNA treatment compared to its GUS-dsRNA equivalent dose by 68.2% (one-way ANOVA, $p < 0.0001$), while the Boscalid positive control showed reduced growth by 80.5% compared to its equivalent GUS dose. Both 1703-dsRNA doses did not show any significant changes in growth compared to GUS. While total reduction in growth of some 6487-dsRNA replicates matched those treated with Boscalid, the growth patterns of individual hyphae did appear to differ in the two treatments (Fig. 3.8a); the Boscalid treated hyphae appeared short and highly branched, while the 6487-dsRNA treated hyphae were long and minimally branched.

To confirm that *S. sclerotiorum* growth can be inhibited with 1703-targeting dsRNA, a second assay using a higher dose of 100 ng/µL was used (Supplementary Fig 3.4). Both the 50 ng/µL and 100 ng/µL doses showed significant reduction in growth (one-way ANOVA, $p < 0.01$), with a 71.2% and 69.2% reduction, respectively.

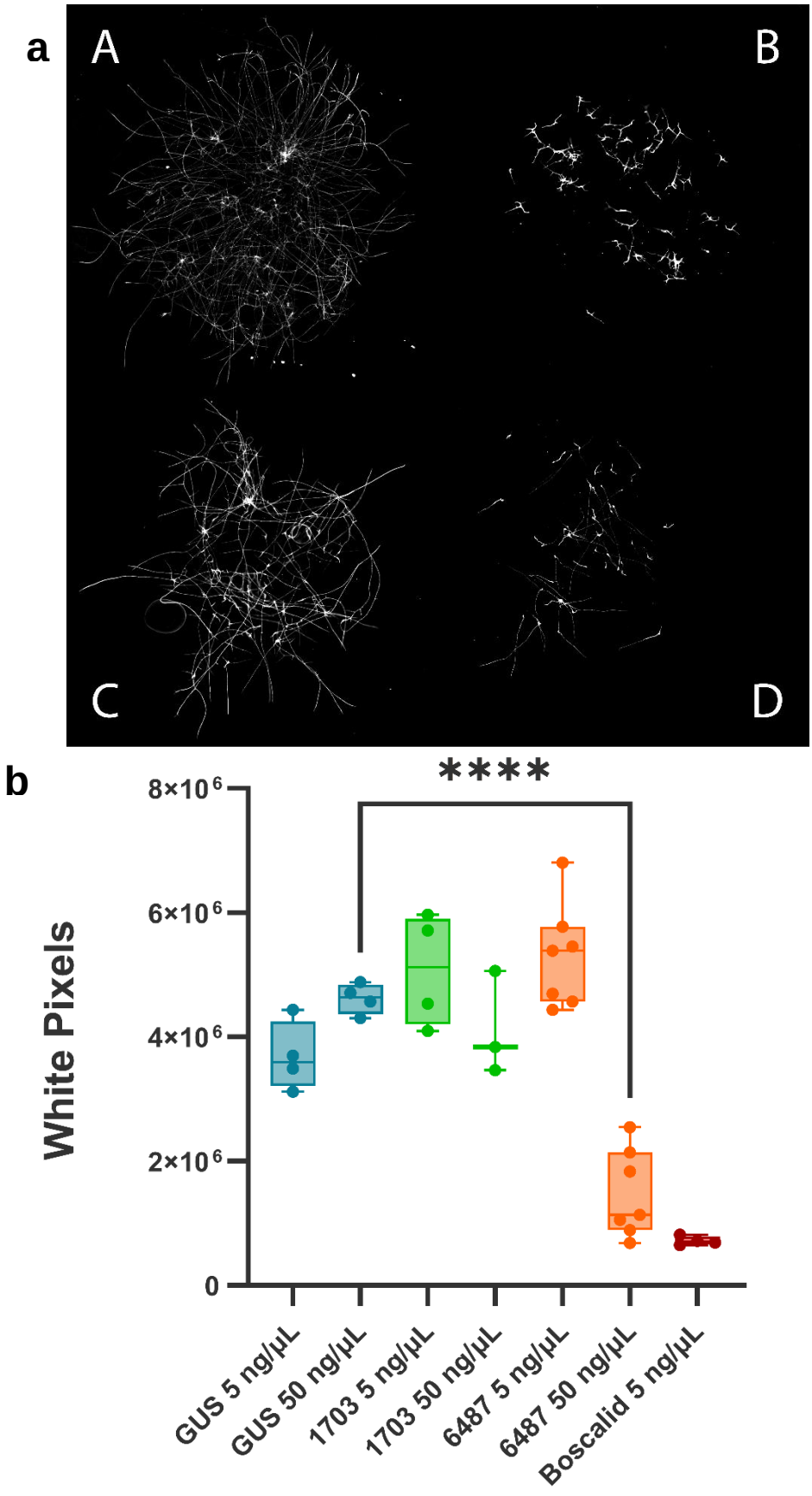
a
A
B
C
D
b
****
White Pixels
8×10^6
6×10^6
4×10^6
2×10^6
0
GUS 5 ng/µL
GUS 50 ng/µL
1703 5 ng/µL
1703 50 ng/µL
6487 5 ng/µL
6487 50 ng/µL
Boscalid 5 ng/µL

Figure 3.8. Impact of dsRNA dose is evident after only 48 hours of growth. (**a**) Representative droplets of *S. sclerotiorum* growth of A: 50 ng/µL GUS dsRNA, B: 5 ng/µL Boscalid, C: 50 ng/µL 1703 dsRNA, and D: 50 ng/µL 6487 dsRNA. (**b**) Boxplot with min/max, interquartile ranges, and median value of total white pixel count of *S. sclerotiorum* growth measured 48 hpi across 3-7 biological replicates per treatment. 50 ng/µL GUS negative control and 50 ng/µL are significantly different (One-way ANOVA, $p < 0.0001$).

3.7 The Evolutionary Analysis of DICER Between Fungi and Oomycetes

With both *S. sclerotiorum* and *H. arabidopsidis* showing the impact of RNAi using similar analytical methods, it is predicted that the key RNAi components are functional across both fungal and oomycete species. One of the key components of RNAi is Dicer, which is responsible for the processing of long dsRNAs into sRNAs. Given the evolutionarily divergence of oomycetes and fungi, it was of interest to see whether the Dicer gene sequences likewise reflected the differences in these two groups of agronomically important pathogens. From a collection of different published sources, putative Dicer amino acid sequences from fungal, oomycete, and other model organisms were retrieved (Supplementary Table 3.2). Full sequences were then aligned using MUSCLE and a phylogenetic tree with was constructed using the Maximum Likelihood method with 500 bootstrap replicates (Fig. 3.9). Of the Dicer sequences aligned, the oomycete and fungi Dicers were segregated from each other, clustering with species of their predicted evolutionary clades. Within both the oomycete and fungi clades, Dicers appeared to segregate again into distinct DCL1 and DCL2 clusters.

Within Dicer is the RNase III domain, the catalytic component responsible for cleavage of dsRNAs into sRNAs. Because of its importance in the Dicer function and its requirement to be highly conserved to stay functional, a phylogenetic analysis of these same Dicer sequences but only of their RNase III domains were carried out. To do so, domains of each amino acid sequence was identified from conserved domain databases, with RNase III sequences

concatenated together. During domain identification, Dicer sequences that lacked any annotated RNase III domains were omitted. Using the same alignment and tree construction parameters as before, a phylogenetic tree was constructed (Fig. 3.10). Instead of being aligned according to their own clades, Dicer sequences were grouped primarily by their homologs, with DCL1 grouping together and DCL2 grouping together. In cases where DCL1 or DCL2 did not group with their expected clade (e.g. [identify one or two]), the sequences may not have been properly annotated or do have similar function to Dicer homologs of other species. To examine more closely the relationship between these Dicer sequences, amino acid residues of high consensus regions of the concatenated RNase III multiple sequence alignment were analyzed (Supplementary Fig. 3.5). Among all aligned Dicers, there are 13 positions with 100% identity, and between *H. arabidopsidis* DCL3, *P. sojae* DCL2, and *P. ultimum* DCL2, there are 33 aligned residues that are identical among them with the rest of the residues showing the same identity across the other oomycete Dicers.

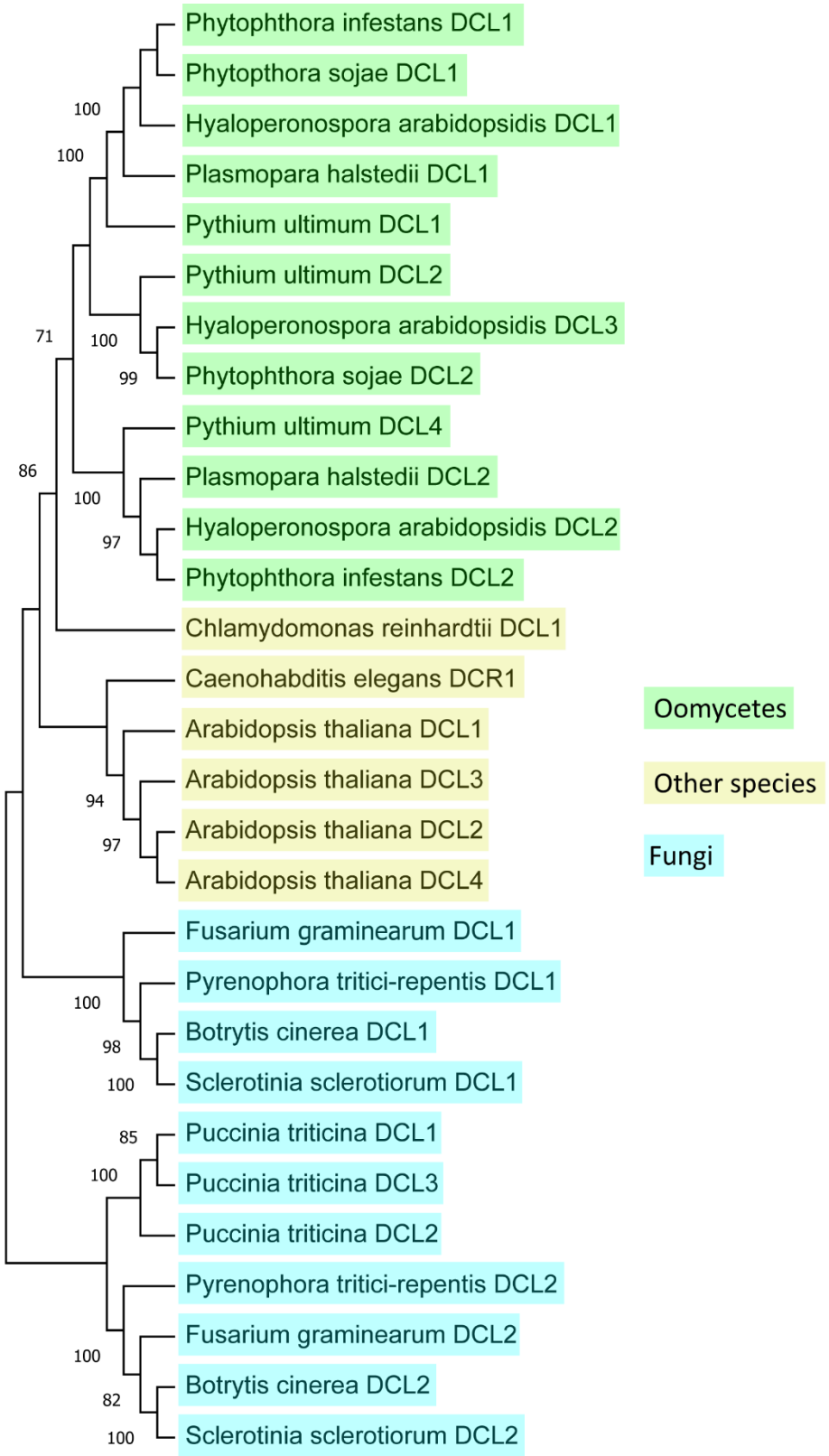

Figure 3.9. Phylogenetic tree of Dicer homologs based on full amino acid sequences. Bootstrap support values above 70 displayed next to nodes.

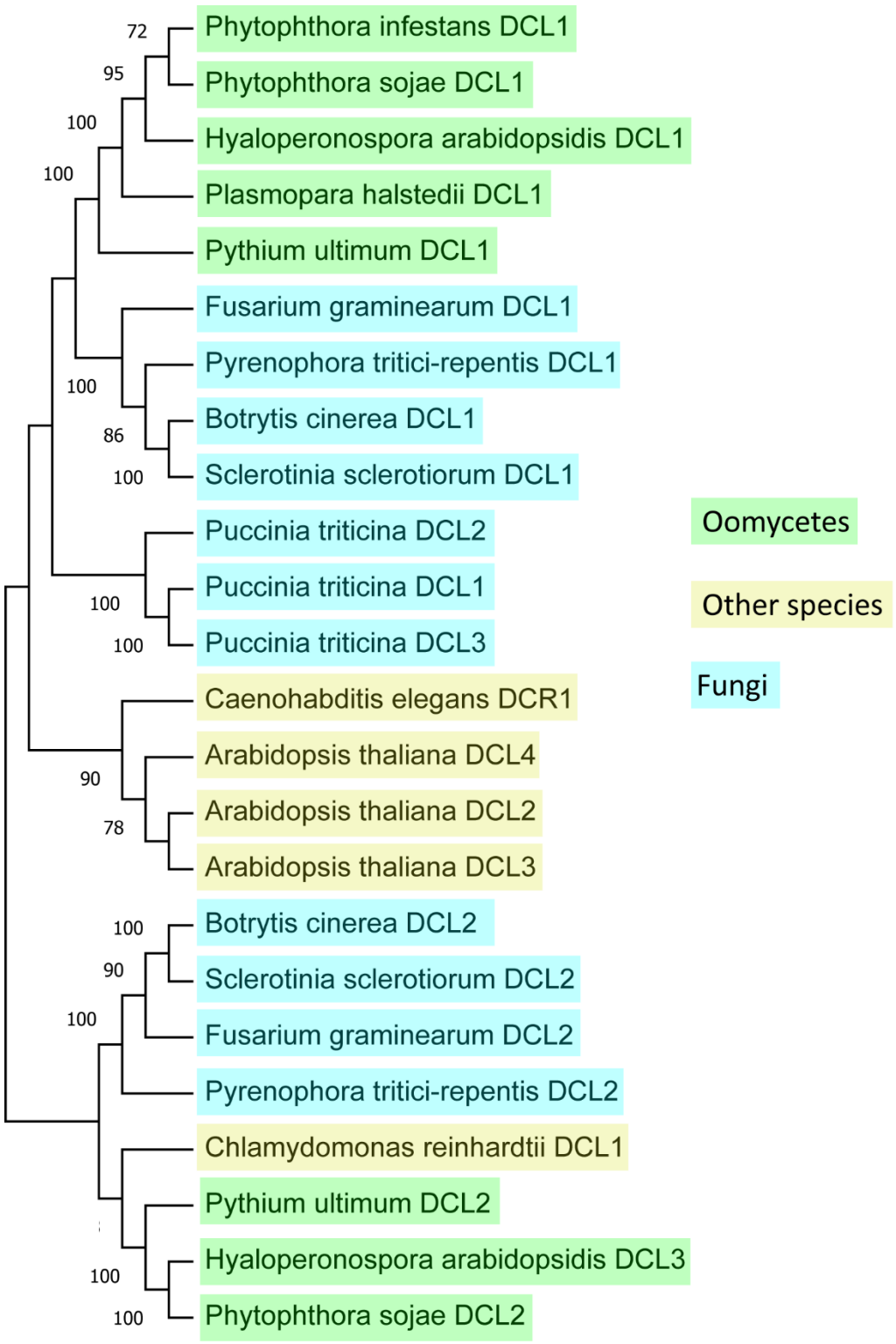

Figure 3.10. Phylogenetic tree of Dicer homologs based on concatenated RNase III amino acid sequences. Bootstrap support values above 70 displayed next to nodes.

CHAPTER 4: DISCUSSION

4.1 Control of *H. arabidopsidis* using Topical Application of dsRNAs

As an alternative to conventional fungicides, SIGS has quickly become a major focus for researchers to protect plants from destructive plant pathogens in a safe and environmentally friendly manner. Much of the focus on developing RNAi solutions against pathogens has been on true fungi, but oomycete pathogens such as downy mildew are worthy species to apply this technology due to the considerable damage they also cause to crops. Here, we have investigated how the topical application of dsRNAs targeting a variety of cellular functions impact growth of the model pathogen *Hyaloperonospora arabidopsidis in vitro*, and how a foliar application of these dsRNAs impacts the growth of *H. arabidopsidis* on *Arabidopsis* seedlings. To accelerate the selection of successful dsRNA targets for future studies and to investigate their impacts on growth of *H. arabidopsidis*, developing an *in vitro* assay is desirable. Previous work from Bilir et al. (2019) demonstrated early-stage growth of this obligate biotrophic pathogen is possible when on cellophane placed over agar, and personal communication with corresponding author Dr. Mahmut Tör emphasized that *H. arabidopsidis* spores require a firm surface and need to be rinsed to remove germination inhibitors. Chemical compounds such as 1-octenol, cinnamic acid, and furanones have been characterized as self-inhibitors of spore germination in true fungi and operate in a spore density-dependent manner, and in pathogenic oomycetes, these chemical self-inhibitors would need to be washed off to achieve successful germination (Kaur and Singh, 2020). Improving upon the assay first described by Bilir, fluorescence microscopy was used to aid in high resolution imaging of germinated spores. Calcofluor white is a common fluorescent stain for staining of beta 1-3 and beta 1-4 polysaccharides found in both cellulose and chitin, and its previous use in detecting pathogenic fungi and oomycetes proves its utility as a stain for *in*

vitro studies observing growth of infective structures (Harrington and Hageage, 2003; Thrane et al., 1999; Ali and Skaar, 2017). Combining the use of an inverted fluorescence microscope with automated focus and stage, germination procedures previously described, and using image analysis programs currently available, researchers can investigate other downy mildew pathogens or even other fungi with similar procedures. This method provides a robust dataset on the early growth of plant pathogens, which is important in developing crop protection products that require elimination of the pathogen before significant damage can occur.

Of the ten dsRNA *H. arabidopsidis* targets tested *in vitro* using this novel spore germination assay, seven showed a significant reduction in germination percentage between 32-95% at a higher dose of 100 ng/µL, with three of the seven showing a greater reduction than the Metalaxyl fungicide at the same concentration. In all 100 ng/µL treatments, any germinated spores showed reduced germination tube lengths, compared to the GUS non-targeting dsRNA negative control. At a lower dose of 20 ng/µL, however, none of the dsRNAs caused any reductions in germination percentage, and the distribution of germination tube lengths were also similar to the GUS negative control. These *in vitro* tests demonstrate the ability of RNAi to reduce growth, and that there is a threshold concentration required for the impact of RNAi to be visibly conspicuous. In other fungal species, growth can be inhibited at lower doses than 100 ng/µL, but recent research suggests that dsRNA uptake by oomycetes may limited, thus requiring a greater dose to achieve similar effects (Qiao et al., 2021). Because these analyses do not investigate the dsRNA's effect on accumulation of the targeted transcript, there may be transcript knockdown in the lower concentration treatments, but the knockdown was insufficient to alter the phenotype. Among the dsRNA targets that showed impacts on germination, three are also targeted by commercial oomycete fungicides (cellulose synthase, ubiquinol cytochrome c

reductase, and oxysterol binding protein). Two of the other targets that showed significant reductions in germination (glucan synthase and protein disulfide isomerase) were identified to be similar in function to targets showing lesion reduction in *S. sclerotiorum* by McLoughlin (2018), while the other target (polysaccharide cellulase) is a novel target that has a role in expanding cell walls during oomycete growth (Judelson and Ah-fong, 2019). Differences in RNAi responses across targets could be attributed to the number of efficacious siRNAs produced by the designed dsRNA and the sequence characteristics of each siRNA (Reynolds et al., 2004; Jagla et al., 2005), mRNA secondary structures (Ding et al., 2014), or protein-mRNA interactions that limit mRNA accessibility (Liu et al., 2014). While many of the dsRNAs selected in this study were predicted to have serious impacts on the pathogens, not all dsRNAs were effective. It is important to recognize that successful targets may not always be easily identified simply based on their predicted importance to the cellular or physiological function of the pathogen; success may also rely on effective dsRNA design and may require multiple revisions to be best optimized for effective or potent RNAi. Current pesticide targets appear to be reasonable RNAi targets in downy mildew, although the sample size is admittedly small, and more need to be tested. This approach to selecting RNAi targets has been used in other fungal pathogens (Song et al., 2018; Koch et al., 2016; Gu et al., 2019), and would be a good place to begin target selection in oomycetes. While the assay developed in this study has potential to be scaled up for faster screening, limitations of this assay are related to the manual work involved in scoring each germinating spore. However, it may be improved by automation, either during imaging using robotically controlled plate readers, or after using machine learning to score the images. Additional studies should investigate the minimum effective concentration of the top performing

targets and design dsRNAs targeting different gene regions to further select for the best SIGS candidates.

To confirm that transcript knockdown occurred in the *H. arabidopsidis* and *A. thaliana* pathosystem, a SIGS assay involving a spray application of dsRNA and a spray application of *H. arabidopsidis* spores was performed. Reduced transcript accumulation was indeed observed in both the protein disulfide isomerase (HpaG809065) and oxysterol binding protein (HpaG807348) targets, but only by 30.7% and 25.4% respectively. At 7 days post-treatment, the limited impact on mRNA accumulation could be explained by the recovery of expression following the dsRNA treatment. Marciano (2021) found gene expression significantly recovered at 7 dpi in grapevine plants treated with dsRNA to protect against the downy mildew *Plasmopara viticola*. Conversely, Koch (2016) found dsRNAs sprayed onto leaves were still detectable in large quantities via Northern blot analysis after 7 days. Regarding SIGS treatments, a likely scenario could be that initial knockdown of the gene target results in low transcript accumulation initially, but gene regulation will cause overexpression to overcome the lack of mRNA transcripts. This would also suggest that the amount of dsRNA applied does not correlate with longer lasting protection. Using the results obtained from *in vitro* studies, we can infer that transcript accumulation is severely impacted at earlier stages of fungal growth but recovers over time. In an agricultural setting where protection is crucial during the critical period of infection, the degree and time of protection via SIGS is an important factor to understand. Extending this period via nanoparticle formulations or targeting genes that are not tightly regulated are important considerations in developing SIGS into a commercial product.

Plant pathogens are often controlled through foliar fungicide applications that provide both contact and systemic protection. When spraying across large areas of land, the correct dose

of active ingredient is important to provide effective control, while also being aware that an excessive dose may not be economically viable. The same case is true for SIGS, and while most SIGS studies mention the concentration of the dsRNA sprayed, there is often no quantification of the total amount applied beyond Northern blot analysis. We set out to quantify the total amount of dsRNA that would have been applied to the leaves of *A. thaliana* and found significant inconsistencies of total amount of dsRNA per unit area across the sprayed area. Using DNA as a proxy for RNA for two replicated tests, the distribution of DNA per square centimeter varied from 9.40 ng/cm^2 to 68.50 ng/cm^2. While efforts were made to maintain a consistent spray pattern between replicates, human error, spray nozzle uniformity, and spray pressure are believed to be the causes for the variability. We did not see that wide variation in our relative transcript abundance measurements from the SIGS assay, but that is likely due to the pooling of seedlings in each biological replicate. To reduce the variability of the spraying method, an automated spray method that applies dsRNA consistently under a constant pressure could provide a more consistent dose over a precise surface and resolve variability even across technical replicates. In a larger scale situation with commercial equipment this is less of an issue but would still require appropriate calibrations.

4.2 Measuring Inhibition of *S. sclerotiorum* using Novel *in vitro* Assays

Screening for effective dsRNA targets is an essential step in developing an effective RNAi product to be brought to market and can be a resource-intensive process. To screen for dsRNA targets within *S. sclerotiorum*, two unique assays were developed to assess the inhibition of *S. sclerotiorum in vitro*. To examine growth of *S. sclerotiorum* in broth culture, a multiwell assay was developed to measure the optical density at 600 nm over time. Previous studies have investigated measuring real-time growth of fungal organisms using OD_{600} values, but limitations

are based on their use of 96-well plates and a single OD_{600} scan per well (Miyazewa et al., 2022; Tøndervik et al., 2014; Aunsbjerg et al., 2015; Natskoulis et al., 2018). For the fast-growing *S. sclerotiorum,* parameters were adjusted to slow its growth by reduction in nutrient concentrations and initial inoculum amount, while expanding the well size to a 24-well plate, allowing sufficient room to grow without overcoming the well entirely and being starved of nutrients.

In the first proof-of-concept analysis with dsRNA treatments, significant differences in mycelial growth were observed across the negative controls, dsRNA treatments, and fungicide positive control. DsRNAs targeting SS1G_06487 exhibited the greatest degree of inhibition, with 66.2% reduction of growth relative to the GUS dsRNA negative control measured at 90 hpi. This pattern is consistent with the effects these dsRNAs have on lesion size caused by *S. sclerotiorum* on *B. napus* leaves as described by McLoughlin (2018). While the SS1G_06487 targeting dsRNA is not statistically different compared to the Boscalid treatment at 90 hours, the overall growth trend indicates that inhibition is only slowed by treatment of dsRNAs, and not halted. The SS1G_06487 gene is predicted to encode the mitochondrial import inner membrane translocase subunit TIM44 and is associated with the heat shock protein Hsp70 (Schiller et al., 2008). A study investigating TIM44 mutants in *Saccharomyces cerevisiae* show lethality when deleted, showing the importance of TIM44 for mitochondrial function and as a good target for RNAi (Schilke et al., 2012). The Boscalid control showed plateaued growth by the 60-hr mark, with OD_{600} values beginning to decline slowly. Boscalid is a succinate dehydrogenase inhibitor, and thereby inhibits fungal respiration by blocking electron transport to ubiquinone. This inhibition is irreversible, causing complete stoppage of further growth (Avenot and Michalides, 2010). The limitation of this OD_{600} assay is in its inability to differentiate between living and

dead cells, which can explain the plateau of growth in the positive control and subsequent decline in OD_{600} values as the fungal cell lysis begins.

With differences between dsRNA treatments and their controls readily elucidated using this assay, a dose response assay with both SS1G_01703 and SS1G_06487-targeting dsRNAs was carried out. Here we show 1 µg/mL doses of both treatments were statistically similar to the negative control, but there were significant differences in levels of inhibition among the 5 µg/mL of both treatments, with SS1G_06487 impacting mycelial growth much more than SS1G_01703 at 96 hours. The growth trends were also unique to each other, with SS1G_01703 beginning to lose efficacy while SS1G_06487 efficacy persisted over the assay's time period. Previous work from McLoughlin (2018) identifies SS1G_01703 as having a role in aminoacyl-tRNA ligase activity and in aflatoxin biosynthesis, which may facilitate pathogenicity *in planta*. Because these assays are *in vitro*, the impact of dsRNA on SS1G_01703 in the liquid culture may not have been as potent as it would have been on the host plant. We also found that combining treatments of both SS1G_01703 and SS1G_06487 at equal concentrations did not result in less mycelial growth than by treatments on their own. This suggests that for these two targets at least, no synergistic effects occurred by reducing these two target transcripts simultaneously. Lastly, we investigated whether applying the half of the dsRNA treatment at the mid-point in the assay would provide better inhibition of mycelial growth. At 96 hpi both the initial 5 µg/mL and 2.5 µg/mL initial with 2.5 µg/mL supplement at 48 hpi were statistically similar, leading us to believe that the bioavailability of the SS1G_01703 dsRNA does not significantly impact mycelial inhibition within this assay, under the conditions used.

In multiple experiments, the GUS negative control experienced a drop in OD_{600} readings after 48 hours, but thereafter, growth recovers. At first glance, it appears that growth is stunted or

inhibited briefly, but as this pattern occurs in both GUS and water negative controls, this can be ruled out. The likely cause of this apparent stalled growth is the aggregation of hyphae within each well. At the beginning each spore begins to germinate, and once the mycelia form, they begin to overlap, and with the help of orbital shaking at each interval, a mycelial mass begins to form. Because the measurement is a top-down scan, hyphal growth may be underreported during this initial aggregation stage. A similar type of aggregation was found by Miyazewa (2022) in *Aspergillus fumigatus*, where cell wall polysaccharides and galactosaminogalactan contribute to hyphal aggregation. While orbital shaking may contribute to this issue, it also prevents attachment to the periphery of the well; future studies would be required to resolve this concern fully.

High resolution imaging and measurement of *S. sclerotiorum* mycelial growth revealed both morphological differences between dsRNA treatments and a dose response within 48 hpi of germination. By measuring total mycelial growth represented as white pixels within a droplet, we found SS1G_01703 dsRNAs at both 5 ng/µL and 50 ng/µL and SS1G_06487 at 5 ng/µL to be statistically similar to the GUS dsRNA equivalent dose, while a significant reduction in mycelial mass was found in the SS1G_06487 50 ng/µL treatment. These results support the notion that SS1G_06487 is a more effective target than SS1G_01703 *in vitro*, and that increasing the concentration creates a more pronounced effect in some targets. To observe a dose response in SS1G_01703, a second assay with a 100 ng/µL found that both 50 ng/µL and 100 ng/µL produced significant reductions in mycelial mass compared to their GUS dsRNA equivalent dose. While experimental parameters were consistent between this assay and the previous one, pipette volumes and hyphal imaging caused by human error may contribute to the differences observed.

Morphological changes within the Boscalid and 6487-dsRNA treatments compared to the GUS-dsRNA were readily apparent in these germination assays. As a succinate dehydrogenase inhibitor, the Boscalid fungicide appears to slow growth by reducing mitochondrial activity. Increased branching of hyphae was a key characteristic, with this feature being found in another study investigating Boscalid treatments on *S. sclerotiorum* (Hu et al., 2018). This morphological feature appears in other SDHI fungicides like fluazinam (Hou et al., 2019), penthiopyrad (Mao et al., 2020), and pyraziflumid (Hou et al., 2018). The research group responsible for these studies theorizes that increased branching is a result of intracellular electrolyte leakage that damages cellular membranes, which could then initiate a branching event. In comparison, the 6487-dsRNA treatment appears to have the opposite effect, with little to no branching present. In *Neurospora crassa*, Hsp70 is highly expressed in early exponential hyphal growth and is an important element in managing stress conditions (Rensing et al., 1998; Roy and Tamuli, 2022). As Tim44 is closely associated with Hsp70, it is possible that interference with this mitochondrial protein import system may result in the reduced hyphal branching of *S. sclerotiorum*.

4.3 RNAi Pathway Comparisons Between *S. sclerotiorum* and *H. arabidopsidis*

Comparison of Dicer genes among agriculturally important pathogens reveals conservation of function between Dicer homologs and reveals evolutionary divergence between oomycetes and fungi. Phylogenetic analysis of entire Dicer genes revealed segregation of species into major clades of oomycetes and fungi. This segregation confirms the evolutionarily divergent relationships between the two groups of pathogens, where oomycetes are within the kingdom Chromista consisting of algae and other unicellular flagellates, while true fungi are within their own kingdom (Beakes et al., 2011). Dicer is a remarkably well-conserved protein across

eukaryotes, with evidence suggesting the first ancestral Dicer arose shortly after the arrival of eukaryotes (Cerutti and Casas-Mollano, 2006). While this Proto-Dicer may have played multiple roles in the regulation of genetic elements and combatting viral defense, evidence suggests that an early duplication event of Dicer allowed their functions to become more specific, as identified in *Drosophila* where Dicer1 facilitates the miRNA pathway and Dicer2 regulates the siRNA pathway (Song and Rossi, 2017). Within Dicer is the highly conserved catalytic domain RNaseIII, which is often the focus of phylogenetic analyses comparing Dicers from multiple species (Bollman et al., 2016; de Jong et al., 2009).

When comparing Dicers of agronomically significant pathogens using concatenated RNaseIII domains, the Dicers did not segregate on an evolutionary basis but instead according to their Dicer homologs. Given that oomycetes and fungi are evolutionarily distant from each other, it is possible that the duplication event occurred very early in eukaryotic evolution, creating the segregation observed.

CHAPTER 5: CONCLUSIONS AND FUTURE DIRECTIONS

In this study, I have examined and refined multiple methods that can be utilized to identify potential RNAi targets for control of *H. arabidopsidis* and *S. sclerotiorum*. Using a combination of techniques such fluorescence microscopy, image analysis, and automated area scanning, we were able to elucidate differences between RNAi targets, dsRNA doses, and the impact these have in early germination of these pathogens. These assays have the potential to be applied in other organisms or to examine other treatments and can be a useful tool for researchers to accelerate treatment evaluation. Additionally, we have examined the relation between a foliar spray application and transcript accumulation and highlighted the phylogenetic differences and similarities of an important gene in the RNAi pathway. The results of these studies suggest that effective control of both fungi and oomycetes can be achieved *in vitro* with an effective concentration that is unique to both pathogens.

Experiments involving the *H. arabidopsidis* pathosystem has revealed that developing dsRNAs that impact the same pathways as current pesticides is an effective way to select successful candidates. This research is of value to other researchers who may choose to examine potential RNAi applications for downy mildews of agricultural plant species and can be adapted to other pathogenic oomycetes. A significant amount of research has been invested into RNAi to control pathogenic fungi, and this work within *H. arabidopsidis* helps lay the groundwork for advancing RNAi research within oomycetes. Building on the work within this study, I would like to develop a way to automate the measurement of germinated spores and evaluate more dsRNA targets *in planta* both molecularly and through histology. Questions yet to be answered involving RNAi within downy mildews include: what mechanisms facilitate dsRNA uptake?; how can

nanoparticle formulations provide extended protection in SIGS?; and can topical applications of dsRNA provide similar levels of protection as pesticides in a real-world scenario?

My investigations of RNAi in *S. sclerotiorum* demonstrated that application of dsRNA on the ascospores could inhibit their germination, which could have significant impacts on suppressing this fungus' infection on host plants. While the effects of RNAi take longer to present themselves compared to pesticides, we have observed effective inhibition after just 48 hours of growth. This is of relevance for researchers who look to develop SIGS products that are effective during the critical period of infection, and that the impacts shown produce similar degrees of hyphal growth as current pesticides. In future studies, I would like to investigate the use of these assays in a high-throughput screening test to identify top-performing dsRNA candidates, and potentially see their use in evaluating other dsRNA structures such as hairpin or paperclip dsRNAs. It will be interesting to explore whether gene expression can be measured at the endpoint of these assays, and if fluorescence microscopy can be measured in real-time, providing information on the impact RNAi has on the rate of growth during early germination.

Together, these experiments shed more light on how we can improve the application of RNAi to control phytopathogens and highlights the similarities and differences in the application of this technology between true fungi and oomycetes. The development of these assays will prove valuable for future research and additional studies will continue to advance our understanding of how to best optimize RNAi to secure a safe and sustainable food supply.

APPENDICES

Supplementary Table 1. Sanger Sequencing Data of dsRNA Target Regions. Plasmid constructs sequenced using pL4440 primer.

Gene	Sequence
HpaG803990	GTGCATACTMGWTAGGGCGATTGGGTACCGGCGACGATCACCTACAAACTGTCGCAGAAGGACTTACCG AAGGAGGTGAAGAGCGATCACAATGCAATGACCAGCGCCATGCGCTTCAAGGCGGACAATGTGAAAGTC TACAACCTTAACATCGCCAATACGGCGGGCAACGTGGGACAAGCTGTCGCGGCGACTGTGGACGGCACC AACTACGGCTTCTACGGCTGCAAGTTCACTGGGTATCAAGACACTTTGTTGACCAAGAAGGGGCTTATCC TGTTTGCCAACTCCTACATCAGTGGCGCCGTTCTCGAGGTCGACGGTATCGATAAGCTTGATATCGAATTC CTGCAGCCCGGGGGATCCACGCGTCACGTGGCTAGCCATGGAACCGGTGGATCCACTAGTTCTAGAGCGG CCGCCACCGCGGTGGAGCTCGAATTCATCGATGATATCAGATCTGCCGGTCTCCCTATAGTGAGTCGTATT AATTTCGATAAGCCAGGTTGCTTCCTCGCTCACTGACTCGCTGCGCTCGGTCGTTCGGCTGCGGCGAGCGG TATCAGCTCACTCAAAGGCGGTAATACGGTTATCCACAGAATCAGGGGATAACGCAGGAAAGAACATGT GAGCAAAAGGCCAGCAAAAGGCCAGGAACCGTAAAAAGGCCGCGTTGCTGGCGTTTTTCCATAGGCTCC GCCCCCCTGACGAGCATCACAAAAATCGACGCTCAAGTCAGAGGTGGCGAAACCCGACAGGACTATAAA GATACCAGGCGTTTCCCCCTGGAAGCTCCCTCGTGCGCTCTCCTGTTCCGACCCTGCCGCTTACCGGATAC CTGTCCGCCTTTCTCCCTTCGGGAAGCGTGGCGCTTTCTCATAGCTCACGCTGTAGGTATCTCAGTTCGGT GTAGGTCGTTCGCTCCAAGCTGGGCTGTGTGCACGAACCCCCCGTTCAGCCCGACCGCTGCGCCTTATCCG GTAACTATCGTCTTGAGTCCAACCCGGTAAGACACGACTTATCGCCACTGGCAGCAGCCACTGGTAACAG ATTAGCAGAGCGAGTATGTAGGCGTGCTACAGAGTTCTTGAAGTGGTGCCTAACTACGGCTACACTAGAG ACAGTATTGTATCTGCGCTCTGCTGAGCAGTTACCTTCGGAAAARGAGTTGGTAGCTCTTGATCCGGCCA MCAACCMCSGCTKGWWAG
HpaG809065	GGGCATACTMTATAGGGCGATTGGGTACCAGGAAGCGAACGATGTGGTTGTGTTTGCCGTCGTCGACGCT GTAGAAGGTGAGGCGCGAGCGTTGCTGGAGAAACTGGCAGATGCCGATGACGTGGCTGTCTACGTGGCG TCCACGCAGCTGGATCTGGTGGCAGACGCTAAGGCCGTGAAGAACGTGGTGCTGTACAAGAAGTTTGAC GAGGGGAAGGTCGTGTACGATGGCGAGTGGGAGAACGAGGCGCTGGCGGCGTTTATCAAGGCCAACAGT CTGCCGCTGGTGATTACGTTCTCGCAGGACAAGGCGCCCATGATCTTTGCTCGAGGTCGACGGTATCGAT AAGCTTGATATCGAATTCCTGCAGCCCGGGGGATCCACGCGTCACGTGGCTAGCCATGGAACCGGTGGAT CCACTAGTTCTAGAGCGGCCGCCACCGCGGTGGAGCTCGAATTCATCGATGATATCAGATCTGCCGGTCT CCCTATAGTGAGTCGTATTAATTTCGATAGGCCCAGGTGGATTCCTCSCYCACTGACTCGCYGCGCTCGG WCSYTCSGYTGCGGSGAGCGGTATCAGCTCACWCRRMGGCGGTRATACGGTTAYCCACAGAWTCAGGGG ATAACGSRSGAAAGAACATGTSAKSAAAAGGCCMGCWAAASGCCRGGAACCGTAARAWKGCCGCGTTGC KGGCGTTTTTCCAKAGGCTCCSCCCCCCYGACKAGCATCACAWAAATCGACSCTCWAGTCASAGGTGGCS ARACYYSYCMGGGACTATAAAGATACSGGGCGTYTYCYCCCTWGAMGMTCYCTCGTGYKCTSTCCYGTT SCSACCMWGCCKYTTACMGGATACMTGTYCMSCCTTTSTSCCWTSGGGARGYRWGGCGSTTTTCTCMYA KYTCACGYTGTATSTATCTCMTTTCRGTGKASGTCKGTYSCTMCAGGMTGRSMTGTGWGCCMGAAMCCC CCRRTTCATSYSRKAYCKCTGSAYMTTATCAGWTWACTMTCGTCTTGAAGTACTRASCCGGTAAAMMMA AYTTWATSSCMMTKGKCAGMAACCWCWGGGTAWMAGATWAGTCGGASSTWGCKRTGWAAGTCGKKG CWACMCASATAYTKWAATKTYKGCACTAACWMACKGSTWMCCTAGCMRWAAACATAATCTGSTAYTC KGACGCTMYGMTTAAAYCCAAGTACMMGTGCGTGAAATAARTWGTGWMGGCYCTCGWTCMGCCATAK MARACCACGGTYGGAWYATCCGTGGGTAGCATCGTCGCCACTGGACTTGGMCASGTCAGGACACTG
HpaG813906	AGGSCAYAWWCGGAGACGGCAGATCTGATATCATCGATGAATTCGAGCTCCACCGCGGTGGCGGCCGCT CTAGAACTAGTGGATCCACCGGTTCCATGGCTAGCCACGTGACGCGTGGATCCCCCGGGCTGCAGGAATT CGATATCAAGCTTATCGATACCGTCGACCTCGAGACTCTCCGCCTTCTTCTCCTCCTCCAGCTGCTCCAGT CGCTGGAGTGACTGTGTATTCCCCACCTCCGTCCTCACTGCTTCGGCCAGTAATTGAGCCTGGGTCAACCG ATTGCCAACCTTCTCGACTGTCCCTTTCTTGTGCTTCGCGGCCAATTTGGCCGCTTTATGCGACGCTTGTCT TCTCATTTCAGACGACTCGGACGACTTCTTCACAGTCGATGAACGAACTGTTGGCGCCACGTACTGATAC AGTGGTGTCATGGACGAAGTAGGAGCTGCAGGGGTACCCAATTCGCCCTATAGTGAGTCGTATTACGCGC GCTCACTGGCCGTCGTTTTACAACGTCGTGACTGGGAAAACCCTGGCGTTACCCAACTTAATCGCCTTGCA GCACATCCCCCTTTCGCCAGCTGGCGTAATAGCGAAGAGGCCCGCACCGATCGCCCTTCCCAACAGTTGC GCAGCCTGAATGGCGAATGGGACGCGCCCTGTAGCGGCGCATTAAGCGCGGCGGGTGTGGTGGTTACGC GCAGCGTGACCGCTACACTTGCCAGCGCCCTAGCGCCCGCTCCTTTCGCTTTCTTCCCTTCCTTTCTCGCCA CGTTCGCCGGCTTTCCCCGTCAAGCTCTAAATCGGGGGCTCCCTTTAGGGTTCCGATTTAGTGCTTTACGG CACCTCGACCCCAAAAAACTTGATTAGGGTGATGGTTCACGTAGTGGGCCATCGCCCTGATAGACGGTTT TTCGCCCTTTGACGTTGGAGTCCACGTTCTTTAATAGTGGACTCTTGTTCCAAACTGGAACAACACTCAAC CCTATCTCGGTCTATTCTTTGATTTATAGGATTTTGCCGATTCGGCCTATTGGTTAAAATGAGCTGATTTAA CAAAAATTAACGCGAATTTACAAAATATACGCTTACATTTAGTGCACTTTCGGGGAAATGTGCGCGACCC TATTGTTATTTCTAATACATCAWTGTWTCCGCTCAKGAACATACTGATATGCTTCAATAATATGAACGAG ATGAATTTCACATTCGTTCGACTTATTCCATTTTGCGCATTGGCCATCG
HpaG810051	GGMAWMAAWGGGGAGACGGCAGATCTGATATCATCGATGAATTCGAGCTCCACCGCGGTGGCGGCCGC TCTAGAACTAGTGGATCCACCGGTTCCATGGCTAGCCACGTGACGCGTGGATCCCCCGGGCTGCAGGAAT TCGATATCAAGCTTATCGATACCGTCGACCTCGAGCGCTTGGCTCTTACTGTTCATCGTGACCGACGGCAT

	CTGCGCCTGTGAGATGCTCACGTCTGGGTTCGCGTCTTCCGACGGCATGGCTTCGCCACACTCCGTGCAGA ATGCCGTGCCGCTGGGCACAGTCGCAAAGCAGTTCTCACAGACGAGACGCACGCGCTCCGTGAGCGTCTG CGCCGGGAGCGTCGCACCCGTGGGCAGCTCCGGTAGCTGCTCCTCCACGGGTCCGAGCTGTGCGTGGGCG CCCACGCGGTTGTAGCACATGAGTCCCCAGCGCATCGAGAGCTGATTGAGGCCGGTACCCAATTCGCCCT ATAGTGAGTCGTATTACGCGCGCTCACTGGCCGTCGTTTTACAACGTCGTGACTGGGAAAACCCTGGCGT TACCCAACTTAATCGCCTTGCAGCACATCCCCCTTTCGCCAGCTGGCGTAATAGCGAAGAGGCCCGCACC GATCGCCCTTCCCAACAGTTGCGCAGCCTGAATGGCGAATGGGACGCGCCCTGTAGCGGCGCATTAAGCG CGGCGGGTGTGGTGGTTACGCGCAGCGTGACCGCTACACTTGCCAGCGCCCTAGCGCCCGCTCCTTTCGC TTTCTTCCCTTCCTTTCTCGCCACGTTCGCCGGCTTTCCCCGTCAAGCTCTAAATCGGGGGCTCCCTTTAGG GTTCCGATTTAGTGCTTTACGGCACCTCGACCCCAAAAAACTTGATTAGGGTGATGGTTCACGTAGTGGG CCATCGCCCTGATAGACGGTTTTTCGCCCTTTGACGTTGGAGTCCACGTTCTTTATAGTGGACTCTTGTTCA AACTGGAACAACACTCAACCCTATCTCGGTCTATTCTTTTGATTTAWAAGGGATTTTGCGATTTCGGCTAT GGTTAAAMATGASTGATTAACAAAATTAACKCGAATTTACAAAWATTACSCTTACATTAGTGMRTTTTCG GGAAATGTGCCGACCCTATGTTATTTTCKAATMMTCAAWTGTATCGCCTATGAAACATACCTGTAATGCT CAAATTATGAACGTAAGTWGAATATCTACAGTCGCGTGTCGCCCCTAT
HpaG806090 (Glucan Synthase 1)	ARAWTWWCGGAGACGGCAGATCTGATATCATCGATGAATTCGAGCTCCACCGCGGTGGCGGCCGCTCTA GAACTAGTGGATCCCACCGGTTCCATGGCTAGCCACGTGACGCGTGGATCCCCCGGGCTGCAGGAATTCGA TATCAAGCTTATCGATACCGTCGACCTCGAGTAATCACCACACCGCCGTACAGCCCAAGTATCGCACCCA AGGATACAGGGTACACTAGACAGCAGAGACCACCAAGTACTAGTCCGCACAGGCATGCAATTGCGGTTT GGACCCACACATAATCTGCAGGAGCGCTAGTACTTAAGACTCCGTAAATCGACGCAGTGAGCCATAGCG AGCTAGCGTAAGCCGACATCGCTTTCGGATGGGAAGTGCCACAAAATGCCATGAAGAGGCCCAGAAGCG CATTCATCAGAGCAAACACCTGCAGAAGACCGATGGGTACCCAATTCGCCCTATAGTGAGTCGTATTACG CGCGCTCACTGGCCGTCGTTTTACAACGTCGTGACTGGGAAAACCCTGGCGTTACCCAACTTAATCGCCTT GCAGCACATCCCCCTTTCGCCAGCTGGCGTAATAGCGAAGAGGCCCGCACCGATCGCCCTTCCCAACAGT TGCGCAGCCTGAATGGCGAATGGGACGCGCCCTGTAGCGGCGCATTAAGCGCGGCGGGTGTGGTGGTTA CGCGCAGCGTGACCGCTACACTTGCCAGCGCCCTAGCGCCCGCTCCTTTCGCTTTCTTCCCTTCCTTTCTCG CCACGTTCGCCGGCTTTCCCCGTCAAGCTCTAAATCGGGGGCTCCCTTTAGGGTTCCGATTTAGTGCTTTA CGGCACCTCGACCCCAAAAAACTTGATTAGGGTGATGGTTCACGTAGTGGGCCATCGCCCTGATAGACGG TTTTTCGCCCTTTGACGTTGGAGTCCACGTTCTTTAATAGTGGACTCTTGTTCCAACTGGAACAACACTCA ACCCTATCTCGGTCTATTCTTTGATTTATAAGATTTTGCCGATTTCGGCCTATTGGTAAAAAATGAGCTGA TTTACAAAATTTACGCGATTTACAAATATACGCTACATTTAGTGGCACTTTCGGAATGTGCGCGACCCTAT TTGTTTATTTCTAATAATCATTGTATCCGCTCATGAACATACCTGATAATGCTCATAATGCAAGAGTWGAT ATCAATCCATTCGCCATTATCTTTTGGCGCCACTTGC
HpaG806090 (Glucan Synthase 2)	AAYATWWACGGAGACGGCAGATCTGATATCATCGATGAATTCGAGCTCCACCGCGGTGGCGGCCGCTCT AGAACTAGTGGATCCACCGGTTCCATGGCTAGCCACGTGACGCGTGGATCCCCCGGGCTGCAGGAATTCG ATATCAAGCTTATCGATACCGTCGACCTCGAGGTACACGGGCGTCACTACTGTGTCCAAAAAGTAACCCG CCTCGCGTTCAGCGTGACGAGCAGACGGAAACTCCTCCTTCATTTTGTGAAACAGGAAGCACACAAACTC CGGAGAGTGACGCAAGTTACTCGCCTCACCCCAAATGAAGAAGAACAAACACAAGTCCACCGAAATCTC ATCCACGCTAGTGAGACCACCTTGAGGCGCCCGATGCTCACTCCAGTGCAATGGCTTAATCATGAGCTTT GAGCACCACTTGTTGTAGTTGGAAAACACCAAAGCGTGCAGTTTCCGATGGTACCCAATTCGCCCTATAG TGAGTCGTATTACGCGCGCTCACTGGCCGTCGTTTTACAACGTCGTGACTGGGAAAACCCTGGCGTTACCC AACTTAATCGCCTTGCAGCACATCCCCCTTTCGCCAGCTGGCGTAATAGCGAAGAGGCCCGCACCGATCG CCCTTCCCAACAGTTGCGCAGCCTGAATGGCGAATGGGACGCGCCCTGTAGCGGCGCATTAAGCGCGGCG GGTGTGGTGGTTACGCGCAGCGTGACCGCTACACTTGCCAGCGCCCTAGCGCCCGCTCCTTTCGCTTTCTT CCCTTCCTTTCTCGCCACGTTCGCCGGCTTTCCCCGTCAAGCTCTAAATCGGGGGCTCCCTTTAGGGTTCCG ATTTAGTGCTTTACGGCACCTCGACCCCAAAAAACTTGATTAGGGTGATGGKTCACGTAGTGGGCCATCG CCCTGATAGACGGTTTTTCGCCCTTTGACGTTGGAGTCCACGTTCTTTAATAGTGGACTCTTGTTMCAAAC TGGAACACACTCAACCCTATCTCGGTCTAWTCTTTGATTATARGGAATTTGCCGACTTCGACTATGGTTAA AATGAGCTGATTTACAAAAATTACGCGAATTTACAAATATTAACGCTACATTAGGTGGCAAGTCSGGGGA ATGKGCGSGGAACYCAWTGCTTATTCAATCTCAAWYTGTWCGCCWAKGACATAGCCTGAWAKGTCAAA TATGAGGGAAAGTAGGATTCACGTTCCGGTCGCTATTCCATATTGCGSACAT
HpaG812588	CGMAYGWWCGGAGACGGCAGATCTGATATCATCGATGAATTCGAGCTCCACCGCGGTGGCGGCCGCTCT AGAACTAGTGGATCCACCGGTTCCATGGCTAGCCACGTGACGCGTGGATCCCCCGGGCTGCAGGAATTCG ATATCAAGCTTATCGATACCGTCGACCTCGAGAATGCTGTGCGTCTTTCCTGCAAAATTGAGTTGCGAGGC GAAACGGTGAATGTAAAGCGGCGGGTCAATGAGCGGTAGATGGATCTGCAATAGCTTGCAAAACTTGAG AAAAACACCTCCTAGCACATAAACGTTGATCTGGAGTTTGTCCGAAAAGTCGATAAGCAAGTGTGGCGAG CGTTCTCGTCGGCATACGACATAGAGGCAGGCGGCGATGACTGTCTGTGTCCTTCGACCGTGGGTAAAGT TTCGCTGCAGCGCCAGCGCATAGAGCCGGAAGGACGAGTGGTACCCAATTCGCCCTATAGTGAGTCGTAT TACGCGCGCTCACTGGCCGTCGTTTTACAACGTCGTGACTGGGAAAACCCTGGCGTTACCCAACTTAATC GCCTTGCAGCACATCCCCCTTTCGCCAGCTGGCGTAATAGCGAAGAGGCCCGCACCGATCGCCCTTCCCA ACAGTTGCGCAGCCTGAATGGCGAATGGGACGCGCCCTGTAGCGGCGCATTAAGCGCGGCGGGTGTGGT GGTTACGCGCAGCGTGACCGCTACACTTGCCAGCGCCCTAGCGCCCGCTCCTTTCGCTTTCTTCCCTTCCTT TCTCGCCACGTTCGCCGGCTTTCCCCGTCAAGCTCTAAATCGGGGGCTCCCTTTAGGGTTCCGATTTAGTG CTTTACGGCACCTCGACCCCAAAAAACTTGATTAGGGTGATGGTTCACGTAGTGGGCCATCGCCCTGATA GACGGTTTTTCGCCCTTTGACGTTGGAGTCCACGTTCTTTAATAGTGGACTCTTGTTCCAAACTGGAACAA CACTCAACCCTATCTCGGTCTATTCTTTGATTTATAAGGGATTTTGCCGATTTCGGCCTATTGGTTAAAAAT GAGCTGATTTACAAAAATTTAACGCGATTACAAATATAACGCTTAMATTTAGTGCACTTTCGGGAATGTSS

	CGAACCCTAGTTGGTATTTTCTAATCTCAATATGTWCCGCTCATGAACATAGCCTGATAAKGCTTCATAAC TGGAAAGGCAGWTAGAATTGCCAGCACGGTGCAGGCTTCGCCGTATATTTACGATGTCTTGTCGAG
HpaG808599	CGAAYAWTAGGAGACGGCAGATCTGATATCATCGATGAATTCGAGCTCCACCGCGGTGGCGGCCGCTCT AGATGCGGACAATACGACCTGAAGGTCGTTCCCCCCTATACGGTCTACAACAACCTGTGGGGTCAAGCCG ATGACTCAAACGGTACCCAGTGCACGGAAGTCACCCGTATTTCGGACGAGTCCATAGCCTGGACGACGGA CTTCAAGTGGGCTGGCAGTCGGTACCAGGTTAAGTCGTTCGCCAATGCAGCACTCACGTTCACGCCCGTG AAGATGTCCCAAGTGGCGAGTATGCCGACGGTGATTGAGTACAAGTACGAGTCCGTCGACGACACCCTCA TCACCAACCTCGAGGGGGGGCCCGGTACCCAATTCGCCCTATAGTGAGTCGTATTACGCGCGCTCACTGG CCGTCGTTTTACAACGTCGTGACTGGGAAAACCCTGGCGTTACCCAACTTAATCGCCTTGCAGCACATCCC CCTTTCGCCAGCTGGCGTAATAGCGAAGAGGCCCGCACCGATCGCCCTTCCCAACAGTTGCGCAGCCTGA ATGGCGAATGGGACGCGCCCTGTAGCGGCGCATTAAGCGCGGCGGGTGTGGTGGTTACGCGCAGCGTGA CCGCTACACTTGCCAGCGCCCTAGCGCCCGCTCCTTTCGCTTTCTTCCCTTCCTTTCTCGCCACGTTCGCCG GCTTTCCCCGTCAAGCTCTAAATCGGGGGCTCCCTTTAGGGTTCCGATTTAGTGCTTTACGGCACCTCGAC CCCAAAAAACTTGATTAGGGTGATGGTTCACGTAGTGGGCCATCGCCCTGATAGACGGTTTTTCGCCCTTT GACGTTGGAGTCCACGTTCTTTAATAGTGGACTCTTGTTCCAAACTGGAACAACACTCAACCCTATCTCGG TCTATTCTTTTGATTTATAAGGGATTTTGCCGATTTCGGCCTATTGGTTAAAAAATGAGCTGATTTAACAA AATTTAACGCGAATTTTAACAAATATTAACGCTTACATTTAGTGGCACTTTTCGGGGAATGTGCGCGGAA CCCTATTTGTTTATTTTTCTAATACATTCAATATGTATCCGCTCATGAGACATAACCTGATAATGCTTCATA ATATTGAAAAGGAGAGTATGAGTATCAACATTCCGTGTCGCATAATCCGTTTTTGGCGCAGTTGCCTCCK GTTTGCTCACCCAGACGCTGTGAGTTAARAKGCTGAGAATCAGTKGGGGTGTCAC
HpaG800629	GCMCWTACGGAGACGGCAGATCTGATATCATCGATGAATTCGAGCTCCACCGCGGTGGCGGCCGCTCTA GAACTAGTGGATCCACCGGTTCCATGGCTAGCCACGTGACGCGTGGATCCCCCGGGCTGCAGGAATTCGA TATCAAGCTTATCGATACCGTCGACCTCGAGTCCCTCAAATGGCTCACGTCCACCTGCTCGGAAATATCAA TCTCCTTGGCCGTCCGGTGCTTGGTAAAGATGGGCTTGCCCCGCCACTTGACTGTCACGGTCGAGCCTTCG CTTATGTTGCTCAAGTCAAACTCAGCGGTGGAGAGAGCCAGCACATCTGCCGACGCGCTCATGCTGCCGA CAAACTTGACCACGGCCAGACGAGCCGCCGTCGCGTAGGCTACACGGGCCCCGCCCAGCATAAAGTACG TGAACGCGCGCTTCGAAGGGTCGCCGGCATCGATGCGGTCCGTCTCAAAGTGGTACCCAATTCGCCCTAT AGTGAGTCGTATTACGCGCGCTCACTGGWGWTYCGTTTTACAACGTCGTGACTGGGAAAACCCTGGSGTT ACCCMACTTAATCGCCTTGCASCACATCCCCCTTTCGCCAGCTGGCGTAATAKCGAAGAGGCCCSCACCG ATCKCCCTTCCCAACAGTTGCGCAGCCTGAATGGSGAATGGGACGCGCCCTGTAGCGGCGCATTAAGCGC GGCGGGTGTGGTGGTTACGCGCAGCGTGACCGCTACACTTGCCAGCGCCCTAGCGCCCGCTCCTTTCKCTT TCTTCYCTTCCTTTCTCGYCRCGTTCGCCGGCTTTCCYCGTCRAGCTCTAAATCRGGGGCTSCCTTTAKGGT TCCGAYTTAGTGCTTTACGGCACCTCGACCCCAAAAAACTTGATTAGGWGATGGWTCRYGTAGTGGGCC RTCGCCCTGMTAGACRGTTKTTCGYCCTTTSGAYGTTGGAGTCCACGWTTCTTTAATARWGGACTCWTST TCCAWACTGAAACRACACTCAGCCTAYCTMGTCTATTCTTTTCGATTTRTATGGGATKTGACCGRTTCRGY CTAKTGGATAGAAAMTGACCTGATTTAACMWAAATKTAACSKCAACTTAACATWAWGWKACGCTTASA TRAGTGGAMGTTTCCGTAATGTGMACGGAACCTATCTGTTTATTTTCCWATCCTTCACTGTACCGCCTCY GGAACTTACCTGATAAGCGKCGCTTCAGTAKGATTGTA
HpaG807348	GGCATACTMGTATAGGGCGATTGGGTACCGGGCATGGGTGGTATGTTCATGTCCTCGAAGACGCCGACG GATTCTCTCCGCGGTGTGATCTTGGACACTTCGGTTACACCCCCGCGTGAGATTTGTGATGTCTCTGGCTC GTGGCTGCACGACCTTGTCTTTGGCAACAAGACGTACTGGGATATCAACAAGTACCAGAGCGGCTACATG GTGCCTTATCCTAAAGATAAGATTTTGGCGTCCGACTCGCGGCACCGCGAGGATCTACATTATCTGGCAA CAGGAGATTTGGATGAATCGCAGGAGTGGAAGGTGCTCGAGGTCGACGGTATCGATAAGCTTGATATCG AATTCCTGCAGCCCGGGGGATCCACGCGTCACGTGGCTAGCCATGGAACCGGTGGATCCACTAGTTCTAG AGCGGCCGCCACCGCGGTGGAGCTCGAATTCATCGATGATATCAGATCTGCCGGTCTCCCTATAGTGAGT CGTATTAATTTCGATAGGCCAGGTGGAKKCCTCGCTCACTGACTCGCTGCGCTCGGTCGTTCGGCTGCGGC GAGCGGTATCARCTCACTCARAGGCGGTAATACGGTTATCCACAGAATCMGGGGATAACRCAGGAAAGA RCATGTGASCRAAAGGSCAGCAAAAGGCCAGGAACCGTAAAAAKGCCGCGTTGCTGGCGTTTTTCCATAG GCTCCSCCCCCCTGACGAGCATCACMAAWATCGACGCTCWWKTCAGAGGTGGCGAARCCYKACASGACT ATAAAGATACCRGGSGTYTCCYCCTGGAAGCTCCCTCGKGCKCTCTSCTGTTCCGACCCTGMMRCTTACSR GAKACMTGTCCGCCTTTCTCCGTTCGGGAAGSRTGRCGCTTTCTCATACCTCACGCTGRARGTATCTYWKT TCRGWGTARGTCKTTSKCTCCAAGSWGGRMYGTGTGCMCRAACYCCSCGTWYAKCYGAYCTRTRGCGSM TWTCSGGTAMYTATRRMTTGGRTCAAACGRGKAWRMAMGAATTKTCSYCMMKAGWASSACRAAGRKW MTAGAATTATSRKRSCKGRSWGWRWGWWKGGYRCAGCTTCTKGWMKTGTTGGYSTAAGWACGAYAKA MYASACGAAAMCWAKTGRGATKCTGCASTCYTGCTRAWAKCGAGTAAMGAWTSGRAAAAYGAKTSAW TCGCCTYGTGMTCCCGSCMAACAATATCYYGCCTGKTGTWMSCTG

Supplementary Table 3.2. List of Dicer genes used in phylogenetic analyses.

Species	DICER Version	Accession/ Sequence ID	Amino Acid Length	Data Origin
Oomycetes				
Hyaloperonospora arabidopsidis	DCL1	HpaG808216	2477	Bollman et. al., 2016 and FungiDB
	DCL2	HpaG802243	739	FungiDB
	DCL3	HpaG801224	820	FungiDB
Plasmopara halstedii	DCL1	XP_024576170	1643	NCBI BLAST of DCL1 dsRNA region from Haile et. al., 2021. 79.53% DNA identity over 96% query cover, retrieved amino acid sequence from NCBI
	DCL2	XP_024581207	712	NCBI BLAST of DCL1 dsRNA region from Haile et. al., 2021. 79.53% DNA identity over 98% query cover, retrieved amino acid sequence from NCBI
Pythium ultimum (Globisporangium ultimum sporangiiferum)	DCL1	PUG3_G008981	1513	FungiDB DICER Query, from species Globisporangium ultimum var. sporangiiferum BR650
	DCL2	PUG3_G007955	963	FungiDB DICER Query, from species Globisporangium ultimum var. sporangiiferum BR650
	DCL4	PUG3_G009498	555	FungiDB DICER Query, from species Globisporangium ultimum var. sporangiiferum BR650
Phytophthora infestans (T30-4)	DCL1	XP_002903577.1	1664	Bollman et. al., 2016 and NCBI NCBI Query
	DCL2	XP_02902496.1	717	Bollman et. al., 2016 and NCBI NCBI Query
Phytophthora sojae	DCL1	AMS24201.1	1675	Bollman et. al., 2016 and NCBI NCBI Query
	DCL2	AMS24203.1	933	Bollman et. al., 2016 and NCBI NCBI Query
Fungi				
Sclerotinia sclerotiorum	DCL1	XP_001585179	1867	de Jong et. al., 2009 and NCBI Query
	DCL2	XP_001588821	1515	de Jong et. al., 2009 and NCBI Query
Botrytis cinerea	DCL1	XP_024552373	1968	NCBI BLASTp of DCL1 of *S. sclerotiorum*, 84.5% identity over 97% query cover
	DCL2	XP_024553022	1523	NCBI BLASTp of DCL2 of *S. sclerotiorum*, 74.52% identity over 96% query cover
Fusarium graminearum	DCL1	XP_011328775	1495	Nakayashiki, 2005 and FungiDB Query

	DCL2	XP_011321198	1451	Nakayashiki, 2005 and FungiDB Query
Pyrenophora tritici-repentis	DCR1	KAA8627380	1572	BLASTp of *S. sclerotiorum* DCL1 in *P. tritici-repentis*
	DCL2	KAG9383795	1410	BLASTp of *S. sclerotiorum* DCL1 in *P. tritici-repentis*
*Puccinia triticina (*BBBD Race 1)	DCL1	OAV89275	1401	Dubey et. al., 2020 and BLASTp of *S. sclerotiorum* DCL1 in *P. triticina*
	DCL2	OAV99053	1465	Dubey et. al., 2020 and BLASTp of *S. sclerotiorum* DCL1 in *P. triticina*
	DCL3	OAV89272	1556	Dubey et. al., 2020 and BLASTp of *S. sclerotiorum* DCL1 in *P. triticina*
Other Species				
Arabidopsis thaliana	DCL1	AEZ02176.1	1033	Bollman et. al., 2016
	DCL2	NP_001189798.1	1388	Bollman et. al., 2016
	DCL3	NP_001154662.2	1580	Bollman et. al., 2016
	DCL4	NP_001190348.1	1688	Bollman et. al., 2016
Chlamydomonas reinhardtii	DCL1	ACA63429	2243	BLASTp of *A. thaliana* DCL1 in *C. reinhardtii*
Caenohabditis elegans	DCR1	P34529ii_DCL1	1910	de Jong et. al., 2009

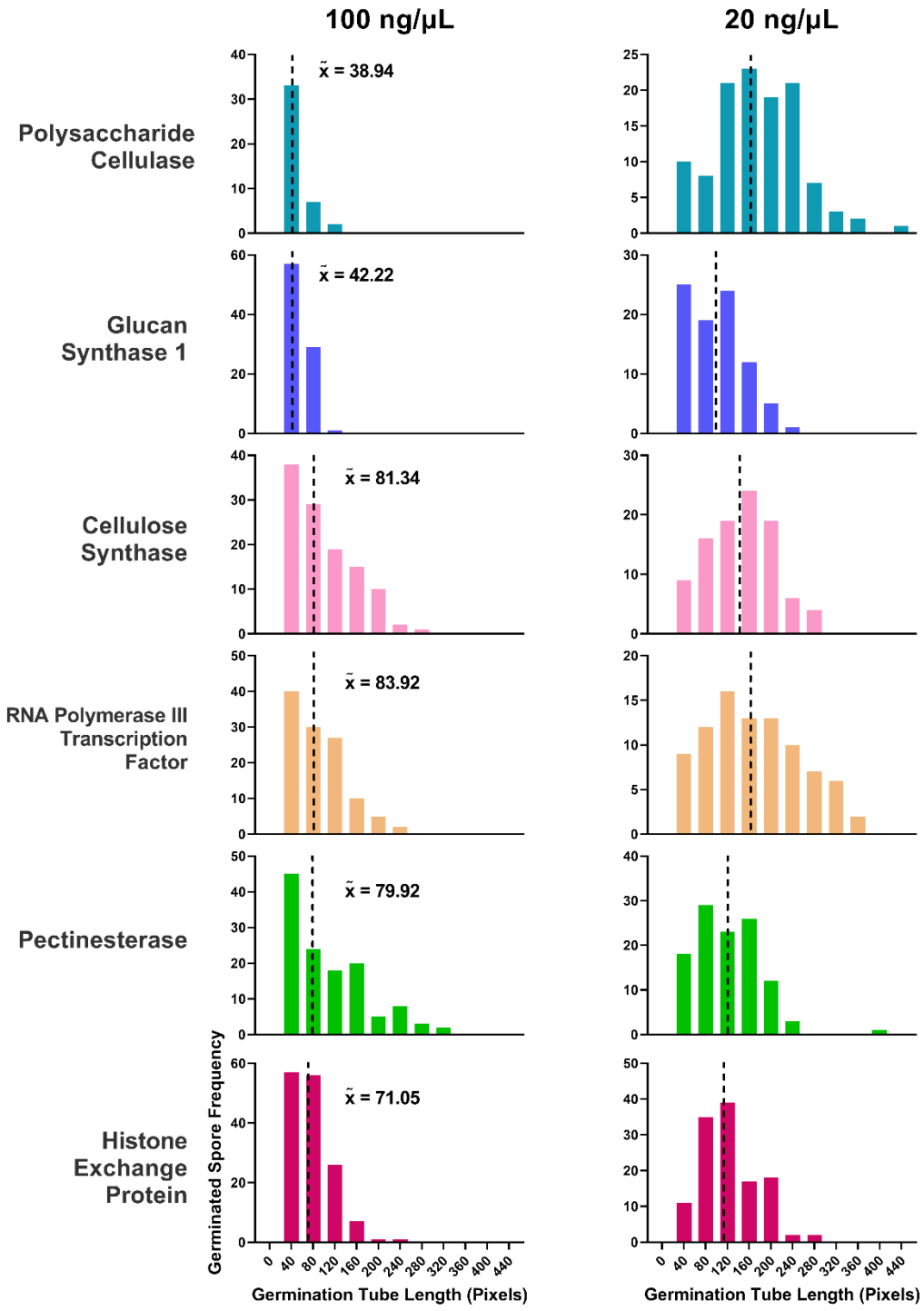

Supplementary Figure 3.1. Frequency distribution of *H. arabidopsidis* germination tubes. Total number of germinated tubes across 3 biological replicates for each treatment distributed across 40-pixel length bin ranges. Dotted line indicates median value.

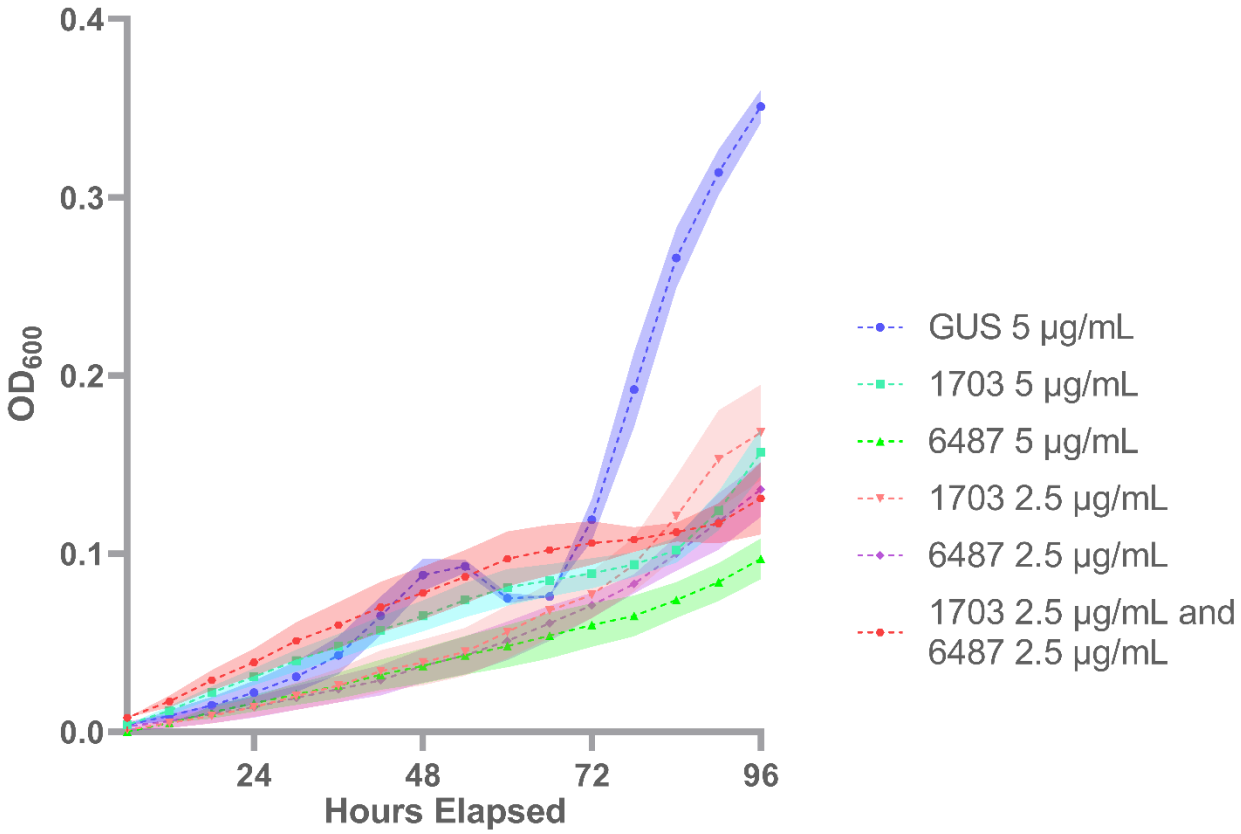

Supplementary Figure 3.2. DsRNA treatment dosage and combination impacts the growth inhibition of *S. sclerotiorum*. OD_{600} measurements scanned every 6 hours in a 9x9 scan grid in each well. Time point 0 hrs measurement subtracted from each subsequent time point. Plotted points represent mean value across 4 biological replicates with standard error plotted as shaded area.

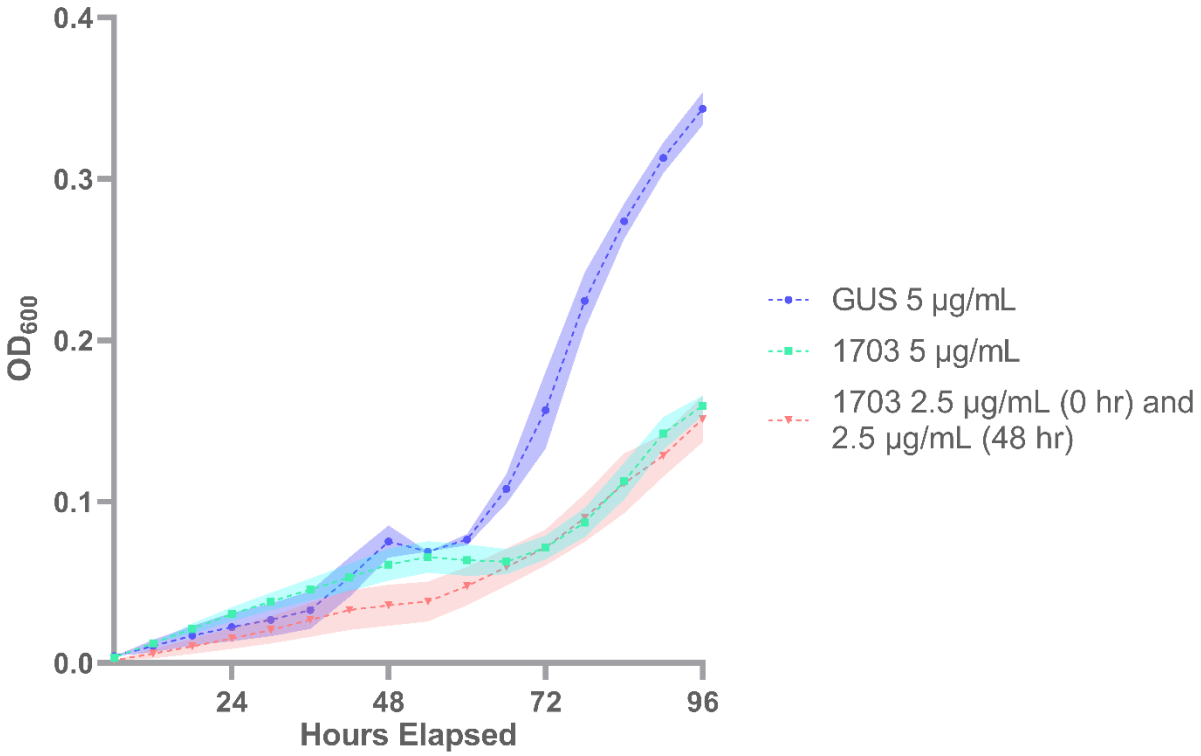

Supplementary Figure 3.3. DsRNA treatment supplemented over time does not increase the inhibition of *S. sclerotiorum*. OD_{600} measurements scanned every 6 hours in a 9x9 scan grid in each well. Time point 0 hrs measurement subtracted from each subsequent time point. Plotted points represent mean value across 4 biological replicates with standard error plotted as shaded area.

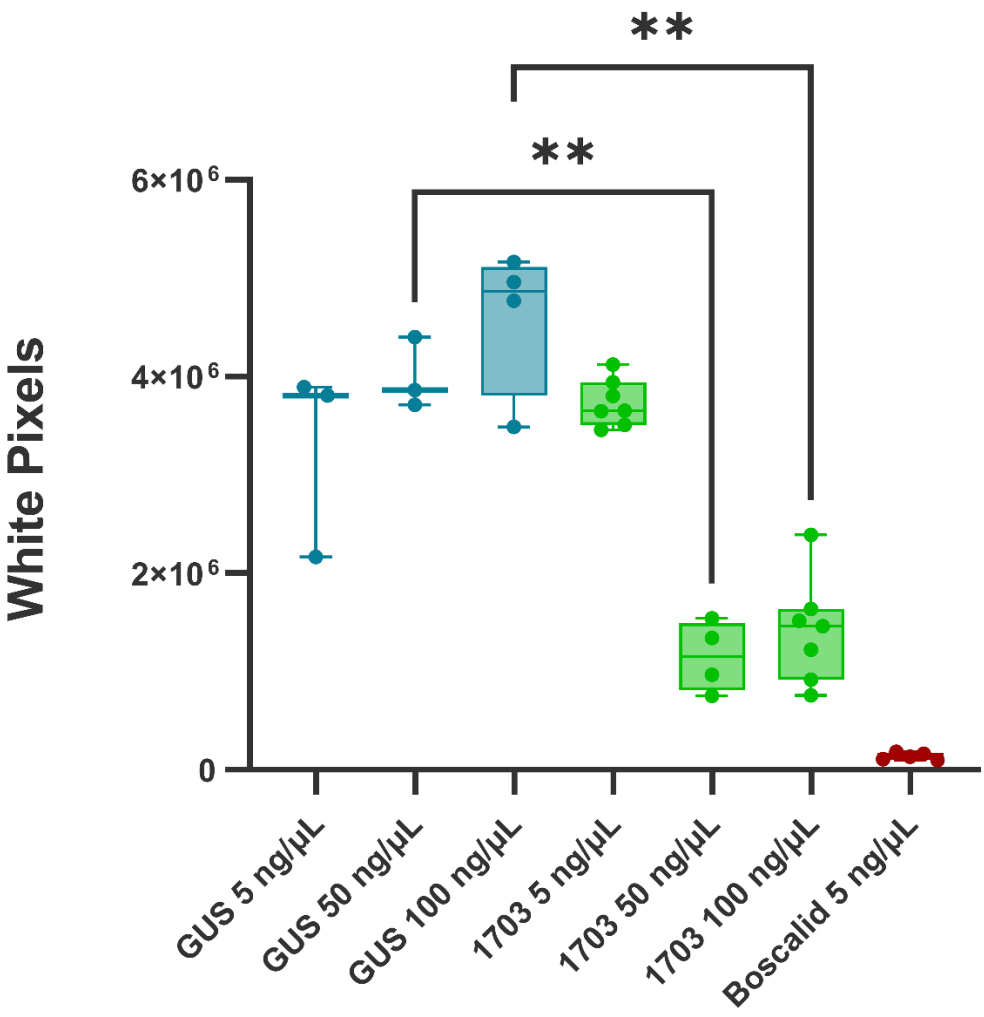

Supplementary Figure 3.4. A higher dose of 1703-targeting dsRNA is required for reduced *S. sclerotiorum* growth. Boxplot with min/max, interquartile ranges, and median value of total white pixel count of *S. sclerotiorum* growth measured 48 hpi across 3-7 biological replicates per treatment. 50 ng/µL and 100 ng/µL doses of GUS and 1703 dsRNA are significantly different (One-way ANOVA, $p < 0.01$).

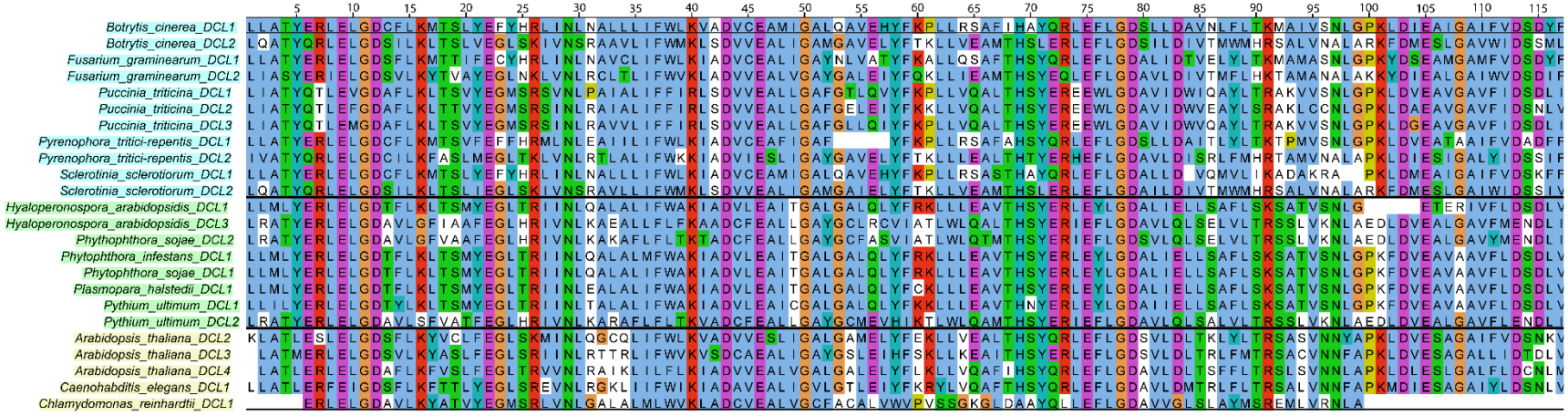
Botrytis_cinerea_DCL1
Botrytis_cinerea_DCL2
Fusarium_graminearum_DCL1
Fusarium_graminearum_DCL2
Puccinia_triticina_DCL1
Puccinia_triticina_DCL2
Puccinia_triticina_DCL3
Pyrenophora_tritici-repentis_DCL1
Pyrenophora_tritici-repentis_DCL2
Sclerotinia_sclerotiorum_DCL1
Sclerotinia_sclerotiorum_DCL2
Hyaloperonospora_arabidopsidis_DCL1
Hyaloperonospora_arabidopsidis_DCL3
Phythophthora_sojae_DCL2
Phytophthora_infestans_DCL1
Phytophthora_sojae_DCL1
Plasmopara_halstedii_DCL1
Pythium_ultimum_DCL1
Pythium_ultimum_DCL2
Arabidopsis_thaliana_DCL2
Arabidopsis_thaliana_DCL3
Arabidopsis_thaliana_DCL4
Caenohabditis_elegans_DCL1
Chlamydomonas_reinhardtii_DCL1

Supplementary Figure 3.5. Concatenated RNase III amino acid multiple sequence alignment of high consensus regions. Aligned residues selected based on BLOSUM62 matrix scores of 100 or greater. Residues coloured according to Clustalx colour schemes.

LITERATURE CITED

Abbasi, R., Heschuk, D., Kim, B., & Whyard, S. (2020). A novel paperclip double-stranded RNA structure demonstrates clathrin-independent uptake in the mosquito *Aedes aegypti*. *Insect Biochemistry and Molecular Biology*, *127*, 103492. https://doi.org/10.1016/J.IBMB.2020.103492

Ali, S. E., & Skaar, I. (2017). A fluorescence-based assay for in vitro screening of Saprolegnia inhibitors. *Journal of Fish Diseases*, *40*(10), 1333–1339. https://doi.org/10.1111/JFD.12605

Anjanappa, R. B., & Gruissem, W. (2021). Current progress and challenges in crop genetic transformation. *Journal of Plant Physiology*, *261*, 153411. https://doi.org/10.1016/J.JPLPH.2021.153411

Arnason, R. (2017) *Fungicide registration costs skyrocket.* The Western Producer. https://www.producer.com/news/fungicide-registration-costs-skyrocket/

Asai, S., Furzer, O. J., Cevik, V., Kim, D. S., Ishaque, N., Goritschnig, S., Staskawicz, B. J., Shirasu, K., & Jones, J. D. G. (2018). A downy mildew effector evades recognition by polymorphism of expression and subcellular localization. *Nature Communications 2018 9:1*, *9*(1), 1–11. https://doi.org/10.1038/S41467-018-07469-3

Asai, S., Rallapalli, G., Piquerez, S. J. M., Caillaud, M. C., Furzer, O. J., Ishaque, N., Wirthmueller, L., Fabro, G., Shirasu, K., & Jones, J. D. G. (2014). Expression Profiling during Arabidopsis/Downy Mildew Interaction Reveals a Highly-Expressed Effector That Attenuates

Responses to Salicylic Acid. *PLOS Pathogens*, *10*(10), e1004443. https://doi.org/10.1371/journal.ppat.1004443

Aunsbjerg, S. D., Andersen, K. R., & Knøchel, S. (2015). Real-time monitoring of fungal inhibition and morphological changes. *Journal of Microbiological Methods*, *119*, 196–202. https://doi.org/10.1016/J.mimet.2015.10.024

Avenot, H. F., & Michailides, T. J. (2010). Progress in understanding molecular mechanisms and evolution of resistance to succinate dehydrogenase inhibiting (SDHI) fungicides in phytopathogenic fungi. *Crop Protection*, *29*(7), 643–651. https://doi.org/10.1016/J.cropro.2010.02.019

Bachman, P., Fischer, J., Song, Z., Urbanczyk-Wochniak, E., & Watson, G. (2020). Environmental Fate and Dissipation of Applied dsRNA in Soil, Aquatic Systems, and Plants. *Frontiers in Plant Science*, *11*, 21. https://doi.org/10.3389/FPLS.2020.00021/BIBTEX

Bardin, S. D., & Huang, H. C. (2010). Research on biology and control of Sclerotinia diseases in Canada. *Canadian Journal of Plant Pathology*, *23*(1), 88–98. https://doi.org/10.1080/07060660109506914

Barik, S. (2006). RNAi in moderation. *Nature Biotechnology 2006 24:7*, *24*(7), 796–797. https://doi.org/10.1038/nbt0706-796

Barkai-Golan, R. (2001). *Postharvest Diseases of Fruits and Vegetables. Development and Control.* Elsevier Netherlands.

Bartnicki-Garcia, S. (1968). Cell Wall Chemistry, Morphogenesis, and Taxonomy of Fungi. *Annual Review of Microbiology*, *22*, 87–108. https://doi.org/10.1146/ANNUREV.MI.22.100168.000511

Bayer Corn Trait Gains EPA Approval: VT4PRO™ with RNAi Technology to Launch in US as Early as 2024 | Business Wire. (2022, March 2nd). Retrieved March 14, 2022, from https://www.businesswire.com/news/home/20220131005510/en/Bayer-Corn-Trait-Gains-EPA-Approval-VT4PRO%E2%84%A2-with-RNAi-Technology-to-Launch-in-US-as-Early-as-2024

Beakes, G. W., Glockling, S. L., & Sekimoto, S. (2012). The evolutionary phylogeny of the oomycete "fungi." *Protoplasma*, *249*(1), 3–19. https://doi.org/10.1007/S00709-011-0269-2

Bennett, M., Deikman, J., Hendrix, B., & Iandolino, A. (2020). Barriers to Efficient Foliar Uptake of dsRNA and Molecular Barriers to dsRNA Activity in Plant Cells. *Frontiers in Plant Science*, *11*, 816. https://doi.org/10.3389/FPLS.2020.00816

Betti, F., Ladera-Carmona, M. J., Weits, D. A., Ferri, G., Iacopino, S., Novi, G., Svezia, B., Kunkowska, A. B., Santaniello, A., Piaggesi, A., Loreti, E., & Perata, P. (2021). Exogenous miRNAs induce post-transcriptional gene silencing in plants. *Nature Plants 2021 7:10*, *7*(10), 1379–1388. https://doi.org/10.1038/S41477-021-01005-W

Bilir, Ö., Telli, O., Norman, C., Budak, H., Hong, Y., & Tör, M. (2019). Small RNA inhibits infection by downy mildew pathogen *Hyaloperonospora arabidopsidis*. *Molecular Plant Pathology*, *20*(11), 1523–1534. https://doi.org/10.1111/MPP.12863

Blum, M., Gamper, H. A., Waldner, M., Sierotzki, H., & Gisi, U. (2012). The cellulose synthase 3 (CesA3) gene of oomycetes: structure, phylogeny and influence on sensitivity to carboxylic acid amide (CAA) fungicides. *Fungal Biology*, *116*(4), 529–542. https://doi.org/10.1016/J.FUNBIO.2012.02.003

Boland, G. J., & Hall, R. (2009). Index of plant hosts of *Sclerotinia sclerotiorum*. *Canadian Journal of Plant Pathology*, *16*(2), 93–108. https://doi.org/10.1080/07060669409500766

Bollmann, S. R., Fang, Y., Press, C. M., Tyler, B. M., & Grünwald, N. J. (2016). Diverse evolutionary trajectories for small RNA biogenesis genes in the oomycete genus Phytophthora. *Frontiers in Plant Science*, *7*(MAR2016), 284. https://doi.org/10.3389/FPLS.2016.00284

Bolton, M. D., Thomma, B. P. H. J., & Nelson, B. D. (2006). *Sclerotinia sclerotiorum* (Lib.) de Bary: biology and molecular traits of a cosmopolitan pathogen. *Molecular Plant Pathology*, *7*(1), 1–16. https://doi.org/10.1111/J.1364-3703.2005.00316.X

Bradley, C. A., Lamey, H. A., Endres, G. J., Henson, R. A., Hanson, B. K., McKay, K. R., Halvorson, M., LeGare, D. G., & Porter, P. M. (2007). Efficacy of Fungicides for Control of Sclerotinia Stem Rot of Canola. *Https://Doi-Org.Uml.Idm.Oclc.Org/10.1094/PD-90-1129*, *90*(9), 1129–1134. https://doi.org/10.1094/PD-90-1129

Brent, K. J., & Hollomon, D. W. (2007). *Fungicide Resistance in Crop Pathogens: How Can it be Managed? 2nd Revised Edition*. Fungicide Resistance Action Committee. https://www.frac.info/docs/default-source/publications/monographs/monograph-1.pdf

(2020). Canadian Plant Disease Survey 2020 Volume 100: Disease Highlights 2019, *Canadian Journal of Plant Pathology*, *42* (sup1), 1–175. https://doi.org/10.1080/07060661.2020.1752524

Canola Council of Canada. (n.d.). *Canola meal: premium protein for dairy, livestock and fish diets*. https://www.canolacouncil.org/about-canola/meal/

Canola Council of Canada. (n.d.). *Canola's economic impact: growing opportunity for all Canadians*. https://www.canolacouncil.org/about-canola/economic-impact/

Cappelle, K., de Oliveira, C. F. R., van Eynde, B., Christiaens, O., & Smagghe, G. (2016). The involvement of clathrin-mediated endocytosis and two Sid-1-like transmembrane proteins in

double-stranded RNA uptake in the Colorado potato beetle midgut. *Insect Molecular Biology*, *25*(3), 315–323. https://doi.org/10.1111/IMB.12222

Case, P. (2019). *EU chlorothalonil ban another hammer blow for UK arable farmers*. Farmers Weekly. https://www.fwi.co.uk/arable/eu-chlorothalonil-ban-another-hammer-blow-for-growers#:~:text=The%20EU%20has%20voted%20to,on%20Friday%20(22%20March)

Cerutti, H., & Casas-Mollano, J. A. (2006). On the origin and functions of RNA-mediated silencing: From protists to man. *Current Genetics*, *50*(2), 81–99. https://doi.org/10.1007/S00294-006-0078-X

Chang, K. F., Hwang, S. F., Ahmed, H. U., Strelkov, S. E., Conner, R. L., Gossen, B. D., Bing, D. J., & Turnbull, G. D. (2013). Yield loss and management of downy mildew on field pea in Alberta, Canada. *Crop Protection*, *46*, 23–28. https://doi.org/10.1016/J.CROPRO.2012.12.001

Christiaens, O., Dzhambazova, T., Kostov, K., Arpaia, S., Joga, M. R., Urru, I., Sweet, J., & Smagghe, G. (2018). Literature review of baseline information on RNAi to support the environmental risk assessment of RNAi-based GM plants. *EFSA Supporting Publications*, *15*(5). https://doi.org/10.2903/SP.EFSA.2018.EN-1424

Ciancio, A., Mukerji, K. G. (Eds.). (2007) *General Concepts in Integrated Pest and Disease Management*. Springer, Dordrecht. https://doi-org.uml.idm.oclc.org/10.1007/978-1-4020-6061-8

Clarke, A. (2021, March 12). *Research looks to soften effect of mancozeb* ban. Farmers Weekly. https://www-proquest-com.uml.idm.oclc.org/docview/2564179094?parentSessionId=mACWvqcIYe4D%2FgetbIZFdY8OyhtXgeh4buJ2tzzObC4%3D&pq-origsite=primo&accountid=14569

Coates, M. E., & Beynon, J. L. (2010). *Hyaloperonospora arabidopsidis* as a Pathogen Model. *Annual Review of Phytopathology*, *48*, 329–345. https://doi.org/10.1146/ANNUREV-PHYTO-080508-094422

Cohen, Y., van den Langenberg, K. M., Wehner, T. C., Ojiambo, P. S., Hausbeck, M., Quesada-Ocampo, L. M., Lebeda, A., Sierotzki, H., & Gisi, U. (2015). Resurgence of *Pseudoperonospora cubensis*: The causal agent of Cucurbit downy mildew. *Phytopathology*, *105*(7), 998–1012. https://doi-org.uml.idm.oclc.org/10.1094/PHYTO-11-14-0334-FI

Dalakouras, A., Wassenegger, M., Dadami, E., Ganopoulos, I., Pappas, M. L., & Papadopoulou, K. (2020). Genetically Modified Organism-Free RNA Interference: Exogenous Application of RNA Molecules in Plants. *Plant Physiology*, *182*(1), 38–50. https://doi.org/10.1104/PP.19.00570

Das, P. R., & Sherif, S. M. (2020). Application of Exogenous dsRNAs-induced RNAi in Agriculture: Challenges and Triumphs. *Frontiers in Plant Science*, *11*, 946. https://doi.org/10.3389/fpls.2020.00946

Dehio, C., & Schell, J. (1994). Identification of plant genetic loci involved in a posttranscriptional mechanism for meiotically reversible transgene silencing. *Proc. Nati. Acad. Sci. USA*, *91*, 5538–5542.

de Jong, D., Eitel, M., Jakob, W., Osigus, H. J., Hadrys, H., DeSalle, R., & Schierwater, B. (2009). Multiple Dicer Genes in the Early-Diverging Metazoa. *Molecular Biology and Evolution*, *26*(6), 1333–1340. https://doi.org/10.1093/molbev/msp042

del Río, L. E., Bradley, C. A., Henson, R. A., Endres, G. J., Hanson, B. K., McKay, K., Halvorson, M., Porter, P. M., le Gare, D. G., & Lamey, H. A. (2007). Impact of Sclerotinia Stem Rot on

Yield of Canola. *American Phytopathological Society*, *91*(2), 191–194. https://doi.org/10.1094/PDIS-91-2-0191

Derbyshire, M. C., & Denton-Giles, M. (2016). The control of Sclerotinia Stem Rot on oilseed rape (*Brassica napus*): current practices and future opportunities. *Plant Pathology*, *65*(6), 859–877. https://doi.org/10.1111/PPA.12517

Ding, Y., Chen, Y., Yan, B., Liao, H., Dong, M., Meng, X., Wan, H., & Qian, W. (2021). Host-Induced Gene Silencing of a Multifunction Gene Sscnd1 Enhances Plant Resistance Against *Sclerotinia sclerotiorum*. *Frontiers in Microbiology*, *12*, 2891. https://doi.org/10.3389/fmicb.2021.693334

Ding, Y., Tang, Y., Kwok, C. K., Zhang, Y., Bevilacqua, P. C., & Assmann, S. M. (2013). In vivo genome-wide profiling of RNA secondary structure reveals novel regulatory features. *Nature 2013 505:7485*, *505*(7485), 696–700. https://doi.org/10.1038/nature12756

Dubelman, S., Fischer, J., Zapata, F., Huizinga, K., Jiang, C., Uffman, J., Levine, S., & Carson, D. (2014). Environmental Fate of Double-Stranded RNA in Agricultural Soils. *PLOS ONE*, *9*(3), e93155. https://doi.org/10.1371/journal.pone.0093155

Dubey, H., Kiran, K., Jaswal, R., Bhardwaj, S. C., Mondal, T. K., Jain, N., Singh, N. K., Kayastha, A. M., & Sharma, T. R. (2020). Identification and characterization of Dicer-like genes in leaf rust pathogen (Puccinia triticina) of wheat. *Functional and Integrative Genomics*, *20*(5), 711–721. https://doi.org/10.1007/S10142-020-00745-W/figures/4

Eitelberg, D. A., Vliet, J., & Verburg, P. H. (2015). A review of global potentially available cropland estimates and their consequences for model-based assessments. *Global Change Biology*, *21*(3), 1236–1248. https://doi.org/10.1111/gcb.12733

FAO. (2018). *The future of food and Agriculture, Alternative pathways to 2050*. *Summary Version.* https://www.fao.org/3/CA1553EN/ca1553en.pdf

Fire, A., Xu, S., Montgomery, M. K., Kostas, S. A., Driver, S. E., & Mello, C. C. (1998). Potent and specific genetic interference by double-stranded RNA in *Caenorhabditis elegans*. *Nature*, *391*(6669), 806–811. https://doi.org/10.1038/35888

Fisher, A., DeGrandi-Hoffman, G., Smith, B. H., Johnson, M., Kaftanoglu, O., Cogley, T., Fewell, J. H., & Harrison, J. F. (2021). Colony field test reveals dramatically higher toxicity of a widely-used mito-toxic fungicide on honey bees (*Apis mellifera*). *Environmental Pollution*, *269*, 115964. https://doi.org/10.1016/J.envpol.2020.115964

FRAC. (2021). *FRAC Code List 2021: Fungal control agents sorted by cross resistance pattern and mode of action (including coding for FRAC Groups on product labels)*. https://www.frac.info/docs/default-source/publications/frac-code-list/frac-code-list-2021--final.pdf?sfvrsn=f7ec499a_2

Genolution. (2020). *Service Overview – AgroRNA Long dsRNA Synthesis Service*. http://genolution.co.kr/agrorna/service-overview/

Gessler, C., Pertot, I., Perazzolli, M. (2011). *Plasmopara viticola*: a review of knowledge on downy mildew of grapevine and effective disease management. *Phytopathologia Mediterranea*, *50*(1), 3-44. http://www.jstor.org/stable/26458675

Gisi, U., & Sierotzki, H. (2008). Fungicide modes of action and resistance in downy mildews. *European Journal of Plant Pathology*, *122*(1), 157–167. https://doi.org/10.1007/S10658-008-9290-5/figures/6

Gouel, C., & Guimbard, H. (2019). Nutrition transition and the structure of global food demand. *American Journal of Agricultural Economics, 101*(2), 383–403. https://doi.org/10.1093/ajae/aay030

Gu, K. X., Song, X. S., Xiao, X. M., Duan, X. X., Wang, J. X., Duan, Y. B., Hou, Y. P., & Zhou, M. G. (2019). A β2-tubulin dsRNA derived from *Fusarium asiaticum* confers plant resistance to multiple phytopathogens and reduces fungicide resistance. *Pesticide Biochemistry and Physiology*, *153*, 36–46. https://doi.org/10.1016/J.pestbp.2018.10.005

Guan, R., Chu, D., Han, X., Miao, X., & Li, H. (2021). Advances in the Development of Microbial Double-Stranded RNA Production Systems for Application of RNA Interference in Agricultural Pest Control. *Frontiers in Bioengineering and Biotechnology*, *9*, 842. https://doi.org/10.3389/FBIOE.2021.753790

Gullickson, G. (2022, March 3rd). *Corteva Agriscience launches Vorceed Enlist corn technology.* Successful Farming. https://www.agriculture.com/news/technology/corteva-agriscience-launches-vorceed-enlist-corn-technology

Haile, Z. M., Gebremichael, D. E., Capriotti, L., Molesini, B., Negrini, F., Collina, M., Sabbadini, S., Mezzetti, B., & Baraldi, E. (2021). Double-Stranded RNA Targeting Dicer-Like Genes Compromises the Pathogenicity of *Plasmopara viticola* on Grapevine. *Frontiers in Plant Science*, *12*, 735. https://doi.org/10.3389/FPLS.2021.667539

Harrington, B.J., & Hageage, G.J. (2003). Calcofluor White: A Review of its Uses and Applications in Clinical Mycology and Parasitology. *Laboratory Medicine, 5*(34), 361-367. https://doi.org/10.1309/EPH2TDT8335GH0R3

Henderson, I. R., Zhang, X., Lu, C., Johnson, L., Meyers, B. C., Green, P. J., & Jacobsen, S. E. (2006). Dissecting Arabidopsis thaliana DICER function in small RNA processing, gene silencing and DNA methylation patterning. Nature Genetics 2006 38:6, 38(6), 721–725. https://doi.org/10.1038/ng1804

Hinas, A., Wright, A. J., & Hunter, C. P. (2012). SID-5 Is an Endosome-Associated Protein Required for Efficient Systemic RNAi in *C. Elegans*. *Current Biology*, *22*(20), 1938–1943. http://dx.doi.org/10.1016/j.cub.2012.08.020

Holub, E. B., Beynon, J. L., & Crute, I. R. (1994). Phenotypic and genotypic characterization of interactions between isolates of *Peronospora parasitica* and accessions of *Arabidopsis thaliana*. *Molecular Plant-Microbe Interactions*, *7*(2), 223–239. https://doi.org/10.1094/MPMI-7-0223

Hou, Y. P., Mao, X. W., Lin, S. P., Song, X. S., Duan, Y. B., Wang, J. X., & Zhou, M. G. (2018). Activity of a novel succinate dehydrogenase inhibitor fungicide pyraziflumid against *Sclerotinia sclerotiorum*. *Pesticide Biochemistry and Physiology*, *145*, 22–28. https://doi.org/10.1016/J.pestbp.2017.12.009

Hou, Y. P., Mao, X. W., Wu, L. Y., Wang, J. X., Mi, B., & Zhou, M. G. (2019). Impact of fluazinam on morphological and physiological characteristics of *Sclerotinia sclerotiorum*. *Pesticide Biochemistry and Physiology*, *155*, 81–89. https://doi.org/10.1016/J.pestbp.2019.01.009

Hu, S., Zhang, J., Zhang, Y., He, S., & Zhu, F. (2018). Baseline sensitivity and toxic actions of boscalid against *Sclerotinia sclerotiorum*. *Crop Protection*, *110*, 83–90. https://doi.org/10.1016/J.cropro.2018.04.004

Islam, M. T., Davis, Z., Chen, L., Englaender, J., Zomorodi, S., Frank, J., Bartlett, K., Somers, E., Carballo, S. M., Kester, M., Shakeel, A., Pourtaheri, P., & Sherif, S. M. (2021). Minicell-based

fungal RNAi delivery for sustainable crop protection. *Microbial Biotechnology*, *14*(4), 1847–1856. https://doi.org/10.1111/1751-7915.13699

Iwasaki, Y. W., Siomi, M. C., & Siomi, H. (2015). PIWI-Interacting RNA: Its Biogenesis and Functions. *Annual Review of Biochemistry*, *84*, 405–433. https://doi-org.uml.idm.oclc.org/10.1146/annurev-biochem-060614-034258

Jagla, B., Aulner, N., Kelly, P. D., Song, D., Volchuk, A., Zatorski, A., Shum, D., Mayer, T., de Angelis, D. A., Ouerfelli, O., Rutishauser, U., & Rothman, J. E. (2005). Sequence characteristics of functional siRNAs. *RNA*, *11*(6), 864–872. https://doi.org/10.1261/rna.7275905

Judelson, H. S., & Ah-Fong, A. M. V. (2019). Exchanges at the Plant-Oomycete Interface That Influence Disease. *Plant Physiology*, *179*(4), 1198–1211. https://doi.org/10.1104/PP.18.00979

Kalyandurg, P. B., Sundararajan, P., Dubey, M., Ghadamgahi, F., Zahid, M. A., Whisson, S. C., & Vetukuri, R. R. (2021). Spray-Induced Gene Silencing as a Potential Tool to Control Potato Late Blight Disease. *Phytopathology*, *111*(12), 2166–2175. https://doi-org.uml.idm.oclc.org/10.1094/PHYTO-02-21-0054-SC

Kamal, M. M., Savocchia, S., Lindbeck, K. D., & Ash, G. J. (2016). Biology and biocontrol of *Sclerotinia sclerotiorum* (Lib.) de Bary in oilseed Brassicas. *Australasian Plant Pathology*, *45*(1), 1–14. https://doi-org.uml.idm.oclc.org/10.1007/s13313-015-0391-2

Kaur, A., Kumar, A., & Reddy, M. S. (2016). RNA Interference (RNAi) and Its Role in Crop Improvement: A Review. *Plant Tissue Culture: Propagation, Conservation and Crop Improvement*, 379–394. https://doi.org/10.1007/978-981-10-1917-3_16

Kaur, M., & Singh, R. (2020). Volatile self-inhibitor of spore germination in pathogenic Mucorale *Rhizopus arrhizus*. *FEMS Microbiology Ecology*, *96*(9). https://doi.org/10.1093/femsec/fiaa170

Koch, A., Biedenkopf, D., Furch, A., Weber, L., Rossbach, O., Abdellatef, E., Linicus, L., Johannsmeier, J., Jelonek, L., Goesmann, A., Cardoza, V., McMillan, J., Mentzel, T., & Kogel, K. H. (2016). An RNAi-Based Control of *Fusarium graminearum* Infections Through Spraying of Long dsRNAs Involves a Plant Passage and Is Controlled by the Fungal Silencing Machinery. *PLOS Pathogens*, *12*(10). https://doi.org/10.1371/journal.ppat.1005901

Koch, A., Kumar, N., Weber, L., Keller, H., Imani, J., & Kogel, K. H. (2013). Host-induced gene silencing of cytochrome P450 lanosterol C14α-demethylase-encoding genes confers strong resistance to Fusarium species. *Proceedings of the National Academy of Sciences of the United States of America*, *110*(48), 19324–19329. https://doi.org/10.1073/pnas.1306373110

Kuck, K.-H., Leadbeater, A., Gisi, U., Wolfgang Krämer, by, Schirmer, U., Jeschke, P., & Witschel, M. (2012). FRAC Mode of Action Classification and Resistance Risk of Fungicides. *Modern Crop Protection Compounds: Second Edition*, *2*, 539–557. https://doi.org/10.1002/9783527644179.CH14

Kumar, K., Gambhir, G., Dass, A., Tripathi, A. K., Singh, A., Jha, A. K., Yadava, P., Choudhary, M., & Rakshit, S. (2020). Genetically modified crops: current status and future prospects. *Planta 2020 251:4*, *251*(4), 1–27. https://doi.org/10.1007/S00425-020-03372-8

Laurie, J. D., Ali, S., Linning, R., Mannhaupt, G., Wong, P., Güldener, U., Münsterkötter, M., Moore, R., Kahmann, R., Bakkeren, G., & Schirawski, J. (2012). Genome Comparison of Barley and Maize Smut Fungi Reveals Targeted Loss of RNA Silencing Components and Species-Specific

Presence of Transposable Elements. *The Plant Cell*, *24*(5), 1733–1745. https://doi.org/10.1105/TPC.112.097261

Lax, C., Tahiri, G., Patiño-Medina, J. A., Cánovas-Márquez, J. T., Pérez-Ruiz, J. A., Osorio-Concepción, M., Navarro, E., & Calo, S. (2020). The Evolutionary Significance of RNAi in the Fungal Kingdom. *International Journal of Molecular Sciences 2020, Vol. 21, Page 9348*, *21*(24), 9348. https://doi.org/10.3390/IJMS21249348

Leadbeater, A. (2015). Recent developments and challenges in chemical disease control. *Plant Protection Science*, *51*(4), 163–169. https://doi.org/10.17221/83/2015-PPS

Lee, W. S., Rudd, J. J., & Kanyuka, K. (2015). Virus induced gene silencing (VIGS) for functional analysis of wheat genes involved in *Zymoseptoria tritici* susceptibility and resistance. *Fungal Genetics and Biology*, *79*, 84–88. https://doi.org/10.1016/J.FGB.2015.04.006

Li, L., Chang, S. S., & Liu, Y. (2010). RNA interference pathways in filamentous fungi. *Cellular and Molecular Life Sciences 2010 67:22*, *67*(22), 3849–3863. https://doi.org/10.1007/S00018-010-0471-Y

Lin, L., Allemekinders, H., Dansby, A., Campbell, L., Durance-Tod, S., Berger, A., & Jones, P. J. (2013). Evidence of health benefits of canola oil. *Nutrition Reviews*, *71*(6), 370–385. https://doi.org/10.1111/NURE.12033

Liu, Q., Feng, Y., & Zhu, Z. (2009). Dicer-like (DCL) proteins in plants. *Functional and Integrative Genomics*, *9*(3), 277–286. https://doi.org/10.1007/S10142-009-0111-5

Liu, Q., Wang, F., & Axtell, M. J. (2014). Analysis of complementarity requirements for plant microRNA targeting using a *Nicotiana benthamiana* quantitative transient assay. *The Plant Cell*, *26*(2), 741–753. https://doi.org/10.1105/tpc.113.120972

Lu, T., Zhang, Q., Lavoie, M., Zhu, Y., Ye, Y., Yang, J., Paerl, H. W., Qian, H., & Zhu, Y. G. (2019). The fungicide azoxystrobin promotes freshwater cyanobacterial dominance through altering competition. *Microbiome*, *7*(1), 1–13. https://doi.org/10.1186/S40168-019-0744-0

Malaj, E., Liber, K., & Morrissey, C. A. (2020). Spatial distribution of agricultural pesticide use and predicted wetland exposure in the Canadian Prairie Pothole Region. *Science of The Total Environment*, *718*, 134765. https://doi.org/10.1016/J.scitotenv.2019.134765

Mao, X., Wang, Y., Hou, Y., & Zhou, M. (2020). Activity of the succinate dehydrogenase inhibitor fungicide penthiopyrad against *Sclerotinia sclerotiorum*. *Plant Disease*, *104*(10), 2696–2703. https://doi.org/10.1094/pdis-10-19-2253-re

Marcianò, D., Ricciardi, V., Marone Fassolo, E., Passera, A., Bianco, P. A., Failla, O., Casati, P., Maddalena, G., de Lorenzis, G., & Toffolatti, S. L. (2021). RNAi of a Putative Grapevine Susceptibility Gene as a Possible Downy Mildew Control Strategy. *Frontiers in Plant Science*, *12*, 880. https://doi.org/10.3389/FPLS.2021.667319

Maximiano, M. R., Santos, L. S., Santos, C., Aragão, F. J. L., Dias, S. C., Franco, O. L., & Mehta, A. (2022). Host induced gene silencing of *Sclerotinia sclerotiorum* effector genes for the control of white mold. *Biocatalysis and Agricultural Biotechnology*, *40*, 102302. https://doi.org/10.1016/J.BCAB.2022.102302

McDowell, J. M. (2014). *Hyaloperonospora arabidopsidis: A Model Pathogen of Arabidopsis.* In Dean, R., Lichens-Park, A., Kole, C. (Eds.), *Genomics of Plant-Associated Fungi and*

Oomycetes: Dicot Pathogens (pp. 209–234). Springer, Berlin. https://doi.org/10.1007/978-3-662-44056-8_10

McLoughlin, A. G., Wytinck, N., Walker, P. L., Girard, I. J., Rashid, K. Y., de Kievit, T., Fernando, W. G. D., Whyard, S., & Belmonte, M. F. (2018). Identification and application of exogenous dsRNA confers plant protection against *Sclerotinia sclerotiorum* and *Botrytis cinerea*. *Scientific Reports 2018 8:1*, *8*(1), 1–14. https://doi.org/10.1038/S41598-018-25434-4

Miller, S. C., Miyata, K., Brown, S. J., & Tomoyasu, Y. (2012). Dissecting Systemic RNA Interference in the Red Flour Beetle *Tribolium castaneum*: Parameters Affecting the Efficiency of RNAi. *PLOS ONE*, *7*(10), e47431. https://doi.org/10.1371/journal.pone.0047431

Mitani, S., Araki, S., Yamaguchi, T., Takii, Y., Ohshima, T., & Matsuo, N. (2002). Biological properties of the novel fungicide cyazofamid against *Phytophthora infestans* on tomato and *Pseudoperonospora cubensis* on cucumber. *Pest Management Science*, *58*(2), 139–145. https://doi.org/10.1002/PS.430

Mitter, N., Worrall, E. A., Robinson, K. E., Li, P., Jain, R. G., Taochy, C., Fletcher, S. J., Carroll, B. J., Lu, G. Q., & Xu, Z. P. (2017). Clay nanosheets for topical delivery of RNAi for sustained protection against plant viruses. *Nature Plants*, *3*(2), 1–10. https://doi.org/10.1038/NPLANTS.2016.207

Miyata, K., Ramaseshadri, P., Zhang, Y., Segers, G., Bolognesi, R., & Tomoyasu, Y. (2014). Establishing an In Vivo Assay System to Identify Components Involved in Environmental RNA Interference in the Western Corn Rootworm. *PLOS ONE*, *9*(7). https://doi.org/10.1371/journal.pone.0101661

Miyazawa, K., Umeyama, T., Hoshino, Y., Abe, K., & Miyazaki, Y. (2022). Quantitative Monitoring of Mycelial Growth of *Aspergillus fumigatus* in Liquid Culture by Optical Density. *Microbiology Spectrum*, *10*(1). https://doi.org/10.1128/spectrum.00063-21

Molotoks, A., Stehfest, E., Doelman, J., Albanito, F., Fitton, N., Dawson, T. P., & Smith, P. (2018). Global projections of future cropland expansion to 2050 and direct impacts on biodiversity and carbon storage. *Global Change Biology*, *24*(12), 5895–5908. https://doi.org/10.1111/gcb.14459

Mosa, M. A., & Youssef, K. (2021). Topical delivery of host induced RNAi silencing by layered double hydroxide nanosheets: An efficient tool to decipher pathogenicity gene function of Fusarium crown and root rot in tomato. *Physiological and Molecular Plant Pathology*, *115*, 101684. https://doi.org/10.1016/j.pmpp.2021.101684

Nakayashiki, H. (2005). RNA silencing in fungi: Mechanisms and applications. *FEBS Letters*, *579*(26), 5950–5957. https://doi.org/10.1016/j.febslet.2005.08.016

Natskoulis, P. I., Lappa, I. K., & Panagou, E. Z. (2018). Evaluating the efficacy of turbimetric measurements as a rapid screening technique to assess fungal susceptibility to antimicrobial compounds as exemplified by the use of sodium metabisulfite. *Food Research International*, *106*, 1037–1041. https://doi.org/10.1016/J.foodres.2018.01.058

Niño-Sánchez, J., Chen, L. H., de Souza, J. T., Mosquera, S., & Stergiopoulos, I. (2021). Targeted Delivery of Gene Silencing in Fungi Using Genetically Engineered Bacteria. *Journal of Fungi* *7*(2), 125. https://doi.org/10.3390/JOF7020125

Nunes, C. A. (2012). Biological control of postharvest diseases of fruit. *European Journal of Plant Pathology*, *133*(1), 181–196. https://doi.org/10.1007/S10658-011-9919-7

Nunes, C. C., & Dean, R. A. (2012). Host-induced gene silencing: a tool for understanding fungal host interaction and for developing novel disease control strategies. *Molecular Plant Pathology*, *13*(5), 519–529. https://doi.org/10.1111/J.1364-3703.2011.00766

Pandey, P., Irulappan, V., Bagavathiannan, M. v., & Senthil-Kumar, M. (2017). Impact of combined abiotic and biotic stresses on plant growth and avenues for crop improvement by exploiting physio-morphological traits. *Front. Plant. Sci*. 8(537). https://doi.org/10.3389/fpls.2017.00537

Parker, K. M., Barragán Borrero, V., van Leeuwen, D. M., Lever, M. A., Mateescu, B., & Sander, M. (2019). Environmental Fate of RNA Interference Pesticides: Adsorption and Degradation of Double-Stranded RNA Molecules in Agricultural Soils. *Environmental Science and Technology*, *53*(6), 3027–3036. https://doi-org.uml.idm.oclc.org/10.1021/acs.est.8b05576

Pasteris, R. J., Hanagan, M. A., Bisaha, J. J., Finkelstein, B. L., Hoffman, L. E., Gregory, V., Andreassi, J. L., Sweigard, J. A., Klyashchitsky, B. A., Henry, Y. T., & Berger, R. A. (2016). Discovery of oxathiapiprolin, a new oomycete fungicide that targets an oxysterol binding protein. *Bioorganic & Medicinal Chemistry*, *24*(3), 354–361. https://doi.org/10.1016/J.BMC.2015.07.064

Pethybridge, S.J., Cobb, A.C., Dillard, H.R. (2015). Production of Apothecia and Ascospores of *Sclerotinia sclerotiorum*. *The Plant Health Instructor*. https://doi.org/10.1094/PHI-T-2004-0604-01

Pieczynska, M. D., de Visser, J. A. G. M., & Korona, R. (2013). Incidence of symbiotic dsRNA 'killer' viruses in wild and domesticated yeast. *FEMS Yeast Research*, *13*(8), 856–859. https://doi.org/10.1111/1567-1364.12086

PMRA. (2018, May 10). *Re-evaluation Decision RVD2018-11, Chlorothalonil and Its Associated End-use Products for Agricultural and Turf Uses*. Government of Canada. https://www.canada.ca/en/health-canada/services/consumer-product-safety/reports-publications/pesticides-pest-management/decisions-updates/reevaluation-decision/2018/chlorothalonil.html

PMRA. (2020, November 19). *Re-evaluation Decision RVD2020-12, Mancozeb and Its Associated End-use Products*. Government of Canada. https://www.canada.ca/en/health-canada/services/consumer-product-safety/reports-publications/pesticides-pest-management/decisions-updates/reevaluation-decision/2020/mancozeb.html

Purdy, L. H. (1979). *Sclerotinia sclerotiorum*: History, Diseases and Symptomatology, Host Range, Geographic Distribution, and Impact. *Phytopathology*, *69*(8), 875. https://doi.org/10.1094/phyto-69-875

Qiao, L., Lan, C., Capriotti, L., Ah-Fong, A., Nino Sanchez, J., Hamby, R., Heller, J., Zhao, H., Glass, N. L., Judelson, H. S., Mezzetti, B., Niu, D., & Jin, H. (2021). Spray-induced gene silencing for disease control is dependent on the efficiency of pathogen RNA uptake. *Plant Biotechnology Journal*, *19*(9), 1756–1768. https://doi.org/10.1111/PBI.13589

Rana, K., Yuan, J., Liao, H., Banga, S. S., Kumar, R., Qian, W., & Ding, Y. (2022). Host-induced gene silencing reveals the role of *Sclerotinia sclerotiorum* oxaloacetate acetylhydrolase gene in fungal oxalic acid accumulation and virulence. *Microbiological Research*, *258*, 126981. https://doi.org/10.1016/J.micres.2022.126981

Rank, A. P., & Koch, A. (2021). Lab-to-Field Transition of RNA Spray Applications – How Far Are We? *Frontiers in Plant Science*, *12*, 2243. https://doi.org/10.3389/FPLS.2021.755203

Rensing, L., Monnerjahn, C., & Meyer, U. (1998). Differential stress gene expression during the development of *Neurospora crassa* and other fungi. *FEMS Microbiology Letters*, *168*(2), 159–166. https://doi.org/10.1111/J.1574-6968.1998.TB13268.X

Reynolds, A., Leake, D., Boese, Q., Scaringe, S., Marshall, W. S., & Khvorova, A. (2004). Rational siRNA design for RNA interference. *Nature Biotechnology 2004 22:3*, *22*(3), 326–330. https://doi.org/10.1038/NBT936

Richards, T. A., Dacks, J. B., Jenkinson, J. M., Thornton, C. R., & Talbot, N. J. (2006). Evolution of Filamentous Plant Pathogens: Gene Exchange across Eukaryotic Kingdoms. *Current Biology*, *16*(18), 1857–1864. https://doi.org/10.1016/j.cub.2006.07.052

Romano, N., & Macino, G. (1992). Quelling: transient inactivation of gene expression in *Neurospora crassa* by transformation with homologous sequences. *Molecular Microbiology*, *6*(22), 3343–3353. https://doi.org/10.1111/j.1365-2958.1992.tb02202.x

Saleh, M. C., van Rij, R. P., Hekele, A., Gillis, A., Foley, E., O'Farrell, P. H., & Andino, R. (2006). The endocytic pathway mediates cell entry of dsRNA to induce RNAi silencing. *Nature Cell Biology*, *8*(8), 793–802. https://doi.org/10.1038/NCB1439

Sanju, S., Siddappa, S., Thakur, A., Shukla, P. K., Srivastava, N., Pattanayak, D., Sharma, S., & Singh, B. P. (2015). Host-mediated gene silencing of a single effector gene from the potato pathogen *Phytophthora infestans* imparts partial resistance to late blight disease. *Functional and Integrative Genomics*, *15*(6), 697–706. https://doi.org/10.1007/S10142-015-0446-Z

Savary, S., Willocquet, L., Pethybridge, S. J., Esker, P., McRoberts, N., & Nelson, A. (2019). The global burden of pathogens and pests on major food crops. *Nature Ecology & Evolution*, *3*(3), 430–439. https://doi.org/10.1038/s41559-018-0793-y

Sharma, P., Meena, P. D., Verma, P. R., Saharan, G. S., Mehta, N., Singh, D., & Kumar, A. (2015). *Sclerotinia sclerotiorum* (Lib.) de Bary causing Sclerotinia rot in oilseed Brassicas: A review. *Journal of Oilseed Brassica, 6*:1–44

Slusarenko, A. J., & Schlaich, N. L. (2003). Downy mildew of *Arabidopsis thaliana* caused by *Hyaloperonospora parasitica* (formerly *Peronospora parasitica*). *Molecular Plant Pathology, 4*(3), 159–170. https://doi.org/10.1046/J.1364-3703.2003.00166

Smith, H. A., Swaney, S. L., Parks, T.D., Wernsman, E. A., & Dougherty, W. G. (1994). Transgenic Plant Virus Resistance Mediated by Untranslatable Sense RNAs: Expression, Regulation, and Fate of Nonessential RNAs. *The Plant Cell, 6*(10), 1441–1453. https://dx.doi.org/10.1105%2Ftpc.6.10.1441

Snijders, C. H. A. (1990). Fusarium head blight and mycotoxin contamination of wheat, a review. *Neth. J. PI. Path, 96*, 187–198. https://doi.org/10.1007/BF01974256

Taylor, A., Coventry, E., Jones, J. E., & Clarkson, J. P. (2015). Resistance to a highly aggressive isolate of *Sclerotinia sclerotiorum* in a *Brassica napus* diversity set. *Plant Pathology, 64*(4), 932–940. https://doi.org/10.1111/PPA.12327

Thines, M. (2014). Phylogeny and evolution of plant pathogenic oomycetes-a global overview. *European Journal of Plant Pathology*, *138*(3), 431–447. https://doi.org/10.1007/S10658-013-0366-5

Tomar, G., Chakrabarti, S. K., Sharma, N. N., Jeevalatha, A., Sundaresha, S., Vyas, K., & Azmi, W. (2018). RNAi-based transgene conferred extreme resistance to the geminivirus causing apical leaf curl disease in potato. *Plant Biotechnology Reports, 12*(3), 195–205. https://doi.org/10.1007/S11816-018-0485-8

Tomoyasu, Y., Miller, S. C., Tomita, S., Schoppmeier, M., Grossmann, D., & Bucher, G. (2008). Exploring systemic RNA interference in insects: A genome-wide survey for RNAi genes in Tribolium. *Genome Biology*, *9*(1), 1–22. https://doi.org/10.1186/GB-2008-9-1-R10

Statistics Canada. (2019, December 3rd). *Table 32-10-0209-01 Type of pesticides used on farms* [Data set]. https://doi.org/10.25318/3210020901-eng

van Blokland, R., van der Geest, N., Mol, J. N. M., & Kooter, J. M. (1994). Transgene-mediated suppression of chalcone synthase expression in *Petunia hybrida* results from an increase in RNA turnover. *The Plant Journal*, *6*(6), 861–877. https://doi.org/10.1046/J.1365-313X.1994.6060861

Wang, H., Gong, L., Qi, J., Hu, M., & Zhong, G. (2014). Molecular Cloning and Characterization of a SID-1-Like Gene in *Plutella xylostella*. *Archives of Insect Biochemistry and Physiology*, *87*(3), 164–176. https://doi.org/10.1002/arch.21189

Wang, M., Weiberg, A., Lin, F. M., Thomma, B. P. H. J., Huang, H. da, & Jin, H. (2016). Bidirectional cross-kingdom RNAi and fungal uptake of external RNAs confer plant protection. *Nature Plants 2016 2:10*, *2*(10), 1–10. https://doi.org/10.1038/NPLANTS.2016.151

Wang, Y., Akhavan, A., Hwang, S. F., & Strelkov, S. E. (2020). Decreased sensitivity of *Leptosphaeria maculans* to pyraclostrobin in Alberta, Canada. *Plant Disease*, *104*(9), https://doi.org/10.1094/pdis-11-19-2461-re

Whitfield, R., Anastasaki, A., Truong, N. P., Cook, A. B., Omedes-Pujol, M., Loczenski Rose, V., Nguyen, T. A. H., Burns, J. A., Perrier, S., Davis, T. P., & Haddleton, D. M. (2018). Efficient Binding, Protection, and Self-Release of dsRNA in Soil by Linear and Star Cationic Polymers. *ACS Macro Letters*, *7*(8), 909–915. https://doi-org.uml.idm.oclc.org/10.1021/acsmacrolett.8b00420

Wynant, N., Santos, D., van Wielendaele, P., & vanden Broeck, J. (2014). Scavenger receptor-mediated endocytosis facilitates RNA interference in the desert locust, *Schistocerca gregaria*. *Insect Molecular Biology*, *23*(3), 320–329. https://doi.org/10.1111/imb.12083

Wytinck, N., Manchur, C. L., Li, V. H., Whyard, S., & Belmonte, M. F. (2020). dsRNA Uptake in Plant Pests and Pathogens: Insights into RNAi-Based Insect and Fungal Control Technology. *Plants 2020, Vol. 9, Page 1780*, *9*(12), 1780. https://doi.org/10.3390/plants9121780

Wytinck, N., Sullivan, D. S., Biggar, K. T., Crisostomo, L., Pelka, P., Belmonte, M. F., & Whyard, S. (2020). Clathrin mediated endocytosis is involved in the uptake of exogenous double-stranded RNA in the white mold phytopathogen Sclerotinia sclerotiorum. *Scientific Reports 2020 10:1*, *10*(1), 1–12. https://doi.org/10.1038/S41598-020-69771-9

Yang, P., Yi, S. Y., Nian, J. N., Yuan, Q. S., He, W. J., Zhang, J. B., & Liao, Y. C. (2021). Application of Double-Strand RNAs Targeting Chitin Synthase, Glucan Synthase, and Protein Kinase Reduces *Fusarium graminearum* Spreading in Wheat. *Frontiers in Microbiology*, *12*, 1729. https://doi.org/10.3389/FMICB.2021.660976

Yin, X., Yi, B., Chen, W., Zhang, W., Tu, J., Fernando, W. G. D., & Fu, T. (2010). Mapping of QTLs detected in a *Brassica napus* DH population for resistance to *Sclerotinia sclerotiorum* in multiple environments. *Euphytica*, *173*(1), 25–35. https://doi.org/10.1007/S10681-009-0095-1

Zamani-Noor, N., & Molinero-Ruiz, L. (2021). Baseline Sensitivity and Control Efficacy of Various Group of Fungicides against *Sclerotinia sclerotiorum* in Oilseed Rape Cultivation. *Agronomy 2021, Vol. 11, Page 1758*, *11*(9), 1758. https://doi.org/10.3390/agronomy11091758

Zhang, Z., Chang, S. S., Zhang, Z., Xue, Z., Zhang, H., Li, S., & Liu, Y. (2013). Homologous recombination as a mechanism to recognize repetitive DNA sequences in an RNAi pathway. *Genes & Development*, *27*(2), 145–150. https://doi.org/10.1101/GAD.209494.112